



Cape Peninsula
University of Technology

**RECONFIGURABLE PHOTOVOLTAIC MODULES FOR ROBUST
NANOSATELLITE POWER SYSTEMS**

by

LÉON TCHONKO NJOUAKOUA

Thesis submitted in fulfilment of the requirements for the degree

Master of Engineering: Electrical Engineering

in the Faculty of Engineering

at the Cape Peninsula University of Technology

Supervisor: Dr. Atanda Kamoru Raji

Bellville Campus

November 2017

CPUT copyright information

The dissertation/thesis may not be published either in part (in scholarly, scientific or technical journals), or as a whole (as a monograph), unless permission has been obtained from the University

DECLARATION

I, Léon Tchonko Njouakoua, declare that the contents of this dissertation/thesis represent my own unaided work, and that the dissertation/thesis has not previously been submitted for academic examination towards any qualification. Furthermore, it represents my own opinions and not necessarily those of the Cape Peninsula University of Technology.

Léon Tchonko Njouakoua

2nd November 2017

Signed

Date

ABSTRACT

Until recently, the focus of most solar technology development for space was towards more efficient, more radiation-resistant and increasingly powerful arrays. During a space mission, solar cells are not only exposed to irradiation by electrons, but also to a range of other particles, like protons. Thus, solar cells on robust nanosatellites are extremely exposed to an environment, which includes the high-energy electrons and protons of the earth's radiation belts, which leads towards the degradation process of the individual solar cell. Solar cell radiation shielding design ensures the protection of the solar cells from the particular radiation environment found in space. While the design principles of a solar photovoltaic automatic switching fault tolerant system which can detect and bypass faulty photovoltaic cells will be presented through this research work. The ability of such a system to be reconfigured using implemented switching matrix system makes it efficient under various environments and faulty conditions.

ACKNOWLEDGEMENTS

I wish to thank:

- *Kleyn's family for their support and for encouraging me to take a step further with my education*
- *Dr Atanda Raji for his encouragement, support and understanding shown through my steps at Cape Peninsula University of Technology*
- *Dr. Senthil Krishnamurthy for always being there when I stand by his door.*
- *Prof. Dina Burger for the University Research Awards*
- *Prof. Mellet Moll for being my Lawyer and my role model in student leadership*
- *The whole Engineering Faculty Staff*
- *The entire Electrical Department Staff*
- *The Directors and the staff of FSATI*
- *The students of Cape Peninsula University of Technology*
- *My family members and friends*
- *Guinness-Cameroun for the precious awards*
- *South Africa*

The financial assistance of the National Research Foundation (NRF) towards this research is acknowledged. Opinions expressed in this thesis and the conclusions arrived at, are those of the author, and are not necessarily to be attributed to the National Research Foundation.

DEDICATION

To the Almighty, the most high and the only provider.

To my father, Mr. Emmanuel Tchonko Njouakoua

To my mother, Christine Tchamko

To the Tchonko family

Contents

DECLARATION	ii
ABSTRACT.....	iii
ACKNOWLEDGEMENTS	iv
Chapter 1: <i>General concept of the study</i>	1
1.1 Background and introduction:	1
1.2 Problem statement:	3
1.2 Objectives of the research work:	4
1.3 Research methodology:	5
1.4 Delineation of study:	7
1.5 Literature study:	8
1.6 Simulation and Modelling:	8
1.7 Thesis outline:	8
Chapter 2: <i>Nanosatellite's Electrical Power System</i>	10
2.1 Background:	10
2.2 Nanosatellites Electrical Power Systems:	11
2.2.1 Orbit trajectory modelling of Zacube-2 in space:	12
2.2.2 General overview of Zacube-2 mounted subsystems:	16
Chapter 3: <i>A literature survey on the photovoltaic energy systems</i>	19
3.1 Introduction:	19
3.2 Photovoltaic effect in the solar cells:	20
3.3 Solar cells and their Generations:.....	20
3.3.1 First Generation of solar cells:	21
3.3.2 Second Generation of solar cells:	21
3.3.3 Third Generation of solar cells:	21
3.3.4 Fourth Generation of solar cells:	23
3.4 Performance analysis of a solar cell:	23
3.4.1 Solar spectrum and Irradiance:.....	23
3.4.2 Power conversion efficiency:	23
Chapter 4: <i>Modelling of solar cells for space photovoltaic energy systems</i>	30
4.1 Introduction:	30
4.2 Solar Cell Modelling:.....	30
4.2.1 Ideal Model of a Single junction Solar Cell:	31
4.2.2 Two diodes Single Junction Solar Cell Model:	37
4.2.3 Power Model of a Single junction Solar Cell:.....	38

4.2.4 General Model for a space triple junction Solar Cell:	38
Chapter 5: <i>Degradation in Different Solar Cell Technologies</i>	41
5.1 Introduction:	41
5.2 Degradation principle in various types of solar cells:	42
5.2.1 Degradation in Silicon Wafer Solar cells:	42
5.2.2 Degradation in Hydrogenated Amorphous Silicon (a-Si:H) Solar cells:	42
5.2.3 Degradation in Copper Indium Gallium Diselenide (CIGS) Solar cells:	43
5.2.4 Degradation in Cadmium Telluride (CdTe) Solar cells:	43
5.2.5 Degradation in III-V Multijunction Solar cells:	44
5.2.6 Degradation in Dye-Sensitized Solar Cells (DSSC):	44
5.2.7 Degradation in Organic Solar cells (OSC):	45
5.3 On- Orbit solar cell Degradation Approach:	45
5.3.1 Space-based solar cells Power Systems:	46
5.3.2 Solar Cells Performance Parameters:	47
5.3.3 The effects of radiation on solar cells:	51
Chapter 6: <i>A literature survey on reconfigurable photovoltaic systems</i>	53
6.1 Introduction:	53
6.2 Reconfigurable solar photovoltaic array:	54
6.2.1 Total-Cross-Tied connection topology:.....	63
6.2.2 Bridge-Linked connection topology:.....	64
6.2.3 Hybrid Configuration connection topology:	65
Chapter 7: <i>Degradation fault detection algorithm and system</i>	66
<i>Optimization of solar cells</i>	66
7.1 Introduction:	66
7.2 Failures occurring in photovoltaic system:	66
7.3 Degradation in photovoltaic system:	67
7.3.1 Front surface soiling:.....	68
7.3.2 Optical degradation:	68
7.3.3 Solar cell degradation:.....	69
7.3.4 Mismatched solar cells:	70
7.3.5 Light-Induced degradation:	70
7.3.6 Temperature-Induced degradation:	71
7.4 Degradation Analysis in photovoltaic system:	71
7.5 Degraded solar cells detection in photovoltaic system:	72
7.5.1 Detection of the degraded solar cell using the short-circuit current:.....	72

7.5.2 Degraded solar cell detection algorithm:.....	74
Chapter 8: <i>The constructed reconfigurable photovoltaic module</i>	83
8.1 Introduction:	83
8.2 Modelling and simulation of the reconfigurable module:	83
8.3 Design of the printed circuit board of the reconfigurable module:	86
8.4 Experimental setups:	88
8.5 Conclusion:	90
Chapter 9: <i>Recommendations and Future work</i>	93
9.1 Recommendations:	93
9.2 Future research work:.....	93
References:.....	94

LIST OF FIGURES

<i>Figure 1.1: Schematic of an individual integrated power electronic switch (“reconfigurable-PV - CAD4X Laboratory,” n.d.).....</i>	<i>3</i>
<i>Figure 1.2: Long-term monitoring data of the photovoltaic module.....</i>	<i>5</i>
<i>Figure 1.3: Block diagram of the reconfiguration scheme block.....</i>	<i>6</i>
<i>Figure 1.4: Solar cells long term monitoring.....</i>	<i>7</i>
<i>Figure 2.1: Illustration of the 3U ZACUBE-2 nanosatellite layout (“ZACUBE-2 - eoPortal Directory - Satellite Missions,” n.d.).....</i>	<i>12</i>
<i>Figure 2.2: Zacube-2's sun synchronous circular orbit trajectory of 600Km using STK10 software ..</i>	<i>13</i>
<i>Figure 2.3: Ground track of the nanosatellite Zacube_2 with the geographical position of its ground station.....</i>	<i>13</i>
<i>Figure 2.4: Geometrical representation of the conditions of visibility of the Nanosatellite by its ground station (“ECLIPSE ET VISIBILITE D’UN SATELLITE,” n.d.).</i>	<i>14</i>
<i>Figure 2.5: Zacube-2 visibility over a period of 3 days using STK10 software.....</i>	<i>15</i>
<i>Figure 2.6: Period of the nanosatellite visibility approximately equal to 11 minutes</i>	<i>15</i>
<i>Figure 2.7: Conceptual Layout of the nanosatellite Zacube-2 (“ZAcube-2 schematics - Google Search,” n.d.).....</i>	<i>17</i>
<i>Figure 2.8: An overview of the systems mounted on the nanosatellite Zacube-2 (“Image,” n.d.)</i>	<i>18</i>
<i>Figure 3.1: I-V characteristics of a solar cell under illumination (Solid curve). Dashed curve represents the corresponding inverted power graph (Kumar, 2017).....</i>	<i>25</i>
<i>Figure 3.2: Equivalent circuit of a p-n junction solar cell illumination (Single-diode model)</i>	<i>28</i>
<i>Figure 3.3: Equivalent circuit of a p-n junction solar cell illumination using two diodes</i>	<i>29</i>
<i>Figure 4.1: Simplified equivalent circuit of a single junction Solar cell.....</i>	<i>31</i>
<i>Figure 4.2: Simplified equivalent circuit of a single junction solar cell with Ohmic losses.....</i>	<i>33</i>
<i>Figure 4.3: The five-parameter model of a single junction solar cell.....</i>	<i>36</i>
<i>Figure 4.4: Dual-diode model of a single junction solar cell</i>	<i>37</i>
<i>Figure 4.5: General equivalent circuit of a single junction Solar cell</i>	<i>39</i>
<i>Figure 4.6: General model for a triple junction solar cell</i>	<i>40</i>
<i>Figure 5.1: I-V characteristic curves of a triple junction solar cell.(Messmer, 2013).....</i>	<i>48</i>
<i>Figure 5.2: Schematic diagram of the circuit used to measure current-voltage curves of the solar cell experiments in space. (Walker and Statler, 1988).....</i>	<i>49</i>
<i>Figure 5.3: I-V characteristic curve of a solar array</i>	<i>49</i>
<i>Figure 5.4: P-V characteristic curve of a solar array</i>	<i>50</i>
<i>Figure 5.5: I-V characteristics of a solar cell under illumination (Solid curve). Dashed curve represents the corresponding inverted power graph</i>	<i>50</i>
<i>Figure 6.1: Photovoltaic arrays power system generator of a 3U nanosatellite.....</i>	<i>55</i>
<i>Figure 6.2: Interconnection of an array of solar cell with bypass and series diodes inserted</i>	<i>56</i>
<i>Figure 6.3: Interconnection of two parallel faces of the nanosatellites photovoltaic system.....</i>	<i>57</i>
<i>Figure 6.4: Series -Connection of solar cells known as the S-Connection mode</i>	<i>57</i>
<i>Figure 6.5: Series - Parallel Connection of solar cells known as the SP-Connection mode.....</i>	<i>58</i>
<i>Figure 6.6: Parallel Connection of solar cells known as the P-Connection mode</i>	<i>58</i>

<i>Figure 6.7: Current-Voltage characteristic of a face made of 6 healthy XTJ solar cells in Series – Connection</i>	59
<i>Figure 6.8: Power-Voltage characteristic of a face made of 6 healthy XTJ solar cells in Series – Connection</i>	59
<i>Figure 6.9: Electrical parameters readings of the series-connection topology</i>	60
<i>Figure 6.10: Photovoltaic system of a 3U-Nano satellite with series diodes</i>	60
<i>Figure 6.11: Solar cells arrays with 3 degraded solar cells among them</i>	61
<i>Figure 6.12: Current-Voltage characteristic of a photovoltaic system under degradation circumstances</i>	61
<i>Figure 6.13: Power -Voltage characteristic of a photovoltaic system under degradation circumstances</i>	62
<i>Figure 6.14: Total-Cross-Tied interconnection topology</i>	64
<i>Figure 6.15: Bridge-Linked interconnection topology</i>	64
<i>Figure 6.16: Honey-Comb interconnection style</i>	65
<i>Figure 7.1: Impact of soiling the top surface of a solar cell in a solar cells array</i>	68
<i>Figure 7.2: Equivalent circuit of a solar cell using the two diodes model</i>	69
<i>Figure 7.3: Unidirectional short-circuit current sensing system of a solar cell unit</i>	72
<i>Figure 7.4: Zacube 2 power supply system</i>	75
<i>Figure 7.5: X+ face interconnection used for degradation fault detection and fault elimination</i>	76
<i>Figure 7.6: Short-circuit current monitoring results of the X+ face of the Zacube 2</i>	78
<i>Figure 7.7: Snapshot of the command window after capturing the measured short-circuit current of each photovoltaic cell</i>	79
<i>Figure 7.8: Six solar cells (XTJ-Prime) connected in series using simple wires</i>	81
<i>Figure 7.9: Six solar cells (XTJ-Prime) connected in series using simple Mosfets</i>	81
<i>Figure 8.1: Reconfigurable photovoltaic module architecture of the X+ Face using Simulink</i>	83
<i>Figure 8.2: Current-Voltage Characteristic Simulink model of a healthy X+ Face of the Zacube 2</i> ...	84
<i>Figure 8.3: Individual Current-Voltage Characteristic curve of a healthy X+ Face of the Zacube 2</i> .	85
<i>Figure 8.4: Current-Voltage (I-V) Characteristic curve of a healthy X+ Face of the Zacube 2</i>	85
<i>Figure 8.5: Power-Voltage (P-V) Characteristic curve of a healthy X+ Face of the Zacube 2</i>	86
<i>Figure 8.6: Implemented reconfigurable architecture of the X+ face photovoltaic module</i>	86
<i>Figure 8.7: Top and Bottom layer PCB tracks of the implemented reconfigurable photovoltaic module architecture</i>	87
<i>Figure 8.8: Populated Top-layer of the reconfigurable photovoltaic module's PCB</i>	87
<i>Figure 8.9: Populated Bottom-layer of the reconfigurable photovoltaic module's PCB</i>	88
<i>Figure 8.10: Block diagram of the experimental setup layout of the designed reconfigurable photovoltaic module</i>	89
<i>Figure 8.11: Experimental setup for measurement of the produced output</i>	89

Chapter 1: General concept of the study

1.1 Background and introduction:

Nanosatellites or any other spacecraft are designed to operate dependably throughout their operational life, ordinarily a number of years. This can be done through stringent quality control and testing of parts and subsystems before they are used in the construction of the satellites or spacecraft. Redundancy of key components is often built in so that if there is a failure of a particular part, assembly or subsystem; another subsystem or unit can perform its functions. Furthermore, hardware and software on the satellite or spacecraft are often designed so that ground controller or the onboard computers can reconfigure the satellite to operate around a part that has failed. Generally speaking, the majority of failures have taken place during launch or during initial deployment and checkout of the satellite or spacecraft. Nanosatellites have popped up within the last decade starting as a tool for education and capacity building but are now rapidly becoming a technology considered for the implementation of operational surveillance and communication services operated by national authorities. Nanosatellites provide a cost-efficient and relative fast option for deploying new spaceborne assets to support data gathering to improve situational awareness leading to increased operational efficiency.

It is stated that Nanosatellites like other spacecraft use photovoltaic modules to fulfil the power demand of the payload. Due to some size and mass constraints, while dealing with nanosatellites, redundancy of components will not be useful in some areas, for instance the photovoltaic modules mentioned in this case. In general, photovoltaic modules are used in most long-mission spacecraft for power generation. The mission design life is generally limited to about fifteen years due to degradation in the Van Allen radiation belts. Degradation leading to failure in photovoltaic modules follows a progression that is dependent on multiple factors, some of which interact causing degradation that is difficult to simulate in the ground laboratory during the design and the testing of the Nanosatellites (*Quintana et al., 2002*). Permanent degradation of photovoltaic modules can be classified as:

- Degradation of packaging materials, like for instance glass cover damage;
- Delamination issues in other words loss of adhesion of layers leading to module overheating;
- Degradation of the cell or module as a result of temperature cycling;

- Degradation caused by moisture; and
- Degradation of the semiconductor device

Extensive studies have been conducted towards the degradation of the photovoltaic modules level over the past forty years. A median annual degradation rate of 0.5 percent based on the nearly two thousands degradation rates from more than hundred publications has been proposed (*Jordan and Kurtz, 2013*). Moreover, at least a couple of different ways can be used to discover the degradation effect on a photovoltaic module such as the following (*Kiefer et al., 2010*):

- Field inspections focusing on individual modules or subsystems;
- Laboratory measurements of individual cells or modules; and
- Analyzing logged monitoring data

It should be noted that, solar cells in space need to operate under harsh environmental conditions as high energy protons and electrons harm the semiconductor material leading to a continuous degradation of the solar cell efficiency (*Patel, 2005a*). Therefore in planning a space mission engineers will require a known method of predicting the expected cell degradation in the space radiation environment. Different kinds of cell technologies respond differently to irradiation depending on the materials used, the thickness of the active regions and the types and concentrations of dopant employed (*Bekhti, 2013*). Significantly, space solar cell degradations calculations can be done using the following (*Suparta and Zulkeple, 2015*):

- NASA Jet propulsion Laboratory equivalent fluence method;
- NAVAL Research Laboratory displacement damage dose “D_d” method;
- Nonionizing energy loss (*NIEL*); and
- SPENVIS implementation (*Walters et al., 2007*)

On the other hand, the logged data gotten from the nanosatellite in space can be used practically and physically to calculate solar cells degradation and to monitor the condition of photovoltaic modules in space during its lifetime. The contribution of this project to what has been already covered by other researchers will be to develop reconfigurable photovoltaic module architecture with integrated switches in a string photovoltaic system that gives each cell the capability to connect with other healthy solar cell of the module to fulfil the permanent loss caused by the degradation of a particular solar cell in the photovoltaic module. The solar cell’s connectivity will be achieved based on the result obtained from the solar cell degradation calculator program using the logged data.

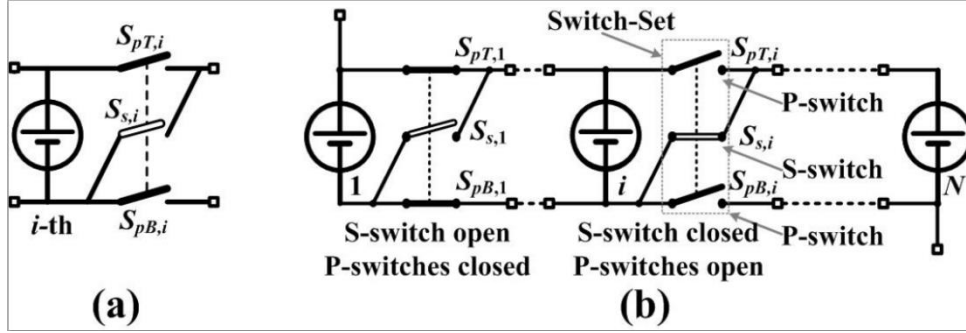


Figure 1.1: Schematic of an individual integrated power electronic switch (“reconfigurable-PV - CAD4X Laboratory,” n.d.)

1.2 Problem statement:

Like any other electrical devices, nanosatellites, which orbit in space, require electrical energy to perform its operation. The electrical energy required by the nanosatellites comes from the radiation of the sun. Thus, photovoltaic modules are used to generate, to store and distribute that energy (*“Comment les satellites transforment-ils l’énergie du soleil en électricité - Articles | Airbus Defence and Space,” n.d.*). Most often, nanosatellites use solar energy as primary energy to generate electrical power immediately. They are equipped with a solar generator system made of photovoltaic arrays which will directly convert the energy from the sun’s radiation into electrical energy. Together with photovoltaic arrays, nanosatellites have rechargeable batteries to store the produced electrical energy which will be in return used to power the nanosatellites when the photovoltaic arrays are unable to produce enough or the required power needed for the operation of the Nanosatellite due to variations of the time of the day, temperature and solar radiation (*Kim et al., 2013*). For nanosatellites where the charging and discharging process frequently takes place, the lifetime of their batteries is limited henceforth the nanosatellites lifetime as well. It is important to note that battery failure in a nanosatellite allows the nanosatellite to operate only when it receives the required power from the Photovoltaic arrays; this is process is known as direct energy transfer “DET”(Wertz and Larson, 1999). Even though the operation of the nanosatellite can be done using the Photovoltaic arrays after the battery fails, its operation depends on: the time of the day; the weather; and the condition of each individual cell available on the photovoltaic panels. Indeed, the operation of the nanosatellite also depends on the efficiency of the photovoltaic arrays at that particular

time. In reality, the efficiency of photovoltaic arrays decreases with time after the launch of the nanosatellite in space. The efficiency's change of the nanosatellites photovoltaic module will be observed based on the comparison of the results or logged data collected from the nanosatellites while orbiting in space and the expected results found by the engineers in the ground laboratory during the design and the testing of the nanosatellites before the launch process took place. The observed performance nonconformities can instantly take place due to catastrophic events for example. Under those circumstances, the performance loss can either be temporal or permanent. The temporal performance loss normally occurs during terrestrial application of photovoltaic arrays through the shading effects of the photovoltaic module. While the perpetual losses in performance rapidly happen during space missions through disintegration of the sun powered cells caused by the high radiation belts found in space by the nanosatellites during their missions.

With those highlighted factors in mind, the main idea of this research is to highlight how to ensure or increase the reliability efficiency of photovoltaic systems used to power the Nanosatellites as described above; when temporal or permanent loss occurs on the battery or the photovoltaic system due to high radiation effect faced by the nanosatellites used in space applications.

1.2 Objectives of the research work:

The objective of this research topic is to form an elastic photovoltaic structure module using a flexible switch array matrix integrated with the photovoltaic modules to solve temporal or permanent losses on each solar cell or bypass diodes when they fail. In other words, the reconfigurable photovoltaic module should be able to increase the reliability and efficiency of the photovoltaic module while solving the degradation of solar cells and bypass diodes due to high radiation belts for space applications. Certain objectives have been set to meet the required outcome of this Master of Engineering research project. The set objectives are listed below:

- Analyze the studies done on long-term monitoring data to determine degradation rates or the rate of change which is strongly influenced by the age and size of the selected systems;
- Implement an algorithm which will be used for data collection, data filtering, degradation analysis and finding the location of the faulty solar cell;

- Implement a fault bypassing algorithm which will determine the most favorable configuration of the healthy solar cell such that the photovoltaic system output power losses due to the faulty solar cell are minimized;
- Investigate the suitable power electronic switches that can be used to realize the switching matrix for space applications;
- Produce a built structure to facilitate and to encourage the design of a reconfigurable solar cells system for a nanosatellite; and
- Test of the built structure will be performed to verify and support the simulated results of the reconfigurable system during the simulation using the adequate software.

1.3 Research methodology:

The degradation of each solar cell of the photovoltaic module has to be observed at the first step, frequently the analysis of long-term monitoring data will be also done using the nanosatellites irradiance data, sensor calibration data and the system logs of the photovoltaic module.

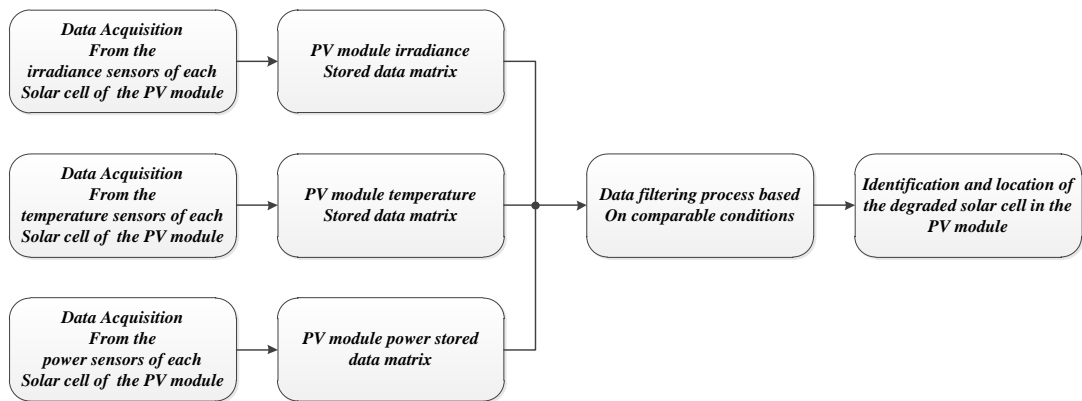


Figure 1.2: Long-term monitoring data of the photovoltaic module

Once the logged measurement data is available, some filtering will be required to obtain failure-free comparable conditions for every time we would like to check the performance of our system. This task will be done through an embedded program, which analyses the data and identifies the faulty stored data of the photovoltaic module made of multiple solar cells whose characteristics will represent an element of the stored data matrix. Now that, the data collection, data filtering, and degradation analysis have been completed; the information regarding the malfunctioning solar cell can be sent to the reconfiguration algorithm to determine the ON/OFF states of the single series switch

(S-switch) and the two parallel switches (P-switch) integrated in each solar cell of the photovoltaic module. The control of the ON/OFF power electronic integrated switches will be given in form of a flexible switch array matrix, which will facilitate the optimal configuration of the faulty or degraded solar cell to be isolated from those healthy solar cells available in the photovoltaic module for the maximum power output of the photovoltaic module.

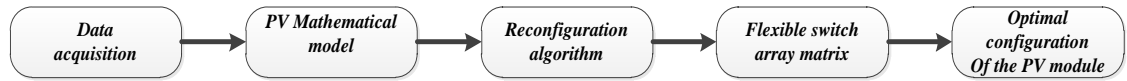


Figure 1.3: Block diagram of the reconfiguration scheme block

A model of the reconfigurable photovoltaic module system will be done to demonstrate the outcomes of this research project using Matlab-Simulink software environment. Matlab/Simulink environment has been chosen due to its powerful simpower systems toolbox. Further, the implementation of the switching matrix system will be realized using the switch block available in Simulink Library while a control system of those row and column switches has to be done using a two level Matlab function to implement the control scheme of the switches.

In our simulation and prototype process, the smart sensors used to measure logged data can be connected to a 10-bit analog to digital converter available on the Arduino or Raspberry Pi board. That board will then be connected to a computer running Labview so that one is able to create a user interface that will display the logged measurement data of each solar cell on the photovoltaic module.

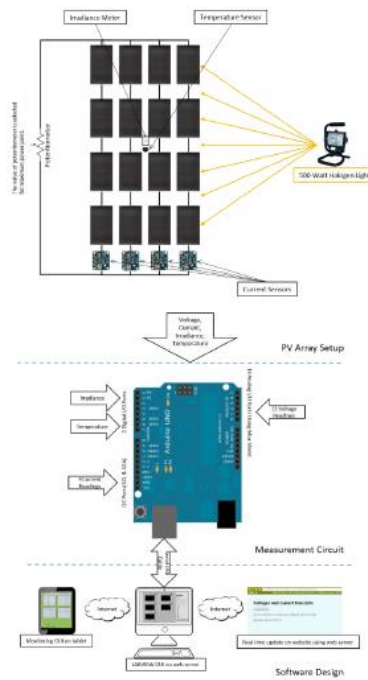


Figure 1.4: Solar cells long term monitoring

1.4 Delineation of study:

The study generated by my master of engineering research’s topic can be centred on the following:

- Nanosatellite’s electrical power system with solar cells system
- Modeling of a solar cell;
- Degradation rates of the single solar cell;
- Fault detection and reconfiguration of solar cells; and
- Implementation of an embedded board to monitor each single cell and optimize their arrangements so that we can operate at approximately a maximum power when some solar cells are faulty.

A built space-engineering prototype of the self-controlled embedded switching board has been designed and tested in the electrical and electronic laboratory available in the university. Based on the space mission analysis and design process, the developed board has to be exposed to various testing scenarios. Thus, the interpreted results were done based on the clear application of scientific and electrical engineering principles for space applications, nanosatellites technology, and advanced power electronic technology.

1.5 Literature study:

Indeed this section presents a well-structured piece of any research process which is frequently constructed from a collection of theory information about Robust nanosatellites, the power system of the nanosatellites, the space radiation effect on the nanosatellites components, the photovoltaic cells, the optimization of the solar cells system, the integrated Nano power electronic switches as well as the switch pattern used for its reconfiguration during the optimization process.

1.6 Simulation and Modelling:

Important to realize, the modelling of the reconfigurable solar cells system has been done based on the mathematical equations, which represent a solar cell. Each solar cell's current, voltage, temperature's values can be obtained by data acquisition system connected to a microchip, which will compute the controlling algorithm implemented in Matlab. Arduino and Raspberry Pi platform environment will be used to perform the data monitoring, data acquisition, data filtering, and fault-finding location. While, Matlab-Simulink will be able to use the result search of the fault-finding algorithm to allow the most favourable configuration of the solar cells, such that photovoltaic system output power loss due to faulty solar cells is minimized using the switching matrix scheme implemented in Simulink. Finally, the space environment information system “*SPENVIS*” will be used as an interface which models the space environment and its effects on the designed reconfigurable system. Truly, the modelling and the simulation of the reconfigurable solar cells system for nanosatellites is covered.

1.7 Thesis outline:

My Master of Engineering Research Project's thesis is structured as stated below:

- *Chapter 2*: An introduction to space technology products: nanosatellites.
- *Chapter 3*: A literature survey on the Photovoltaic energy systems.
- *Chapter 4*: Modeling Methodology for photovoltaic systems.
- *Chapter 5*: Photovoltaic system degradation in space applications.
- *Chapter 6*: A literature survey on reconfigurable photovoltaic systems.

- Chapter 7: Degradation fault detection algorithm and system optimization of Solar cells.
- Chapter 8: Simulation and results of the experimental setup of the proposed solar cells reconfigurable system.

Chapter 2: Nanosatellite's Electrical Power System

2.1 Background:

Based on the man-made satellite's records, one notes that Sputnik I, was the first launched and operated low earth orbit “**LEO**” satellite. After a number of years the American space exploration programs have launched many other Earth orbiting satellites. Consequently, the first manned spacecraft classified as the first commercial geosynchronous satellite was placed in orbit. From there, a huge number of countries in the world have successfully engraved their marks into small and large space innovative programs and businesses. As an illustration we do notice the French South African Institute of Technology in South Africa that runs a space program in the country. One of the benefits of the space program is that the satellite or space engineering system's researchers always contributes to the advancement of the space technology and science through the outcomes of their academic research program or work. Henceforth, today many countries in the world having operating satellites possess the capability of placing them in orbit. It is important to realize that up until the 30th June 2016, a total number of operating satellites came to a value of 1419 (***One thousand four hundred and nineteen***) active satellites in orbit(*tax, n.d.*). Among those satellites, which are still operating in orbit, one of them is known as the first South African launched and operating nanosatellite called ZACUBE-1 (TshepisoSat). The ZACUBE-1 is a student lead endeavour of the French South African Institute of Technology (“*ZACube-1 (TshepisoSAT) / AMSAT-NA,*” *n.d.*).

Moving from the design process to the successful launch of a built nanosatellite which can be used for space science and exploration always appears as an expensive endeavour, something out of reach for most universities and structures (*Bester et al., 2012*). After all, the introduction of the CubeSat design specification in 1999 by aerospace engineering Professor Jordi Puig Sauri from California Polytechnic State University and Professor Robert Twiggs from the department of Aeronautics and Astronautics at Stanford University changed the previous stated vision of those universities and structures (*Toorian et al., 2008*). A good reason of that project was to provide a standard for Picosatellites design which will reduce cost and development time, increase space's accessibility and sustain frequent launches. In fact, CubeSats are a class of research spacecraft called nanosatellites. They are built to standard dimensions or units “U”, for this reason we will have CubeSats built to standard dimensions of 1U

(10x10x10cm), 2U (20x10x10cm), 3U (30x10x10cm) with a weight restriction moving from 1.33Kg for a 1U CubeSat to 4Kg if it's a 3U CubeSat (*Loff, 2015*).

The vision of educational institutions and industries to invest or run space program is to expose humans to space science and innovative technology environment. Thus, students from Cape Peninsula University of Technology are encouraged to join the space program under the French South African Institute of Technology so that they can be exposed and familiarize themselves with satellite engineering systems environment. Through that given opportunity, students have been given chances to develop their skill and to receive some experience in real space applications. Some of the lineaments given by the space program based at the Cape Peninsula University of Technology are:

- A physical layout and design guidelines according to the international standard;
- Coordination of required documentation and export licenses; and
- Confirmation of successful deployment and telemetry information.

First thing to remember, all nanosatellites in orbit need electrical power to successfully operate and fulfil their allocated mission. Consequently, nanosatellites are equipped with an electrical power system that will generate, store, condition, control and distribute power within the specified voltage band to all bus and payload equipment (Patel, 2005a). This chapter will give us an overview of the nanosatellite's electrical power system together with a little breakdown of the stated system from the generation stage to the distribution stage.

2.2 Nanosatellites Electrical Power Systems:

Again, the electrical power system of a nanosatellite has the responsibility to generate, store, condition control and distribute electrical power to the various systems, which are parts of the nanosatellite. Currently, the on-going project at the space program of the Cape Peninsula University of Technology is about the design and the construction of a nanosatellite called Zacube-2 which will act as a pre-cursor mission to a constellation of nanosatellites that will be engineered by the state University of Technology ("*F'SATI*," *n.d.*). The on-going built product named Zacube-2 is a 3U cubesat which is apparently a follow up on a mission of the previous successfully launched cubesat known as zacube-1 ("*ZACUBE-2 - eoPortal Directory - Satellite*

Missions,” n.d.). The nanosatellite will act as technology demonstrator for essential subsystems and from the one which an innovative software define radio platform will be developed as primary payload (*“ZACUBE 2 (ZA 004) - Gunter’s Space Page - Gunter’s Space Page,” n.d.).*

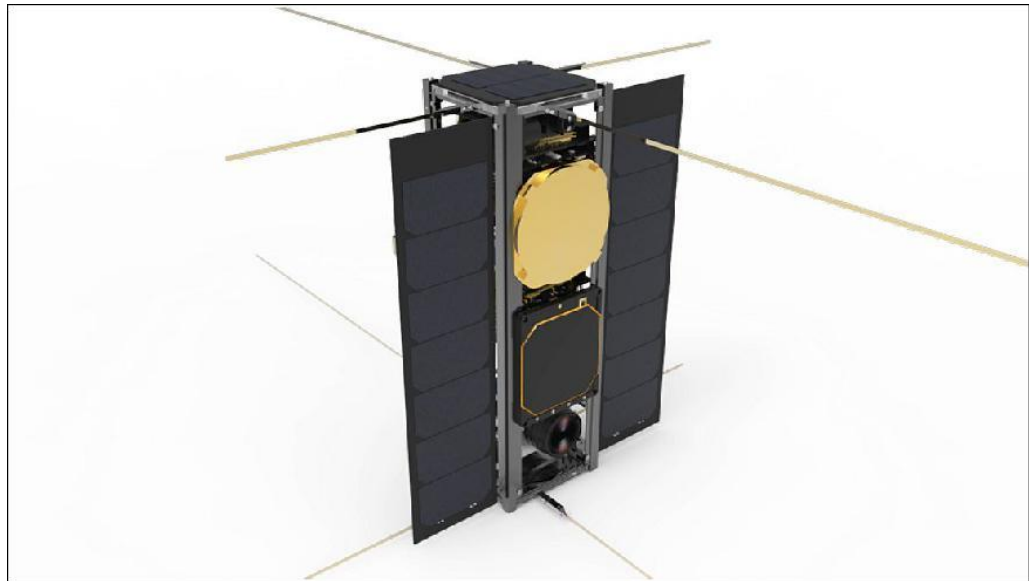


Figure 2.1: *Illustration of the 3U ZACUBE-2 nanosatellite layout (“ZACUBE-2 - eoPortal Directory - Satellite Missions,” n.d.)*

Another key point will be to highlight that the designed nanosatellite will desire a sun synchronous circular orbit of 600Km (*“ZACUBE-2 - eoPortal Directory - Satellite Missions,” n.d.).* Using that information, satellite engineers can predict the accurate or expected time when they can send or receive telemetry information to or from the nanosatellite orbiting in space; in other words they can be able to predict the visibility of the nanosatellite orbiting in space by the ground station available on the university campus.

2.2.1 Orbit trajectory modelling of Zacube-2 in space:

Due to many constraints related to the design and the development of spacecraft; AGI has developed a commercial modelling and analysis software for space, defence and intelligence communities. This will allow engineers and analysts to use STK model to model complex systems along with sensors and communications, in the context of the mission environment (*“Systems Tool Kit - Technology | Space Foundation,” n.d.).* Using some of the core capabilities of the stated software, we can be able to model the orbit trajectory of Zacube-2 in space for a sun synchronous circular orbit of 600Km as illustrated in the figure below:

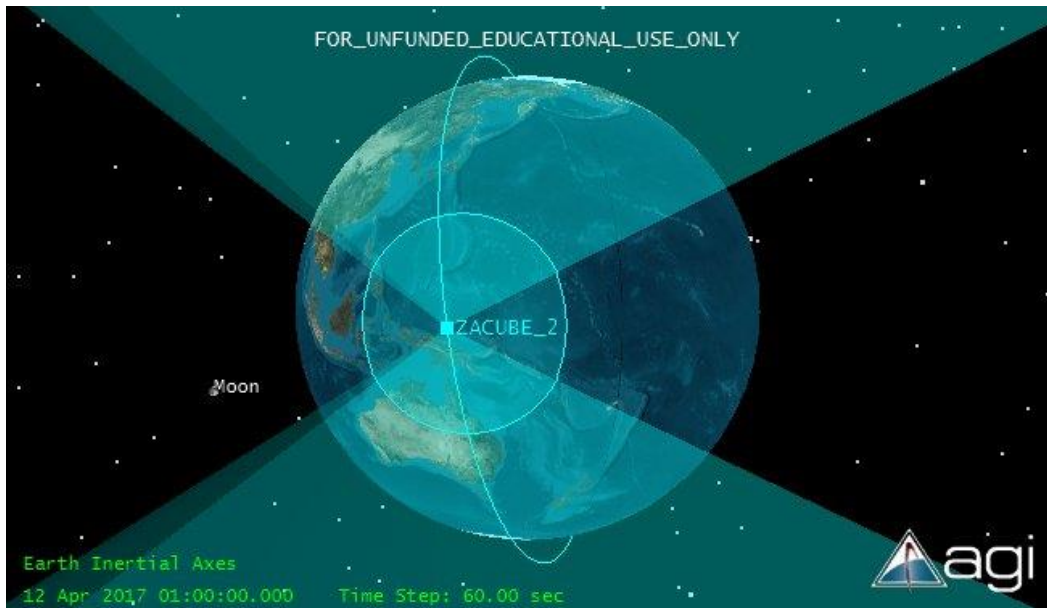


Figure 2.2: *Zacube-2's sun synchronous circular orbit trajectory of 600Km using STK10 software*

Furthermore, we can also model the ground track of the nanosatellite whereby the location of the nanosatellite's ground station will be identified as shown in the figure below:

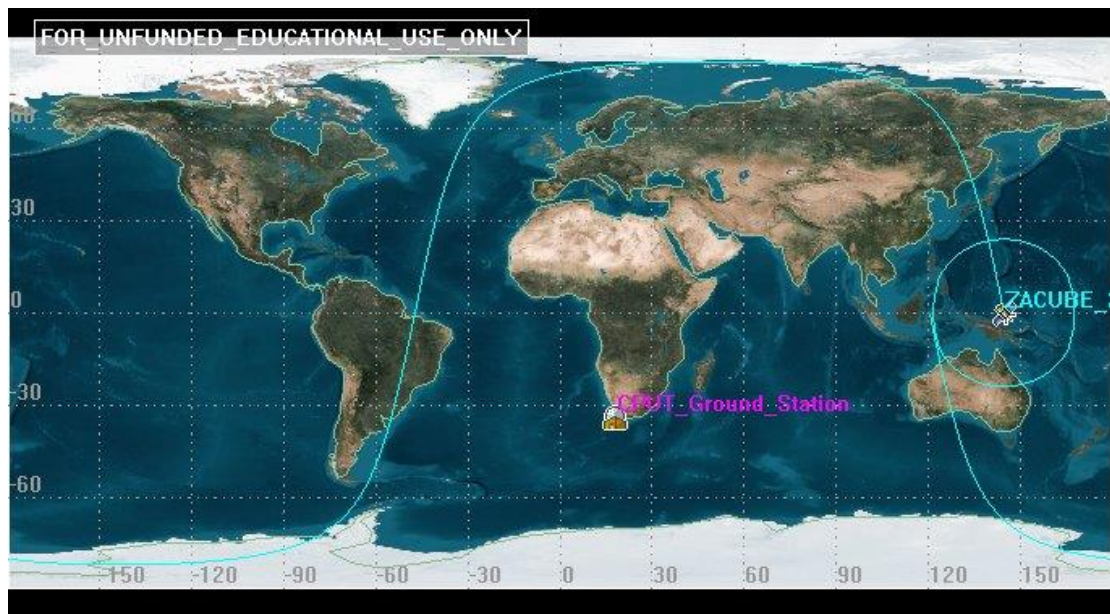


Figure 2.3: *Ground track of the nanosatellite Zacube_2 with the geographical position of its ground station*

In the case where the coordinates of the satellites ' S ' in its orbit is given and the geographical coordinates of the ground station T^* is known as well; both items will appear on the figure of the ground track of the nanosatellite. Through the system tool kit software, we can determine the moment when the nanosatellite is visible by its defined geographical ground station so that we can be able to establish a communication between the nanosatellite in space and the ground station located on the earth. We

- Telemetry reception and orbital restitution; and
- Reception of scientific data, images stored by the nanosatellite in space, coded information produced by the nanosatellite, etc.....

For those reasons, the conditions of visibility of the nanosatellite zacube-2 by the ground station at Cape Peninsula University of Technology has been determined using STK10 software and the result is shown in the figure below:

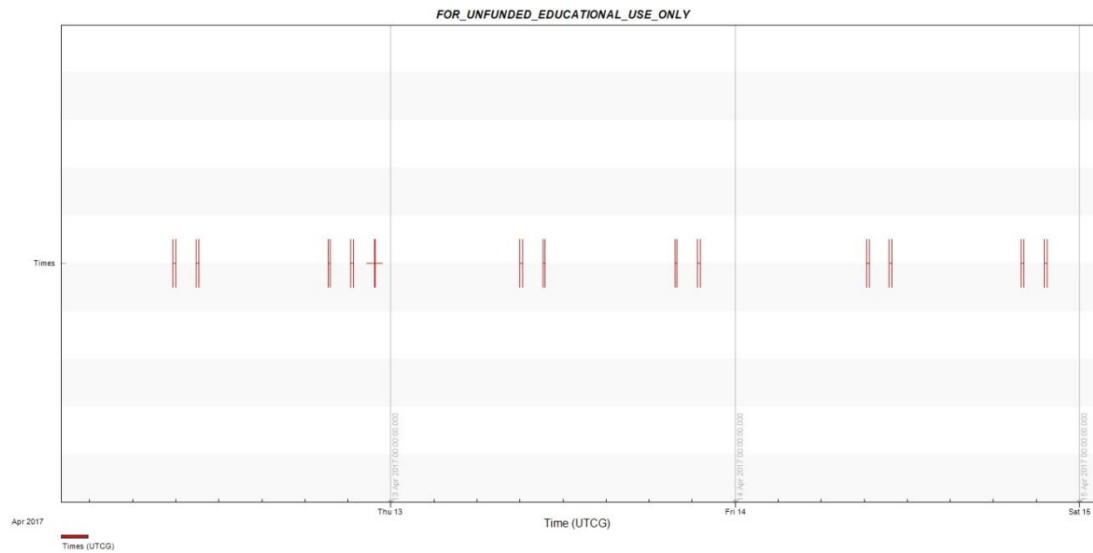


Figure 2.5: *Zacube-2 visibility over a period of 3 days using STK10 software*

It's shown on the image that the nanosatellite will be passing over the ground station at least 4 times a day; the duration of the passing period can be obtained by just zooming in the picture at a certain passing pulse as illustrated in the figure below:

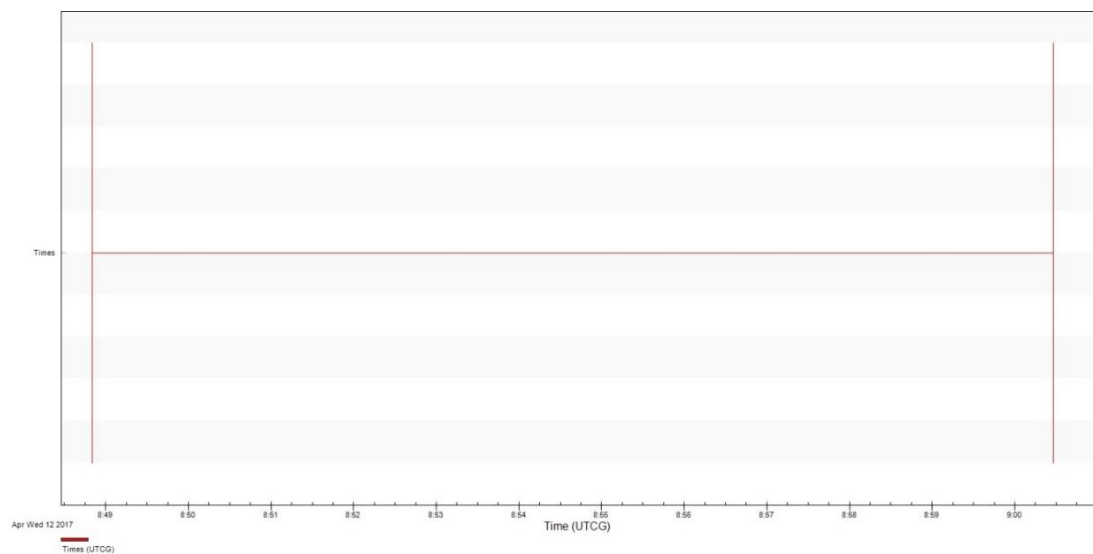


Figure 2.6: *Period of the nanosatellite visibility approximately equal to 11 minutes*

For the case of this research project, this period of visibility will be used to send a telemetry command from the ground station to the nanosatellite so that we can have or receive an updated data information regarding the health of the solar cells, power converters and the battery which have been mounted as part of the electrical power system of the nanosatellite Zacube-2. The received data will be analysed at the ground station level and in case of a failure (degradation of any solar cells) a ground station command will be sent in that visibility interval so that a change may occur in the reconfiguration of the remaining healthy solar cells available on the nanosatellite solar panels in orbit. The new reconfigurable scheme will allow the nanosatellite to have an optimized electrical solar generated power even though the presence of some faulty solar cells has been detected. Consequently, we can still be able to have communication with the nanosatellite and reconfigure its electrical power system so that some of the subsystems or payload can operate instead of having a total failure or death of the nanosatellite related to the failure of a particular subsystem or component. Thus, redundancy and reliability of the subsystem available on the nanosatellite will be subject to modification and therefore will assist on solving problems due to the limitation of space available on the spacecraft where spare subsystem can't be mounted in case we would like to back up any subsystem's failure in the orbit.

Sending a telemetry command to reconfigure the photovoltaic cells available on the nanosatellite is an alternative way in case the design embedded reconfigurable system is a self or remote control system through a telemetry command signal. In reality, the telemetry command scheme will involve extra components and a human capability to establish a communication between the nanosatellite and the station, to analyse the data and to implement the reconfiguration of the system. The presence of all those extra parties will bring up the benefit of the doubt regarding the reliability and the efficiency of the overall or entire whole system. For the purpose of this research project, the reliability of the entire designed embedded system will be achieved by giving the capability to the system to operate all by itself without reception of any telemetry command coming from the ground station.

2.2.2 General overview of Zacube-2 mounted subsystems:

A nanosatellite is formed by different systems designed to adhere to the specific criteria of a particular defined mission. Two groups can be used to classify the common set and additional systems of a nanosatellite as described below (*Patel, 2005a*):

- The payload: all the communication equipment available in the nanosatellite will form this classification group.
- The nanosatellite bus: formed by all remaining equipment having different functionalities used to support the payload.

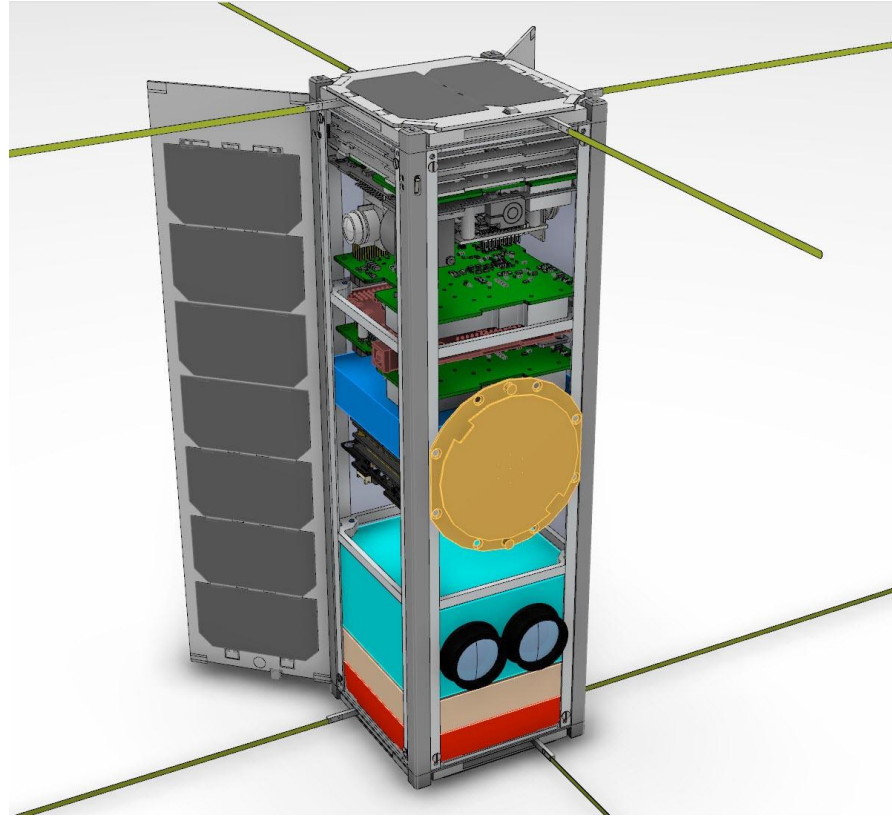


Figure 2.7: Conceptual Layout of the nanosatellite Zacube-2 (“ZAcube-2 schematics - Google Search,” n.d.)

One of the nanosatellite bus systems is known as the power system, which has: the solar arrays, the battery, power electronics, distribution harness and controls. Furthermore, the communications and data handling system to receive commands and return information, telemetry sensors to gage the nanosatellite state, a central computer to coordinate and control activities of all systems are also known as other essential nanosatellite bus systems (*Patel, 2005a*).

The common set and additional systems of a nanosatellite as discussed in the previous paragraphs compiled in a form of block diagram will be shown in the figure below:

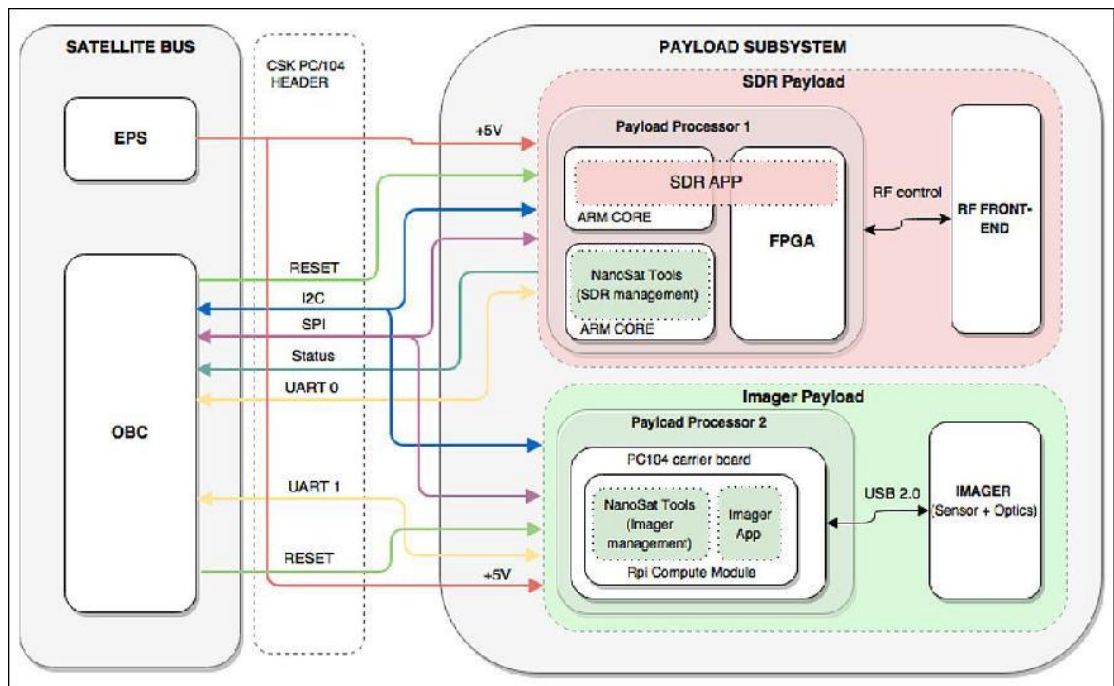


Figure 2.8: An overview of the systems mounted on the nanosatellite Zacube-2 (“Image,” n.d.)

We can clearly notice that the nanosatellite bus system block and the Payload subsystem block are connected to the Electrical power supply block. Thus, the reliability and the efficiency of the electrical power supply needs some improvement so that even in case of degradation of solar cells due to the harsh radiation effect in space some components of the payload subsystem must be powered to allow a partial operation of the nanosatellite in space which is way better that a complete shutdown of the nanosatellite due to some degraded solar cells available on its solar panels.

Chapter 3: A literature survey on the photovoltaic energy systems

3.1 Introduction:

Space has a massive impact on our daily lives and it's one of the major facilitator of the global economy. Consequences of research into space can be highlighted through the given amazing understanding of our universe and the forces that govern it which directly have an effect on our lives on Earth. Moreover, space exploration has extended the envelope of human knowledge and presence throughout the solar energy system. Energy has a very important role in the socioeconomic growth and energy security of a country (*Kumar, 2017*). Since the journey of research into space has started, we can notice the launch of many satellites across the global world. Generally, most of those launched satellites have used the sun's energy as their primary source of electrical power for the spacecraft (*Mac Kenzie, 1967*). An energy resource that can be replaced or renewed rapidly by natural processes is known as a renewable energy or renewable energy source ("*Renewable energy,*" *n.d.*). As an illustration, sunlight, wind power, hydropower, geothermal, biomass, and tides are found among the list of the most important types of renewable energy sources. Looking over the past few decades, we can notice the massive promotion and special attention given to the solar energy system among the above list of renewable energy sources.

In detail, it's the radiant heat and light from the sun, which can be harvested through a number of means like solar thermal, solar photovoltaic, and photosynthesis technologies. Surely, solar photovoltaic also called solar cell does the conversion from solar energy into electricity which can be exploited in all different ways according to their different needs (*Kumar, 2017*). Seeing that nanosatellites are solar powered devices, the reduction of greenhouse gases will be observed. Considering just solar cells as a complete solution of power generation in space will not be sufficient due to the fact that the production of electricity can only be made only if the solar cells are illuminated therefore an energy storage unit needs to be attached the solar power system to improve the efficiency and the reliability of the solar power system (*Mac Kenzie, 1967*).

Now that we have realized a growth of photovoltaic devices and technologies in world, we can say that everybody can generate its own power independently at low operating cost and virtually pollution free. Indeed, solar photovoltaic technology do operate on the principle of the photovoltaic effect (*Kumar, 2017*).

3.2 Photovoltaic effect in the solar cells:

Generation of a voltage or electric current in a material or a device upon illumination of light is known as the photovoltaic effect (*Kumar, 2017*). The photovoltaic effect was first observed in 1839 by French physicist Edmund Becquerel when he found that shining light on an electrode submerged in a conductive solution would create an electric current (*"How do Photovoltaics Work? | Science Mission Directorate," n.d.*). Later in 1873, W.Smith discovered photoconductivity in selenium and then this gave birth to photovoltaic technology. The devices that exhibit photovoltaic effect are known as photovoltaic devices or solar cells (*Stöckmann, 1973*).

In fact, the photovoltaic effect appears in the semiconductor devices where exposure to light causes the photons to get absorbed in the semiconducting material that excites electrons from the valance band to the conduction band. Such electrons in the conduction band are known as electrons, and they leave behind the corresponding holes in the valance band. These electrons and holes need to be extracted out to get electricity (*"Photovoltaic effect - Energy Education," n.d.*). Due to opposite charge electrons (negatively charged) and the holes (positively charged), they have the tendency of recombination, which should be prevented. The solar cells are designed and prepared in a way that the photo generated electrons and holes move in opposite directions via drift and diffusion processes and get collected there. A solar cell possesses two electrodes with the light –absorbing medium sandwiched between them. Collection of photo generated charge carriers on the electrodes in opposite sides of the semiconductor causes an electromotive force; a photovoltage is developed across the device. If an electronic circuit is connected to the device, an electric current would pass through the circuit and this way the light energy gets converted into electricity. The drift is provided by built in electric field, whereas diffusion is caused by the concentration gradient of the photo generated charge carriers. If the energy of incident photons is less than the band gap of the semiconductor, the photons will not be absorbed and no photovoltaic effect will be observed (*Kumar, 2017*).

3.3 Solar cells and their Generations:

Photovoltaic cells have been created for more than hundred years ago; on the negative side we can highlight their poor actual efficiency. The first solid state solar cell was prepared by Charles Fritts in 1883, when he coated a thin film of gold over the selenium semiconductor to form a junction and got around 1% power conversion

efficiency. Due to the non-successful experiments performed on the selenium solar cells, more experiments were performed on other materials and this gave birth to the next generations of solar cells (*Kumar, 2017*).

3.3.1 First Generation of solar cells:

Monocrystalline silicon solar cells, Polycrystalline silicon solar cells, amorphous silicon solar cells and Hybrid silicon solar cells were the first generation of solar cells. These solar cells are also known as conventional, traditional solar cells made from Silicon (*"3 Generations of Solar Cells," n.d.*). In particular, monocrystalline silicon solar cells, polycrystalline silicon solar cells, had a fairly high performance, which made them a reliable source of electricity generation for satellites and space vehicles with a very high operating cost compared to their power out. Due to an expensive cost and complex fabrication processes of these solar cells, the need of giving birth to their next generations took place (*Kumar, 2017*).

3.3.2 Second Generation of solar cells:

For cost effective solar cell technology, new processes and materials were developed which included amorphous Silicon (a-Si) solar cells, copper indium gallium diselenide (CIGS) solar cells, and cadmium telluride (CdTe) solar cells (*Kumar, 2017*). These materials are processed in thin films and the solar cells made of these materials are also known as thin-film solar cells because when compared to the first generation of silicon solar cells they are made from layers of semiconductor materials only a few micrometres thick (*"3 Generations of Solar Cells," n.d.*). These solar cells embody a small amount of active materials and are developed on inexpensive substrates like glass and plastic; they can be easily operated in the large area and when processed on plastic substrates, they can be fabricated roll to roll with ease (*Kumar, 2017*). Comparing these second generation to the first generation solar cells regarding efficiency and cost: one can bring out the fact that the second generation solar cells are less efficient than the crystalline silicon solar cells.

3.3.3 Third Generation of solar cells:

The third generation of solar cells includes multijunction solar cells and emerging photovoltaic technologies like: (*"Types of Solar Cells - Generation of Solar Cells," 2015*)

- Dye-sensitized solar cell (DSSC): is another class of thin-film solar cells that is based on organic dyes. They are quite thin, lightweight, and can be processed at low temperatures on non-expensive substrates like glass, plastic and metal foils. Low cost processing and inexpensive materials make these cells very cost effective (*Kumar, 2017*);
- Organic solar cell (OSC): is solid-state thin film solar cells based on organic semiconductors. Organic semiconductors are special class of aromatic hydrocarbons where carbon atoms are sp^2 hybridized and have alternate single and double bonds. Due to alteration in single and double bonds among C atoms these materials are also known as conjugated semiconductors. In general, these are insulators in pure form; they are called semiconductors because their electrical conductivity increases exponentially with temperature and some others properties like band gap are similar to those of their inorganic semiconductors. Alteration of single and double bonds is responsible for the conductivity in these materials (*Kumar, 2017*);
- Quantum dot solar cell (QDSC): is another solar cells technology based on the concept of minimization of energy loss using semiconductors of different band gaps like planer multijunction cells but with better tenability across the solar spectrum and ease in production (*Kumar, 2017*);
- Multijunction solar cells: based on III-V compound semiconductors like gallium arsenide (GaAs), gallium antimonide (GaSb), and indium phosphide (InP) were also observed to have excellent optical and electrical properties making them potential candidates for solar cells applications. They possessed very high optical absorption coefficients and absorbed most of the incident light within few micrometers. In the 1980s, GaAs-based solar cells surpassed Silicon solar cells efficiency and in 1990s took them over for satellite applications. GaAs-based single-crystal single-junction thin-film solar cells hold the record maximum efficiency of 28.8%, which has remained unchanged since early 1990s. Furthermore, experiments have been done to improve the efficiency of solar cells. This paved a path to develop a GaInP/GaAs/Ge triple junction solar cell, where the GaInP₂/GaAs junction was grown on a Ge substrate and the device exhibited 34.1% efficiency. In 2012, Agui et al achieved 36.9% efficiency in a GaInP/GaAs/GaInAs triple-junction solar cell. The triple junction solar cells hold the current maximum efficiency of 37.9% without any concentrator. Multijunction solar cells are the only third generation solar cells

that are commercially available. They are highly efficient and hold the world records in performance, but these solar cells are very expensive and are being used in satellites and other terrestrial applications only (*Kumar, 2017*).

3.3.4 Fourth Generation of solar cells:

The fourth generation of solar cells is quite futuristic and is expected to have very high power conversion efficiency. They can be prepared in a large area with great ease like Dye-sensitized solar cells and Organic solar cells. In addition, high power conversion efficiency would make them potential candidates for future power generation. The fourth generation solar cell includes the organic-inorganic hybrid and organometal halide perovskite solar cells (*Imalka Jayawardena et al., 2013*).

3.4 Performance analysis of a solar cell:

3.4.1 Solar spectrum and Irradiance:

Several galaxies and numerous stars are the elements of the universe. Every star together with all objects traveling around a star constitutes a solar system (*"Our Solar System - Overview | Planets," n.d.*). Our solar system is made of the sun, nine planets and their natural satellites, dwarf planets, asteroids, and comets. Due to the fact that a solar system is formed by a star and its objects: the sun in this particular system will be the star of our solar system and it is located in the centre with all other objects circling around it. The sun is an abundant source of energy, which originates from nuclear fusion reaction through a series of proton-proton chains where hydrogen is converted into Helium. The temperature of the outer surface of the sun is about 5778 °K.

The solar intensity at the mean distance from the Earth is about 1361 W/m² and is known as solar constant (*Kumar, 2017*). The solar radiation outside the earth's atmosphere is referred as air mass zero (AM0), meaning no atmosphere and no deflection from the original solar spectrum. This spectrum can be equated to that of a black body at 5800 °K. This spectrum is important for the performance analysis of satellite and space-vehicle solar cells (*"Layers of the Sun," 2015*).

3.4.2 Power conversion efficiency:

The percentage of the solar energy shining on top of a solar cell surface that is transformed into useful electricity is seen as the power conversion efficiency of the

particular solar cell ("*Solar Performance and Efficiency*," n.d.). In general, two essential steps contribute to the photovoltaic energy conversion in solar cells known as:

- Firstly, the absorption of light generates an electron-hole pair. The electron and hole are then separated by the structure of the device. Electrons to the negative terminal and holes to the positive terminal, thus the generation of electrical power is made (*Markvart and Castañer, 2003*).

If there is a connected load across the two electrodes or the two terminals, one will notice a flow of an electric current passing through the connected load. In cases where there is no load connected across the terminals of the solar cell or the solar cell is in the open circuit condition state, the potential difference established across the two terminals of the solar cell under illumination is called an open-circuit voltage (V_{oc}). In this case, there will not be a current deriving from the solar cell.

Considering the scenario where the two terminals of the illuminated solar cell are short circuited, a flow of an electric current would pass through the short circuited junction and this would be the maximum possible current that could be established from the illuminated solar cell at a particular given light intensity. The value of that measured current through the short circuit condition is recognized as the short-circuit current (I_{sc}). It is highlighted that during the short-circuit condition, the voltage across the terminal of the illuminated the solar cell will take the value of Zero volts. Comparing the load condition parameters with the open circuit parameters, the current and voltage across the load would be less than I_{sc} and V_{oc} .

The determination of the power conversion efficiency of a particular solar cell has a major role in terms of knowing the maximum electrical generated power given to the load that is connected across the terminals of the solar cell, henceforth the current-voltage characteristic represented by the (I - V) characteristics of the solar cell are measured while the solar cell is illuminated.

The measurement of the stated I-V characteristics can be achieved using the following step:

- Using a source measure unit as an alternate of the load, where a range of voltage from negative to positive values is applied and the corresponding current through the cell is measured and recorded (*Kumar, 2017*).

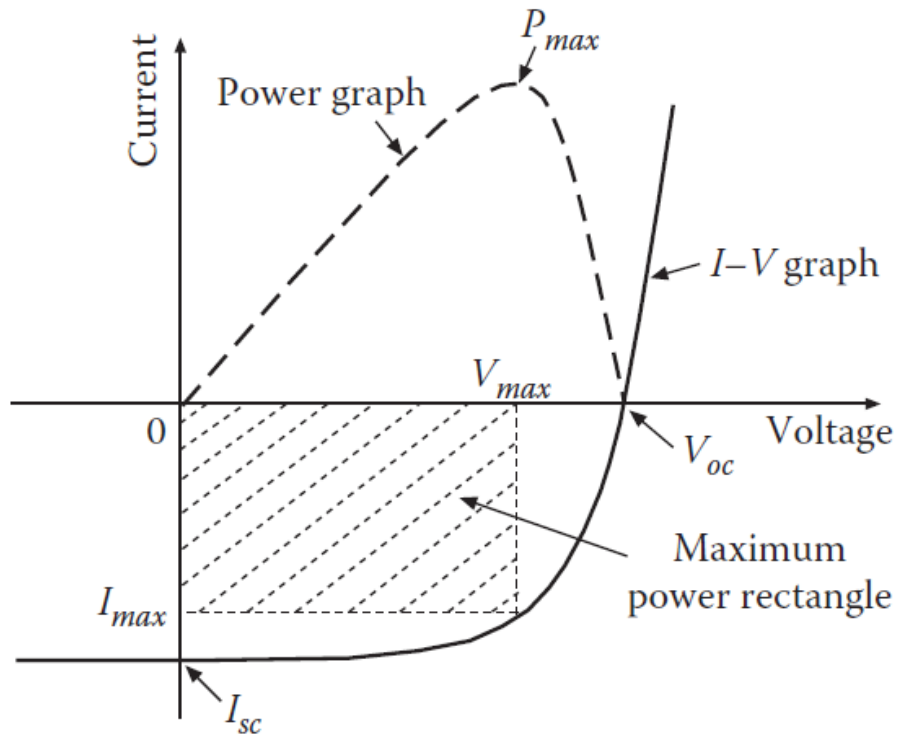


Figure 3.1: I-V characteristics of a solar cell under illumination (Solid curve). Dashed curve represents the corresponding inverted power graph (Kumar, 2017)

The point corresponding to the maximum value on the power graph represents the maximum electrical power derived from the solar cell known as:

$$P_{max} = I_{max} \times V_{max} \quad (\text{Equation 2})$$

Thus, the power conversion efficiency noted (η) of the illuminated solar cell can be calculated using the equation given below:

$$\eta = \frac{P_{max}}{P_{in}} = \frac{I_{max} \times V_{max}}{P_{in}} \quad (\text{Equation 3})$$

Where:

P_{in} : is the value of the incident optical power in Watts (W)

The fill factor is basically defined as the ratio of P_{max} over (I_{sc} multiply by V_{oc}), it can be expressed as:

$$FF = \frac{I_{max} \times V_{max}}{I_{sc} \times V_{oc}} \quad (\text{Equation 4})$$

Practically, the fill factor is the measure of the solar cell quality and defines the shape of the characteristics. A mathematical insertion of equation 2 and 3 into the first formula of the power conversion efficiency of a solar cell will lead to the equation written below as:

$$\eta = \frac{I_{sc} \times V_{oc} \times FF}{P_{in}} \quad (\text{Equation 5})$$

Using a percentage notation, the power conversion efficiency of a solar cell in percentage can be determined using the equation below:

$$\eta = \frac{I_{sc} \times V_{oc} \times FF}{P_{in}} \times 100 \quad (\text{Equation 6})$$

A non-necessity for the laws of the physics to behave in the same way on all components, based on the simple fact that solar cells are made from multiple device architectures. Henceforth, we end up having different types of solar cell generation. Thus, each and every type of solar cell needs to be investigated separately regarding the solar cell's type. Important to realize that a p-n junction solar cell is actually a p-n junction diode, and application of a voltage would cause a current flow through the junction even when the cell is not illuminated (*Kumar, 2017*). Thus, the dark current (I_D) will be the name of the measured current in that case. During the current-voltage measurement under illumination along with the photo-generated current; a dark current also circulates. That parameter should always be considered while looking at the actual value of the photo generated current (*Adamo et al., n.d.*).

Considering an ideal p-n junction diode, the value of the dark current is calculated using the equation below:

$$I_D = I_s \left(\exp^{(qV)/(K_B T)} - 1 \right) \quad (\text{Equation 7})$$

Where: $\begin{cases} I_s = \text{is the reverse saturation current of the diode} \\ q = \text{is the elementary charge} \\ K_B = \text{is the Boltzmann constant} \\ T = \text{is the absolute temperature of the diode} \end{cases}$

The negative photocurrent is obtained due to the flow of photo generated electrons and holes that constitute the photocurrent. Photo generated electrons and holes have to move toward the cathode and the anode, which leads to a flow of the photocurrent from the N-type to the P-type across the junction. An ideal p-n junction will possess no recombination losses and the short circuit current will be same as the photocurrent's value I_L . In reverse bias both dark current and photocurrent will be negative, while the forward bias case will have a positive value of the dark current with a negative photocurrent. Consequently, the total current will decrease until it becomes zero at open circuit voltage value where both the dark current and the photocurrent are at the same amplitude. The value of the total current (I_{Total}) circulating in the solar cell under illumination can be expressed as shown in the equation below (Kumar, 2017):

$$I_{Total} = I_s \left(\exp^{(qV)/(K_B T)} - 1 \right) - I_L \quad (\text{Equation 8})$$

During the short-circuit case (when we have: $V=0$), the expression of the total current through the cell would have the following terms:

$$I_{Total} = I_{sc} = -I_L \quad (\text{Equation 9})$$

Through the open-circuit condition (when we have: $I_{Total}=0$), the voltage across the solar cell known as V_{oc} , will be calculated by:

$$V_{oc} = \frac{K_B T}{q} \times \ln \left(\frac{I_L}{I_s} + 1 \right) \approx \frac{K_B T}{q} \times \ln \left(\frac{I_L}{I_s} \right) \quad (\text{Equation 10})$$

Practically the charge's extraction from a solar cell is obstructed by some parameters and therefore produces the recombination of charge carriers. Some amount of resistivity is surely into all semiconductors which restraint the extraction of charges. Furthermore, the defects in the film and energy barriers at contacts would obstruct the extraction of the charge. All the components responsible for the interruption to the extraction of the charges are characterized by a resistance connected in series (R_s) with the diode. While the recombination of charge carriers is characterized by: shunting the diode with a resistance connected in parallel (R_p). Like all electrical device or component, a solar cell can be model by the equivalent circuit shown in figure 3.2 (Khaligh and Onar, 2010):

Equivalent circuit of a solar cell using PSIM

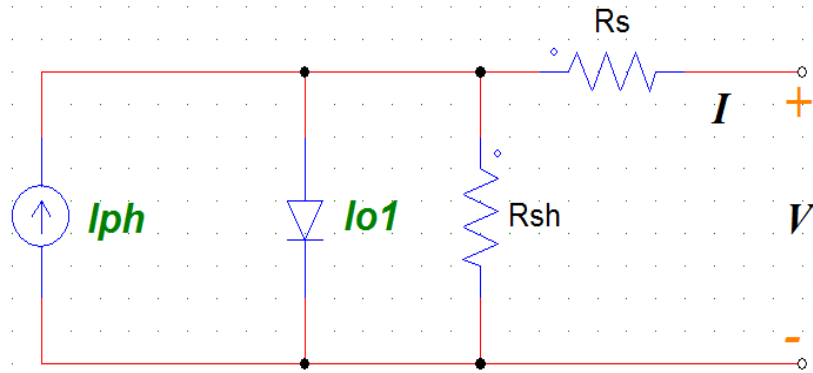


Figure 3.2: Equivalent circuit of a p-n junction solar cell illumination (Single-diode model)

Thus, the total current can be expressed as shown by the equation below:

$$I_{Total} = I_s \left(\exp\left(\frac{qV - IR_s}{nK_B T}\right) - 1 \right) + \left(\frac{V - IR_s}{R_p} \right) - I_L \quad (\text{Equation 11})$$

Where:

n = is the ideality factor of the diode

Identically, the mathematical model of a solar cell can be done adding the parameters that are capable of influencing the behaviour of the solar cell. The parameters listed below are those ones, which can influence the behaviour of a particular solar cell:

- Intensity of the incident light;
- Operative absolute temperature; and
- Degradation by cosmic radiation.

Considering all those factors, the new equivalent circuit of a solar cell can be drawn in figure 3.3:

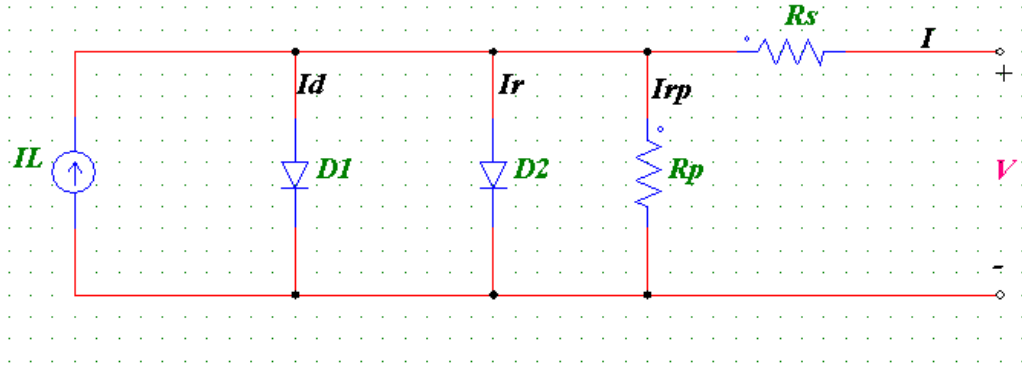


Figure 3.3: Equivalent circuit of a p-n junction solar cell illumination using two diodes

The new drawn model is seen as an alternative model of solar cell called the dual-diode model of a solar cell. The output current (I) of the dual-diode model will be found using the expression below:

$$I = I_L - I_d \left(\exp\left(\frac{(q \times (V - IR_s))}{(k_B T)}\right) - 1 \right) - I_r \left(\exp\left(\frac{(q \times (V - IR_s))}{(2k_B T)}\right) - 1 \right) - \left(\frac{V - IR_s}{R_p} \right) \quad (\text{Equation 12})$$

Chapter 4: Modelling of solar cells for space photovoltaic energy systems

4.1 Introduction:

The foundation of science relies in creating models, which will represent physical experience. In other words, the object of the study's representation is a model. Additionally, models can bring observations and understanding about the object or the case being investigated and form some predictions regarding its performance. Then its accuracy can be evaluated through its capability to predict but its efficiency will rely upon the simplicity and its disposition of bringing out the observation and the understanding of the studied case. After all, it's natural that the same object or case studied may obtain different models based on the calculation procedure, the accuracy and the number of parameters involved during the modelling process to also satisfy different point of interest. The use of experimental data to design mathematical models for dynamical systems is the purpose of system identification (*Ljung, 1998*). Whereby a system will be defined as a process where different variables interact, producing observable signals, which are called outputs. External signals shaped by the observer can often influence the system. Luckily, system identification handles dynamical systems which are processes whose current outputs parameters do not only depend on the current inputs parameters but also on its previous state (*Galrinho, 2016*).

Due to the fair advantages in autonomous systems, the use of space photovoltaic devices has increased. In articles, several mathematical models have been drawn to illustrate the operation and principle behaviour of a solar cell. Based on the natural fact that a same studied case can have different models, we will say that all those models drawn in the articles do differ in calculation method, accuracy and the number of parameters involved during the calculation process.

4.2 Solar Cell Modelling:

Considering the various ways of extracting the equivalent circuit parameters of a solar cell relying on the types of available information regarding the photovoltaic system or solar cell. The elaborated list will come down with the following listed models:

- Ideal model of a single junction solar cell;
- Two diode single junction solar cell model;
- Power model of a single junction solar cell; and
- General model for a space triple junction solar cell.

4.2.1 Ideal Model of a Single junction Solar Cell:

Using a diode and current source, we can actually design a reduced equivalent circuit of a single junction solar cell as illustrated in figure 4.1:

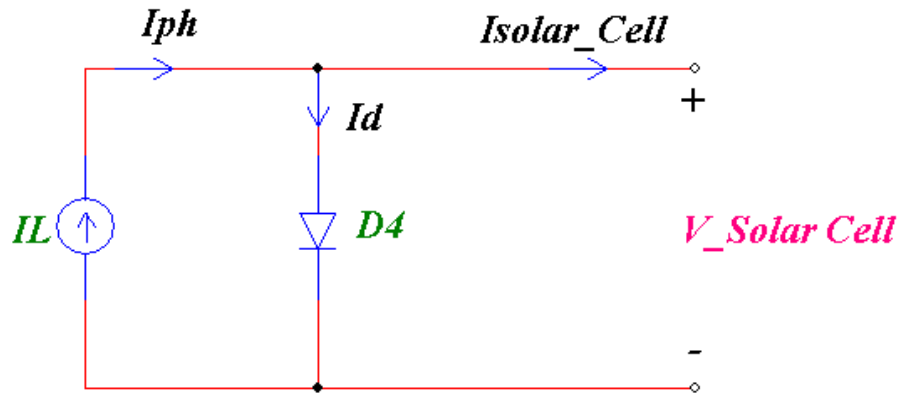


Figure 4.1: Simplified equivalent circuit of a single junction Solar cell

In this reduced equivalent circuit, we have to notice that the photocurrent I_{ph} is generated by the current source element. Comparatively, the value of the produced photo current is immediately proportional to the solar irradiance falling on the surface of the solar cell. The solar irradiance G is defined as the amount of light energy from one thing hitting a square meter of another each second (Zell, 2015). Frequently, solar cell's manufacturer will use the short-circuit current parameter and the open voltage parameter to describe the performance of a solar cell. Through the simplified equivalent circuit of a single junction solar cell, mathematically the expression of the current flowing at the terminal of the solar cell will be given by the equation below:

$$I_{solar_cell} = I_{photocurrent} - I_d \quad (\text{Equation 13})$$

Where:

$$I_d = I_o \times \left[e^{\left(\frac{V_{solar_cell}}{V_T}\right)} - 1 \right] \quad (\text{Equation 14})$$

With:

$$\left\{ \begin{array}{l} I_d = \text{is the current shunted through the intrinsic diode} \\ I_o = \text{is the reverse saturation current of the diode in Amperes} \\ V_T = \text{is the thermal potential} = \frac{(A.K.T_j)}{q} \\ A = \text{is the diode ideality factor} \\ K = \text{is the Boltzmann's constant} = 1.381 \times 10^{-23} \frac{J}{K} \\ T_j = \text{is the junction temperature of the solar cell in degrees Kelvin} \\ q = \text{is the electron charge} = 1.602 \times 10^{-19} C \end{array} \right.$$

Therefore:

$$I_d = I_o \times \left[e^{\left(\frac{q \times V_{solar_cell}}{A.K.T_j} \right)} - 1 \right] \quad (\text{Equation 15})$$

Thus, a substitution of the current shunted flowing through the intrinsic diode in equation 1 will give:

$$I_{solar_cell} = I_{photocurrent} - \left\{ I_o \times \left[e^{\left(\frac{q \times V_{solar_cell}}{A.K.T_j} \right)} - 1 \right] \right\} \quad (\text{Equation 16})$$

Seeing that the photocurrent is equal to the short-circuit current of the solar cell, the solar cell's current can have the expression below:

$$I_{solar_cell} = I_{short_circuit} - \left\{ I_o \times \left[e^{\left(\frac{q \times V_{solar_cell}}{A.K.T_j} \right)} - 1 \right] \right\} \quad (\text{Equation 17})$$

$$I_{solar_cell} = I_{sc} - \left\{ I_o \times \left[e^{\left(\frac{q \times V_{solar_cell}}{A.K.T_j} \right)} - 1 \right] \right\} \quad (\text{Equation 18})$$

By setting both the current flowing through the terminal of the solar cell equal to zero and the voltage across the terminal of the solar cell equals to the open circuit voltage of the solar cell, we can be able to get the expression of the reverse saturation I_o as shown below:

$$I_{solar_cell} = I_{photocurrent} - \left\{ I_o \times \left[e^{\left(\frac{q \times V_{solar_cell}}{A.K.T_j} \right)} - 1 \right] \right\} = 0 \quad (\text{Equation 19})$$

$$I_{photocurrent} - \left\{ I_o \times \left[e^{\left(\frac{q \times V_{open_circuit}}{A.K.T_j} \right)} - 1 \right] \right\} = 0 \quad (\text{Equation 20})$$

$$I_o = \frac{I_{photocurrent}}{\left[e^{\left(\frac{q \times V_{open_circuit}}{A.K.T_j} \right)} - 1 \right]} = \frac{I_{short_circuit}}{\left[e^{\left(\frac{q \times V_{open_circuit}}{A.K.T_j} \right)} - 1 \right]} \quad (\text{Equation 21})$$

Putting it on another way, the short-circuit current can be expressed as a function of the illuminated area as shown below:

$$I_{short_circuit} = I_{sc} = Area \times J_{sc} \quad (Equation\ 22)$$

In case we are interested about working out the value of the open circuit voltage, we can have it using the expression below:

$$V_{open_circuit} = V_{oc} = V_T \times \ln\left(1 + \frac{I_{sc}}{I_o}\right) \quad (Equation\ 23)$$

Surely using the current-voltage characteristic of an illuminated solar cell, the maximum output power of the solar cell can be obtained as well as the fill factor of the solar cell via the equation given below:

$$MPPT = P_{max} = I_{max} \times V_{max} \quad (Equation\ 24)$$

$$Fill\ Factor = FF = \frac{I_{max} \times V_{max}}{I_{oc} \times V_{oc}} \quad (Equation\ 25)$$

4.2.1.1 Single diode Model of a Single junction Solar Cell with Ohmic losses:

An implementation can be brought to the simplified equivalent circuit of a single junction solar cell drawn in the previous section whereby the material resistivity and the ohmic losses due to levels of contact are taken into consideration during the modelling of the solar cell. The sum of the losses generated by those elaborated factors will be characterized by a resistance R_s , connected in series in the simplified equivalent circuit of the single junction solar cell as shown in figure 4.2:

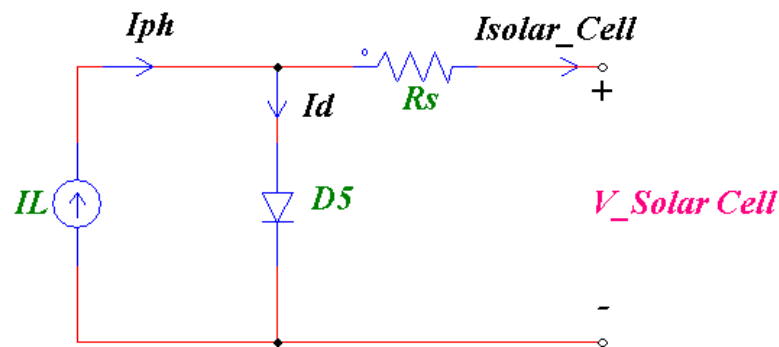


Figure 4.2: Simplified equivalent circuit of a single junction solar cell with Ohmic losses

Considering that drawn circuit, the new expression of the current voltage equation will be written as shown in the equation below:

$$I_{solar_cell} = I_{photocurrent} - \left\{ I_o \times \left[e^{\left(\frac{q \times [V_{solar_cell} + (I_{solar_cell} \times R_s)]}{A.K.T_j} \right)} - 1 \right] \right\} \quad (Equation 26)$$

Assuming that the photocurrent is equal to the short-circuit current of the solar cell; we will turn that equation into the one below:

$$I_{solar_cell} = I_{short_circuit} - \left\{ I_o \times \left[e^{\left(\frac{q \times [V_{solar_cell} + (I_{solar_cell} \times R_s)]}{A.K.T_j} \right)} - 1 \right] \right\} \quad (Equation 27)$$

Provided a given junction temperature " T_j ", the short-circuit current can be expressed as shown in the equation below:

$$I_{sc-Gref} = I_{sc-ref} \times [1 + (\alpha_{sc} \times \Delta T)] \quad (Equation 28)$$

Where:

$$\Delta T = T_j - T_{jref} \quad (Equation 29)$$

Here:

$$\left\{ \begin{array}{l} I_{sc-ref} = \text{is the short - circuit current measured under the} \\ \text{reference irradiance equal to } 1000 \text{ W/m}^2 \\ T_{jref} = \text{is the reference junction's temperature found in} \\ \text{the datasheet of the solar cell equal to } 25 \text{ }^\circ\text{C} \\ \alpha_{sc} = \text{is the temperature coefficient of the short - circuit current in } ^\circ\text{K}^{-1} \\ T_j = \text{is the junction's temperature in degrees kelvin (} ^\circ\text{K)} \end{array} \right.$$

In addition, the short-circuit current generated at any other amount of solar energy on the solar cell surface can be determined by using the equation below:

$$I_{sc-G} = I_{sc-Gref} \times \left[\frac{G}{G_{ref}} \right] \quad (Equation 30)$$

In the case of an open-circuit scenario at a reference junction's temperature, we will have the current flowing at the terminal of the solar cell equals to zero. Therefore, the reverse saturation current will take the expression below:

$$I_{o-T_{jref}} = \frac{I_{shortcircuit-T_{jref}}}{\left[e^{\left(\frac{q \times V_{opencircuit-T_{jref}}}{A.K.T_{jref}} \right)} - 1 \right]} \quad (Equation 31)$$

Let's:

$$V_{Th-T_{jref}} = \frac{(A.K.T_{jref})}{q} \quad (\text{Equation 32})$$

Then:

$$I_{o-T_{jref}} = \frac{I_{shortcircuit-T_{jref}}}{\left[e^{\left(\frac{V_{opencircuit-T_{jref}}}{V_{Th-T_{jref}}} \right)} - 1 \right]} \quad (\text{Equation 33})$$

So the expression of the reverse saturation current at any given temperature in degrees kelvin will be found using the expression below:

$$I_o = I_{o-T_{jref}} \times \left[\exp\left(\frac{-q \cdot \frac{E_g}{A.K}}{\frac{1}{T_j} - \frac{1}{T_{jref}}} \right) \right] \times \left(\frac{T_j}{T_{jref}} \right)^{3/A} \quad (\text{Equation 34})$$

Also the solar cell current will have a new term into its expression as shown in the equation below:

$$I_{solar_cell} = I_{sc-ref} \times \left[\frac{G}{G_{ref}} \right] \cdot [1 + (\alpha_{sc} \times (T_j - T_{ref}))] \quad (\text{Equation 35})$$

$$- \left(\frac{I_{shortcircuit-ref}}{\left[e^{\left(\frac{q \times V_{opencircuit-ref}}{A.K.T_{jref}} \right)} - 1 \right]} \right)$$

$$\times \left[\left[\exp\left(\frac{-q \cdot \frac{E_g}{A.K}}{\frac{1}{T_j} - \frac{1}{T_{jref}}} \right) \right] \right]$$

$$\times \left(\frac{T_j}{T_{jref}} \right)^{3/A} \cdot \left(\exp\left(\frac{q \times [V_{solar_cell} + (I_{solar_cell} \times R_s)]}{A.K.T_j} \right) - 1 \right)$$

Where: E_g characterizes the gap energy

Finally, the output power of the solar cell would be calculated using the basic formula shown below:

$$P_{solar_cell} = I_{solar_cell} \times V_{solar_cell} \quad (\text{Equation 36})$$

Recalling the expression of the current of the solar cell:

$$I_{solar_cell} = I_{short_circuit} - \left\{ I_o \times \left[e^{\left(\frac{q \times [V_{solar_cell} + (I_{solar_cell} \times R_s)]}{A.K.T_j} \right)} - 1 \right] \right\} \quad (Equation 37)$$

By neglecting the added term "- 1", this can lead us to the way of calculating the value of the resistance connected in series into the simplified equivalent circuit of the solar cell to introduce the losses due to the material resistivity and the levels of contact:

$$R_s = \left(- \frac{d V_{solar_cell}}{d I_{solar_cell}} \Big|_{V_{solar_cell} = V_{open_circuit}} \right) - \left(\frac{1}{w} \right) \quad (Equation 38)$$

Where:

$$w = q \cdot \left[\frac{I_{short_circuit}}{A.K.T_j} \right] \quad (Equation 39)$$

4.2.1.2 Single diode Model of a Single junction Solar Cell with parallel resistance:

The single diode model of a single junction solar cell with parallel resistance is an equivalent circuit of a practical solar cell. This practical equivalent circuit of the solar cell is also known as a five parameter model of the solar cell (Tamrakar et al., 2015).

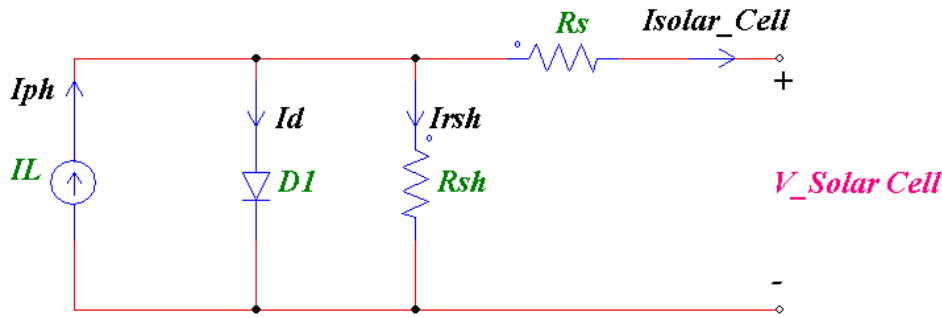


Figure 4.3: The five-parameter model of a single junction solar cell

Although this five parameter model of a single junction solar cell takes in consideration both the voltage drops and internal losses due to the current flowing through the solar cell via " R_s "; and the leakage current to the ground when the diode is reverse biased via " R_{sh} ", we can see that in the five parameter model the recombination effect of the diode is neglected.

This model has been made of a single diode playing the cell polarization phenomena and two resistors representing the losses. In addition, manufacturers are using this model by giving the technical characteristics of the manufactured solar cells. The current voltage characteristics of the five-parameter model will be given by:

$$I_{solar_cell} = I_{photocurrent} - I_d - I_{rsh} \quad (Equation 40)$$

Where:

$$\begin{cases} I_d = I_o \times \left[e^{\left(\frac{q \times [V_{solar_cell} + (I_{solar_cell} \times R_s)]}{N_s - cell \cdot K \cdot T_j} \right)} - 1 \right] \\ I_{rsh} = \frac{V_{solar_cell} + (I_{solar_cell} \times R_s)}{R_{sh}} \end{cases}$$

4.2.2 Two diodes Single Junction Solar Cell Model:

Although the single diode model of a single junction solar cell is widely used for practical photovoltaic applications, and seeing that it is also satisfactory when it comes to the representation of the solar cell characteristics and dynamics; a second method or way of modelling a single junction solar cell has been developed which is known as the dual-diode model or two diodes model of a single junction solar cell. The dual-diode model of a single junction solar cell can be illustrated in figure 4.4:

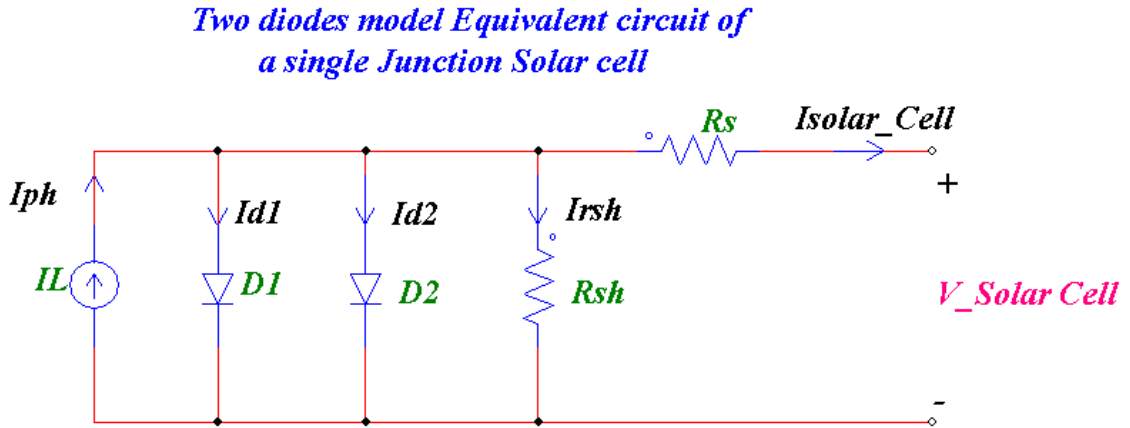


Figure 4.4: Dual-diode model of a single junction solar cell

In this particular model, extra rates of freedom are added for more accuracy. Basically, the dual-diode model considers into its account the mechanism of electric transport of charges inside the single junction solar cell. Using this model, the PN junction polarization development is characterized by the two diodes, which also represent the minority carriers' recombination located at both the material's surface and within the material's volume. Analysing the dual-diode model, the current flowing through the terminal of the single junction solar cell can be found using the equation given below:

$$I_{solar_cell} = I_{photocurrent} - I_{d1} - I_{d2} - I_{rsh} \quad (\text{Equation 41})$$

Whereby the recombination currents I_{d1} and I_{d2} will be given by:

$$I_{d1} = I_{o1} \times \left[e^{\left(\frac{q \times [V_{solar_cell} + (I_{solar_cell} \times R_s)]}{A \cdot N_{s-cell} \cdot K \cdot T_j} \right)} - 1 \right] \quad (\text{Equation 42})$$

$$I_{d2} = I_{o2} \times \left[e^{\left(\frac{q \times [V_{solar_cell} + (I_{solar_cell} \times R_s)]}{2A \cdot N_{s-cell} \cdot K \cdot T_j} \right)} - 1 \right] \quad (\text{Equation 43})$$

With their saturation current written as shown below:

$$I_{o1} = P_4 \cdot T_j^3 \cdot \exp\left(\frac{-E_g}{k \cdot T_j}\right) \quad (\text{Equation 44})$$

$$I_{o2} = P_4 \cdot T_j^3 \cdot \exp\left(\frac{-E_g}{k \cdot T_j}\right) \quad (\text{Equation 45})$$

Due to the fact that we are only having a single junction solar cell, the value of N_{s-cell} , which stands for the number of cells connected in series, will be equal to one. We can quickly pick up the complexity in terms of deriving the expression of the solar cell characteristic parameters even though the consideration of those little details contributes to the increase of the efficiency given by the particular model; the two diode model will not be widely used regarding its complexity level.

4.2.3 Power Model of a Single junction Solar Cell:

Due to the fact that a polycrystalline silicon module will be used to design the hardware prototype of this research project a model that would give the same power of the solar cells when operating at maximum power point known as polynomial model of a single junction solar cell needs to be modelled.

The maximum power can be found using the equation below:

$$P_{solar_cell_max} = k_1 \cdot (1 + k_2 \cdot [T_j - T_{jref}]) \cdot (k_3 + G) \quad (\text{Equation 46})$$

Where: k_1, k_2 and k_3 are constant taken from the datasheet of the solar cell's manufacturer.

4.2.4 General Model for a space triple junction Solar Cell:

Having different semiconductor layers that have different bandgaps into the multijunction solar cells, we can achieve a better use of the solar spectrum.

Whereby each layer made of various materials, probably an III-V semiconductor type which will absorb a different portion of the spectrum. Generally, the most energetic photons are absorbed by the top layer having the largest bandgap. In addition, each layer moving from the top layer to the bottom layer has a smaller bandgap compared to the previous layer (Lansel, 2005). Keeping in mind that multijunction solar cells are primarily manufactured from gallium arsenide GaAs and its compounds with other III-VI group materials (Shekoofa and Wang, 2015). Increasing the efficiency boundary of a single junction solar cell is the principle cause of the design and the manufacturing process of multijunction solar cells.

Thus we can see that a multiple junction solar cell will only be a product of successive single junction solar cell. Based on the different models drawn for the modelling of a single junction solar cell, we can draw a general equivalent circuit of a single junction solar cell as shown in figure 4.5:

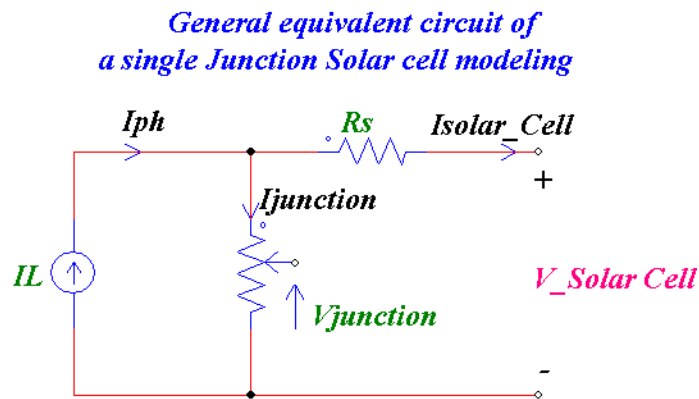


Figure 4.5: General equivalent circuit of a single junction Solar cell

Thus, decomposition can occur when it comes to the modelling of a multijunction solar cell, which is constituted of n-layer of semiconductors. In case we have an n-layer of semiconductors into a multijunction solar cell, we can break it's modelling into n-single junction sub cells connected in series as shown in figure 4.6:

General equivalent circuit of a triple Junction Solar cell modeling

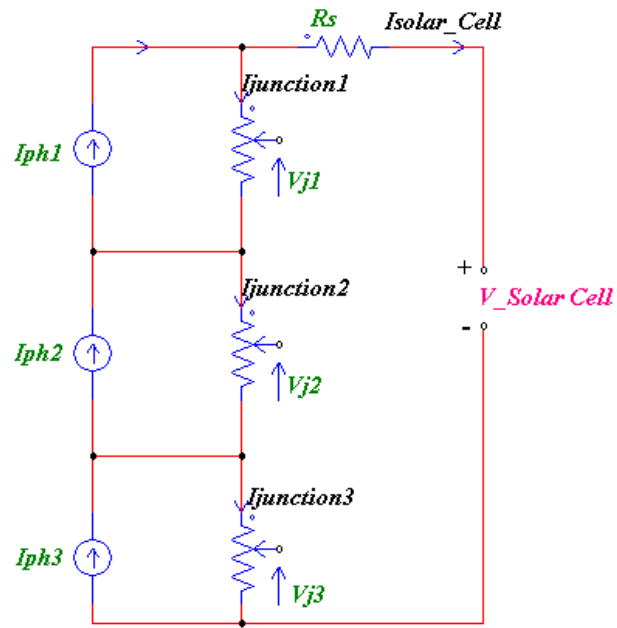


Figure 4.6: General model for a triple junction solar cell

The equations describing this new model can be expressed as shown below:

$$\begin{aligned}
 J_{solar-cell} &= J_{short-circuit(Bottom\ layer)} = J_{short-circuit(Middle\ layer)} && (Equation\ 47) \\
 &= J_{short-circuit(top\ layer)}
 \end{aligned}$$

$$V_{solar-cell} = (V_{j1} + V_{j2} + V_{j3}) - [(R_s) \cdot (I_{solar-cell})] \quad (Equation\ 48)$$

Chapter 5: Degradation in Different Solar Cell Technologies

5.1 Introduction:

The validation of experimental results shows that solar cells can be classified as reliable devices. But some evidence has however been put together which reflects the service life of these solar cells as a limited service in case the solar cells are exposed to irradiation by high-energy particles. According to the work done by Loferski and Rappaport, it was shown that the solar cell output was reduced to 75 percent of its initial value by irradiation with 5×10^{13} electrons per square centimetres having an energy of 1.7 Mev; 3.5×10^{10} protons per square centimetres having an energy of 17.6 Mev; or 4.4×10^9 alpha particles having an energy of 40 Mev. We have to mention that: the stated work has been done with insufficient data on the Van Allen Belts which will assess the effect of this radiation on the life of the solar cells. Recently, Dennet carried more study on the radiation damage in satellite solar power systems and he found that the effect of radiation damage will decrease the open circuit voltage only slightly and to cause a very large decrease in the short-circuit current (*Dryden and Von Doenhoff, 1961*). Furthermore, we have to note that the rapid degradation of these solar cells can be allocated to low energy protons of the outer region of the Van Allen Belt entering the bare surface and damaging the diode junction (*LE, n.d.*).

Over time, gradually losses on the performance are observed on every solar cell or solar module available on the nanosatellite. In some cases due to the degradation of the solar cells and the solar modules, the deterioration in performance is either very slow or very fast. Long term energy production from the photovoltaic systems has got the deterioration in performance as a very serious issue and as a big obstacle (*Kumar, 2017*). Seeing the impact of degradation alone on the commercialization of the solar cell technologies, consequently action must be taken to solve the degradation impact issue on that stated technology before its introduction on the shelves in the market. Numerous factors do contribute to the degradation process of solar cells and photovoltaic modules; that degradation process does occur independently of the use of the solar cells or the photovoltaic modules then again the degradation process has a fast speed during the operation of the solar cells (*Kumar, 2017*).

Important to realize that during the degradation process, we can notice a few cases where the electrode materials decompose themselves and a loss of their optical and electrical properties can be observed. Thus, the factors in charge of accelerating the degradation in those solar cells are the following: sunlight, temperature, humidity and oxygen. This chapter will cover the degradation process in different solar cell technologies and modules, which will lead

to a better understanding of that degradation process. Henceforth, the preventive solution to that big obstacle will be implemented.

5.2 Degradation principle in various types of solar cells:

Harsh environmental radiation exposure, temperature, atmospheric conditions, bias, humidity, oxygen and their combinations are not the only factors where the degradation of a solar cell will take its dependence from. Different from those listed factors, the structure and the fabrication procedures are also some factors on which the degradation of a solar cell will depend on as well. With this in mind, we can see the complexity of the degradation of a solar cell. Based on the structure and the fabrication procedures, the degradation effect of a solar cell will be different from one type of structure of solar cell to the other type due to the different degradation mechanism associated to the particular structure of the solar cell (*Kumar, 2017*). Henceforth, the reliability of a solar cell is irretrievably connected to the solar cell degradation. Thus, firstly it will be a benefit to have a proper understanding of the cell level degradation.

5.2.1 Degradation in Silicon Wafer Solar cells:

Assuming that crystalline silicon represented as “c-Si” is a very stable material, after several hours of exposure to sunlight, silicon solar cells experience light-induced degradation, which can decrease their efficiency of the energy conversion by up to 10% (“*Study raises questions on what causes silicon solar cell degradation,*” *n.d.*). Thus, the degradation will have a direct impact on the current density-voltage characteristic curve of the solar cells. The light induced degradation in the crystalline silicon solar cells appears in two different steps. The light induced degradation effect is usually ascribed to boron-oxygen defects in the wafer itself; consequently it’s expected to have an interface or surface component, if ionization of this charge occurs or if there is an increase in the density of interface states. Investigations have been done on the light induced degradation effects whereby it has been found that in some cases the light induced degradation is fully recoverable in the silicon solar cells via thermal annealing when the solar cells are annealed at around 200 degrees Celsius for about 30 minutes; while it can’t be recoverable in other cases (*Sopori et al., 2012*).

5.2.2 Degradation in Hydrogenated Amorphous Silicon (a-Si:H) Solar cells:

Basically, the structure of Hydrogenated amorphous silicon solar cells is the opposite compared to the structure of the Silicon wafer solar cells. A comparison between hydrogenated

amorphous silicon thin solar cells and the classic Silicon wafer solar cells will show that hydrogenated amorphous silicon solar cells are very cost effective; they possess low power conversion efficiency and a faster degradation effect (*Deneuille et al., 1980*). Based on literature, studies demonstrate that the faults occurring on hydrogenated amorphous silicon solar cells could have a native originality or could be induced by the light. Both types of faults are due to threefold-coordinated silicon atoms containing dangling bonds which are defined as unsaturated bonds that are peopled by only a single electron and therefore will play a decisive function in the degradation of the amorphous silicon solar cell (*Fehr et al., 2011*). The causes of an increase on the fault's level of the solar cell will be occasioned by:

- The recombination of the photo-induced charge carriers; and
- The reduced lifetime of the charge carriers

Consequently, a reduced power conversion efficiency of the solar cell will be observed. The light-induced faults are assessable and could be removed through thermal annealing while the native faults produced during film processing are stable with respect to annealing (*Vasudevan et al., 2017*).

5.2.3 Degradation in Copper Indium Gallium Diselenide (CIGS) Solar cells:

A well understanding of the degradation effect in copper indium gallium solar cells is not really achieved seeing that according to every type of structures there will be a different types of degradation (*Kumar, 2017*). At the same time, high temperature-induced and humidity-induced degradation behaviours were investigated through the analysis of those solar cells and it has been found that the moisture and elevated temperatures have a negative impact on the performance of the copper indium gallium diselenide solar cells (*Lee et al., 2015*). In some cases, degradation in copper indium gallium diselenide solar cell can be caused by light exposure whereas in some cases light exposure has shown no effect or improvement in performance (*Kenny et al., 2006*).

5.2.4 Degradation in Cadmium Telluride (CdTe) Solar cells:

Although cadmium telluride solar cells have shown stability over thousands of hours of field testing, they haven't yet reached the reliability record of the crystalline silicon solar cells (*Meyers et al., 1996*). The lifetime testing of the cadmium telluride solar cells displays a deterioration in their performance with weighty losses in the open circuit voltage and the fill factor of the cadmium telluride solar cells due to formation of blocking interfaces at the electrodes, increased charge carrier recombination at the junction and the increment in overall

bulk resistivity of the cell (*Meyers et al., 1996*). Two independent mechanisms give a clear understanding of the degradation phenomena in the cadmium telluride solar cell which can be listed as follows (*Visoly-Fisher et al., 2003*):

- An excessive Copper doping into the cadmium telluride and
- A depletion of the back contact barrier

5.2.5 Degradation in III-V Multijunction Solar cells:

Multijunctions solar cells can be seen as a group of generators which connected in series, therefore the open circuit voltage V_{oc} will be the addition of the individual open circuit voltages of the subcells while their short circuit current will be the short circuit current of the sub cell with the lowest value among them (*Plantevin et al., n.d.*). Thus, we can express those two parameters for the n-junction solar cells using the equations below:

$$V_{oc} = V_{oc1} + V_{oc2} + \dots + V_{ocn} \quad (\text{Equation 49})$$

$$I_{sc} = \min(I_{sc1}, I_{scn}) \quad (\text{Equation 50})$$

Important to realize that those equations can be used regardless of the amount of degradation of the multijunction solar cell; due to the fact that firstly those sub cells are made using different types of materials and secondly because the energy of an incident particle will decrease with the penetration depth, the rates of the degradation of V_{oc} , I_{sc} , and the power are different for each individual sub cell.

5.2.6 Degradation in Dye-Sensitized Solar Cells (DSSC):

For cost effective energy generation, Dye-sensitized solar cells are gifted but the fact that their lifetime span is so short leaves some distance in terms of their adequate utilization. Like the previous other solar cells, dye-sensitized solar cells show devaluation in their performance over a certain period of time. Nevertheless the degradation process in Dye-sensitized solar cells is still a nightmare but some degradation studies performed on this type of solar cell recommended that the performance of dye-sensitized solar cell relies upon their construction structure and constituent materials (*Kumar, 2017*). Generally, the degradation in Dye-sensitized solar cell could be either a physical degradation or chemical degradation. In addition, physical degradation in Dye-sensitized solar cell is connected to the leakage or drying of the electrolyte medium; while the chemical degradation is connected to the decomposition of dye and electrolyte components. According to studies done on the dye sensitized solar cells,

six elemental characteristics contribute to the dye sensitized solar cell degradation which can be listed as follows (*Sauvage, 2014*):

- Iodine consumption in electrolyte;
- Dye desorption at elevated temperatures for instance higher than sixty degrees Celsius;
- Lack of Chemical or Photochemical Stability of Benchmark Ruthenium Sensitizers;
- Platinum dissolution for electrolytes free of thiocyanate;
- Formation of a polymeric solid electrolyte interphase; and
- Ultra violet irradiation, which will consequently lead to conceivable dye or electrolyte component oxidation.

5.2.7 Degradation in Organic Solar cells (OSC):

Although organic solar cells are quite fascinating and highly cost effective, they suffer from rapid degradation in air (*Kumar, 2017*). In fact the word degradation points out the change in the properties of a material or a device affecting negatively its efficiency over a period of time (*Azzouzi, 2016*). Degradation in organic solar cells is a complex issue and it's principally generated by adsorption and diffusion of ambient molecules that react with cell components which will lead them to lose either their electrical properties or their optical properties (*Kumar, 2017*). Furthermore, metal or organic interfacial charge injection has a crucial role in the organic solar cell degradation process whereby the dark injection current and the photocurrent can all together determine the shapes of the voltage –current characteristics curve, and the correlation between them may have particular influence on the output performance of the organic solar cells (*Yang et al., 2013*).

5.3 On- Orbit solar cell Degradation Approach:

Since the launch of the world's first solar-powered satellite on the 17th March 1958, solar cells have been identified as a primary power source for satellites and spacecraft (*Bailey and Raffaele, 2003*). In fact, the world's first solar-powered is called Vanguard I; it was just a small satellite with a low electrical power demand of few watts. Since that time, we have noticed the growth in the space and satellite industries for the design, manufacturing and launch of different size of satellites based on the type of payloads they will be carrying. Thus, nowadays satellites together with geostationary communications satellites, produce a lot of kilowatts electrical power with the solar cells that have been mounted on the satellites joint with adequate embedded systems designed to ensure the normal operations of the subsystems through end of life known as the lifetime of the mission allocated to the satellite (*Walker and Statler, 1988*).

Previous sections have defined and explained the degradation in different solar cell technologies. In the next paragraph of this chapter, we will describe space-based solar cells power systems. The solar cell degradation monitoring's methods and furthermore the radiation effect on the solar cells. The current methods for modelling solar cell degradation over mission lifetime will be presented in this chapter, and a description of our approach to using on-orbit data to establish a comparison with these models. While the closing section of this chapter will show a description of the scheme for solar cell degradation analysis using on-orbit telemetry and space environment data.

5.3.1 Space-based solar cells Power Systems:

Important to realize that the satellite's power subsystem design is said to be fully successful if the electrical power demand has been satisfied during the lifetime mission of the designed satellite. Thus, the space-based solar cells power system will be seen as a system, which encompasses solar cells, which ensure the generation of electrical power to the payloads of the spacecraft. Those solar cells can be mounted in series to form a string of solar cells then put in parallel to form parallel strings of solar cells. In case we decided to form a group of those different solar cells arrangement, we will end up with solar panels which is nothing than being a group of parallel strings of solar cells (*Taherbaneh et al., 2011*). In space the generation of electrical power energy is done using a primary source of energy known as the solar light energy, and the conversion of the solar light energy to electrical energy (*which will a direct current electrical energy for this case*) is achieved by the use of some semiconductor devices known as solar cells (*Ibrahim et al., 2011*). In general, the generation of the electric current in the semiconductor device takes place where exposure to light causes the photons to get absorbed in the semiconducting material that excites electrons from the valance band to the conduction band. Photo generated electrons are those electrons in the conduction band. They leave behind the corresponding holes in the valance band. These electrons and holes need to be extracted out to get electricity (*Kumar, 2017*). Basically the production of the photocurrent is done through the incoming photons that generate minority carriers on the front surface of the solar cells that diffuse into the solar cell junction. In space applications, systems are continuously exposed to radiation which procreates defects that prevent the carriers from reaching the cell junction and decrease the generated photocurrent (*Faraday et al., 1968*). Solar cells are classified among the least shielded satellite components group based on theirs functions (*O'Brien, 2009*). The front surface of a solar cell is shield using a thin transparent cover glass while the back surface is shielded using the cell substrate material and the panel structure. The cover glass is coated with antireflection and conductive coatings, and bonded to the solar cell using a form of transparent

adhesive (*Messenger et al., 2011*). It will absorb low energy protons and electrons due to the fact that glass causes a slowdown of the incident particles, preventing the particles from reaching the active volume of the cell and causing degradation of the solar cells (*Bailey and Raffaele, 2003*). Furthermore, the thickness of the shield materials is one of the most important parameters during the design missions for the end of life power requirements. A cover glass of 75 micrometers thickness is capable to stop all incident protons with energies less than 2.8MeV (*Messenger et al., 2010*).

5.3.2 Solar Cells Performance Parameters:

Three important parameters can be used to monitor the performance of a solar cell and state the occurrence of degradation. Those parameters can be listed below:

- The short- circuit current known as: I_{sc} ;
- The open circuit voltage known as: V_{oc} ; and
- The maximum power of the solar cell known as: P_{max}

Though, the parameter that characterizes the ability of the solar cell in terms of converting incoming photons into electricity is known as the solar cell efficiency; it won't be useful to monitor the performance of solar cells in space after the launching process. The short circuit current parameter of the solar cell is obtained under two different scenarios:

- Firstly, it's obtained when the load resistance or the voltage across the solar cell is equal to Zero.
- Secondly, we can also obtain that parameter when the solar cell is short-circuited.

Another key point is the short-circuit current represents the largest amount of current that can be drawn from the solar cell which has been produced from the collection of light-generated carriers in the cell structure (*Ibrahim et al., 2011*).

Especially for a triple junction solar cell, the short circuit current quantity will be determined by the junction that has the lowest current output of all three junctions because the solar cells are connected in series (*Sumita et al., 2003*). This can be expressed using the equation below:

$$I_{sc} = \min(I_{sc1}, I_{sc3}) \quad (\text{Equation 51})$$

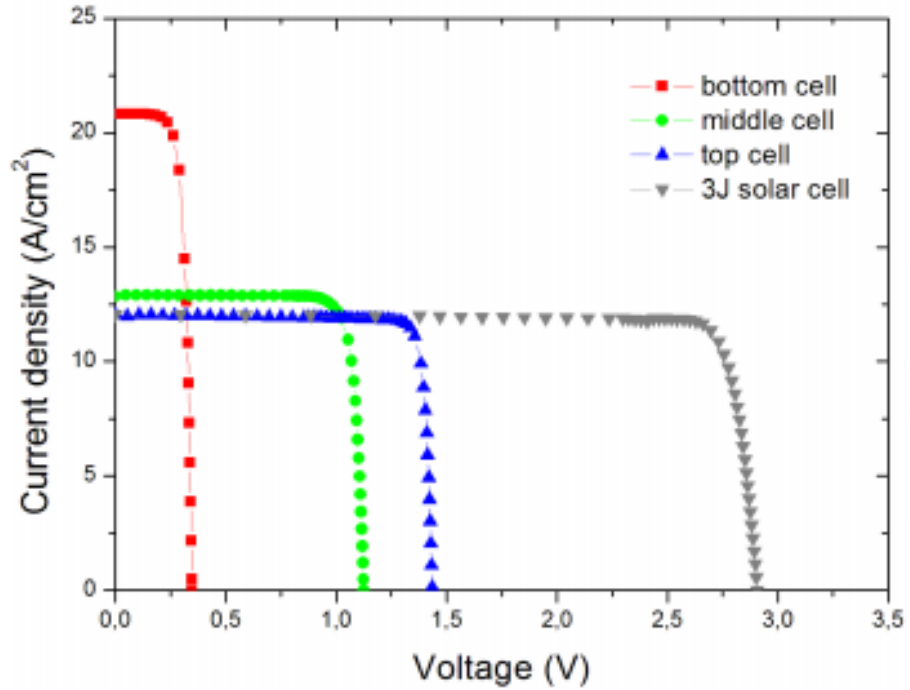


Figure 5.1: I-V characteristic curves of a triple junction solar cell. (Messmer, 2013)

While the open circuit voltage will be generated by the solar cells for infinite load resistance or Zero current (Walker and Statler, 1988). That open circuit parameter will also be the sum of the voltages generated at each solar cell connected in series to form a string of the solar panel as shown in the equation below:

$$V_{oc} = V_{oc1} + V_{oc2} + \dots + V_{ocn} \quad (\text{Equation 52})$$

Practically, any damage or degradation on each solar cell will immediately affect the value of that parameter (Sumita et al., 2003). The mathematical expression of the open circuit voltage of a solar cell can be shown below:

$$V_{oc} = \frac{K_B T}{q} \times \ln\left(\frac{I_L}{I_s} + 1\right) \approx \frac{K_B T}{q} \times \ln\left(\frac{I_L}{I_s}\right) \quad (\text{Equation 53})$$

We can clearly see that a change of the temperature value will modify the value of the open circuit voltage of a solar cell; therefore we will say that it depends on the temperature of the solar cell in space. In figure 5.2, the current-voltage characteristic of a solar cell used for space application in sequence, perusing out equally dispersed focuses from the short circuit current to the open circuit voltage parameters. Through this measurement process, each solar cell is short circuited but not when it is being stepped through the current voltage characteristic. The short

circuit current and the open circuit voltage are both obtained when the load resistance is respectively equal to zero and infinity.

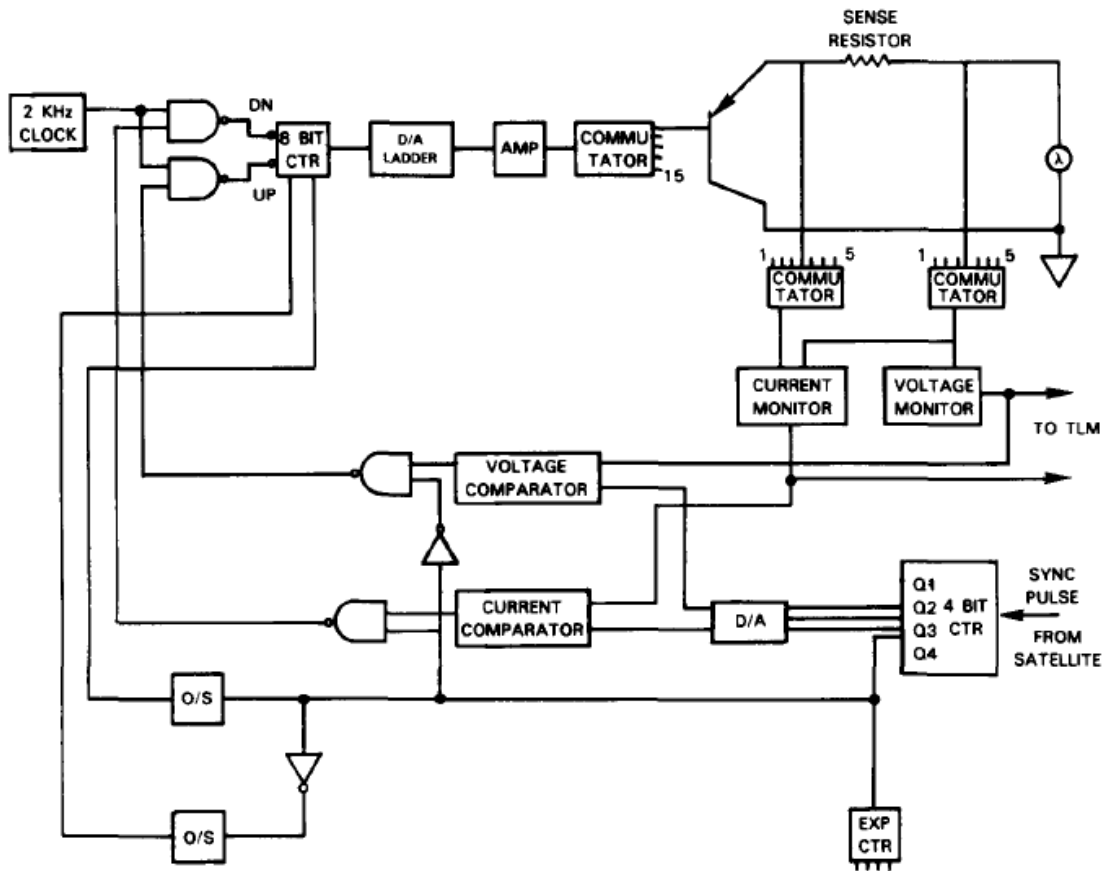


Figure 5.2: Schematic diagram of the circuit used to measure current-voltage curves of the solar cell experiments in space. (Walker and Statler, 1988)

The isolation of the solar cell temperature impacts from the degradation of the solar cell should be done for the analysis process of the open circuit voltage parameter of a solar cell in space. Using those different parameters, the current-voltage (I-V) characteristic curve and the power-voltage (P-V) characteristic curve can be drawn as shown in figure 5.3 and in figure 5.4 to illustrate the characteristics of the particular solar cell or solar array also called solar panel:

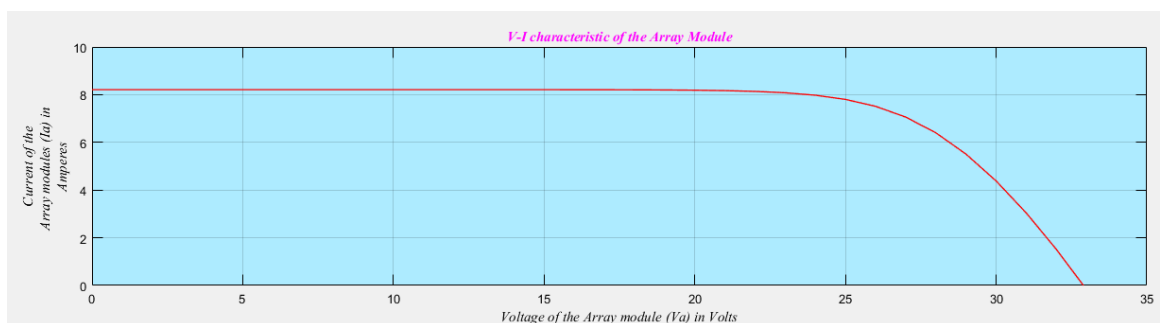


Figure 5.3: Current-Voltage characteristic curve of a solar array

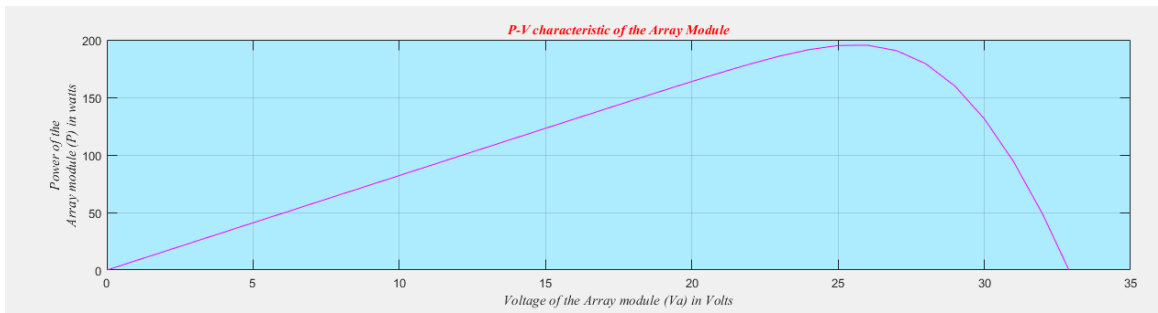


Figure 5.4: Power-Voltage characteristic curve of a solar array

The point corresponding to the maximum value on the power graph represents the maximum electrical power derived from the solar cell known as:

$$P_{max} = I_{max} \times V_{max} \quad (\text{Equation 54})$$

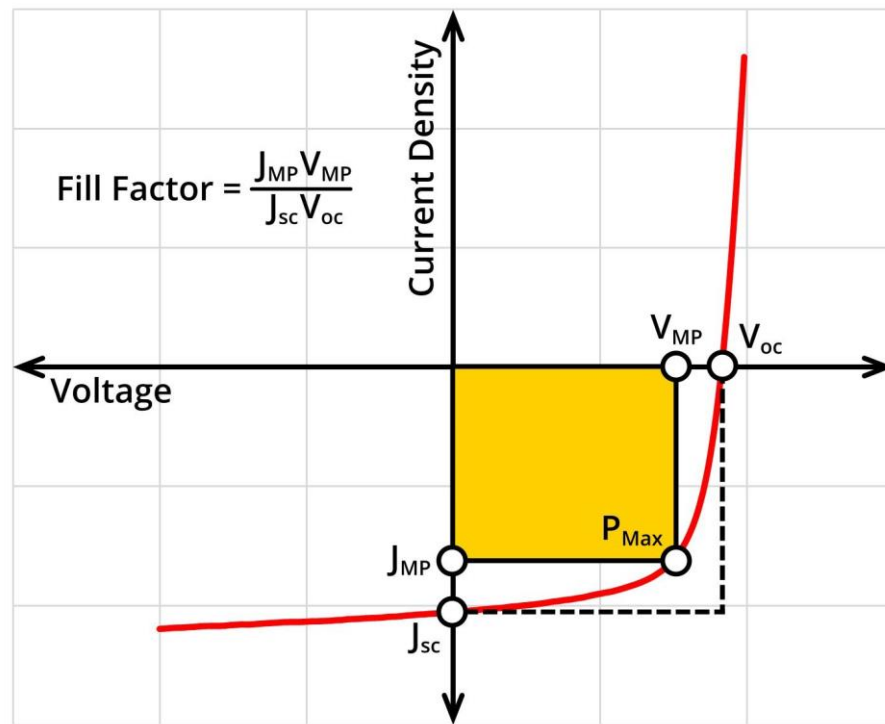


Figure 5.5: Current-Voltage characteristics of a solar cell using the short circuit current density. (“Solar Cells: A Guide to Theory and Measurement – Ossila,” n.d.)

The characteristic shown in figure 5.5 describes the ability of the particular solar to transform solar energy into electricity. The short circuit current density has been used during the drawing of this characteristic to turn around the generated current’s dependency on the area of the solar cell.

The property of the solar cell material and its structure will influence the degradation rates of the three main parameters used to monitor the performance of a solar cell in space (Alurralde, 2004).

5.3.3 The effects of radiation on solar cells:

For space applications, two semiconductor materials are commonly used. They are called Silicon (Si) and gallium (GaAs). In the earlier decades, the use of silicon solar cells was the state of the art solar cell for space applications. To this point one can notice that silicon solar cells are still operating on-board numerous satellites, but gallium solar cells which were firstly launched in 1996 are said to be actually the most advanced cells in flight (*Odenwald and Green, 2007*).

On the negative side, we have to highlight that both types of solar cells due to the radiation found in the space environment have to experience the phenomenon of solar cell degradation caused by the space environment's radiation. Significant progress has been achieved in advancing the overall solar cell efficiency and radiation resistivity over the past fifty years through the use of ground based radiation damage experiments (*Alurralde, 2004*). Based on the mission and the type of orbit of the satellite, the electrical power demand of the satellite payload will definitely vary. Due to the high efficiency and radiation tolerance of solar cells made with gallium (GaAs), we can notice an increase in terms of the use of the stated solar cells (*Hacke et al., 1994*).

Important to realize that charged particles in the space environment do traverse material, and through both ionizing and non-ionizing means they lose energy. In the case of solar cells, the primary energy loss mechanism is through non-ionizing effects that imply the displacement of atoms in the semiconductor lattice. The displacement of atoms results in lattice defects such as vacancies, interstitials and the formation of defect energy levels in the semiconductor material (*Weinberg and Brinker, 1988*). These defects produce carrier-trapping centers in the semiconductor bandgap, as well as generate carriers. Carrier generation contributes to an increase in the forward bias dark current-voltage curve and degrades the open circuit voltage (*Walters et al., 1996*).

The consequences of the recombination centers are: the reduction of minority carrier diffusion length, or minority carrier life time; and the decrease of the photovoltaic output of the solar cell (*Srouf and McGarrity, 1988*). Especially for gallium (GaAs) and Silicon (Si) solar cells, radiation-induced recombination centers operate as a primary mechanism for solar cell performance degradation. In addition, the degradation of the open circuit voltage will be achieved by an increased forward biased dark current-voltage curve. While the decrease in the minority carrier diffusion length will degrade the short circuit current I_{sc} , the increased forward biased dark current –voltage curve is done the decrease process in the minority carrier diffusion length (*Walters et al., 1991*). The generation of the photocurrent output is performed through the diffusion of charge carriers to the junction before the recombination takes place

(*Yamaguchi, 2001*). Degradation of the minority carrier diffusion length reduces the cell's efficiency (*Walters et al., 1991*). In comparison to the junction distance, the average diffusion length of the photo-generated carrier is large for gallium (GaAs) solar cells. On the other hand, the average diffusion length is compared to the thickness of the photo-carrier generating region of the silicon solar cells. Whereby, a decrease in the diffusion length of carriers in silicon will represent a decrease in efficiency of the silicon solar cells. While, a smaller decrease in efficiency of gallium solar cells will be observed after the contribution effect of the gallium solar cell carrier diffusion length degradation (*Hacke et al., 1994*).

Chapter 6: A literature survey on reconfigurable photovoltaic systems

6.1 Introduction:

Displacement damage dose approach can be used to determine solar cell degradation in space with the space environment information system implementation. Another key point will be other various methods that can be used to perform calculations on space solar cell degradations such as (Messenger et al., 2001):

- Jet Propulsion Laboratory equivalent fluence method: in which the damage coefficients have to be worked out through an extensive set of experimental measurements.
- Naval Research Laboratory displacement damage dose method Known as D_d -Method: whereby the energy dependence of the damage coefficients is determined from a calculation of the non-ionizing energy loss called NIEL.
- SPENVIS implementation method.

It's important to realize that those approaches listed above only assist in terms of a prediction of solar cell degradation in space radiation environments using a single characteristic degradation curve of that particular solar cell. In addition, the end of life solar cell performance for a given mission can be determined through a reading on its characteristic curve once the displacement damage dose for the mission has been given. The explained information gotten from the characteristic curve will assist during the preparation of the mission on the ground floor level.

In reality after the prediction of the solar cell degradation parameters, no action is performed regarding the degraded solar cells mounted on the satellites, which are actually orbiting in the space environment. Actually, more than 750 000 pieces of dangerous debris are now orbiting earth, which leads to an urgent need for coordinated international action to ensure the long-term sustainability of spaceflight. In other word, a coordinated solution to space debris that consequently will keep the earth's orbital environment as clean as possible is highly needed (esa, n.d.). Indeed, part of those space debris are retired satellites and satellites, which have seen the end of their missions due to solar, power systems failures.

Studies on the radiation damage in satellite solar power systems revealed that the effect of radiation damage can be observed through (Dryden and Von Doenhoff, 1961):

- A decrease of the open circuit voltage
- A decrease in the short circuit current

With this in mind, this chapter will present a new reconfiguration system which will improve the efficiency of the nanosatellite's solar cell array by reducing the power losses through the used bypass semiconductor diodes and the series diodes inserted in a photovoltaic system.

6.2 Reconfigurable solar photovoltaic array:

Earth's space environment and solar activity could have deleterious effects on solar technologies that are utilized by the modern space engineering community. Thus, a proper understanding of the originality of those raised effects is crucial for a successful and efficient design, implementation and operation of the new space technologies. It is important to highlight that: for the protection of vulnerable systems against the harmful effects of the space environment; a better new understanding of the constitution of the used technology equipment, its operation, its deterioration process and an access to its key data are valuable at this stage to realize the intended protection scheme. Withstanding the radiation environments that all spacecraft sent into orbit around the Earth or to the far reaches the solar system may encounter; will be the main objective of the designed space technologies. Nevertheless, anomalies produced by space radiation has an effect on the operation of the computer memory and processors aboard these spacecraft and such anomalies appear to become more prevalent as semiconductor devices continue to shrink in size (*Read "The Sun to the Earth -- and Beyond, n.d.*). Due to space environment's threat to spacecraft system and on the other hand the safety of the space environment health when it comes to the reduction of the space debris; an increase demand for more reliable and efficient energy sources with maintenance-free operations capability has been observed in the space industry. The amazing outcome of a collaborative project between the United States department of energy's national renewable energy laboratories and researchers from two Swiss centers is the tested range of multi junction solar cells with an efficiency up to 35.9 percent (*"NREL, Swiss Scientists Power Past Solar Efficiency Records | NREL | NREL," n.d.*). Surprisingly, this new solar cell with efficiency above thirty five percent is the new high record of multi junction space solar cell. Keeping in mind that solar cell power system generation is highly influenced by the harsh environmental radiation exposure in the space environment; therefore intensive research efforts have been conducted on the photovoltaic power generation technologies. Practically, the universal design of a photovoltaic generation system is made of sets of solar cells.

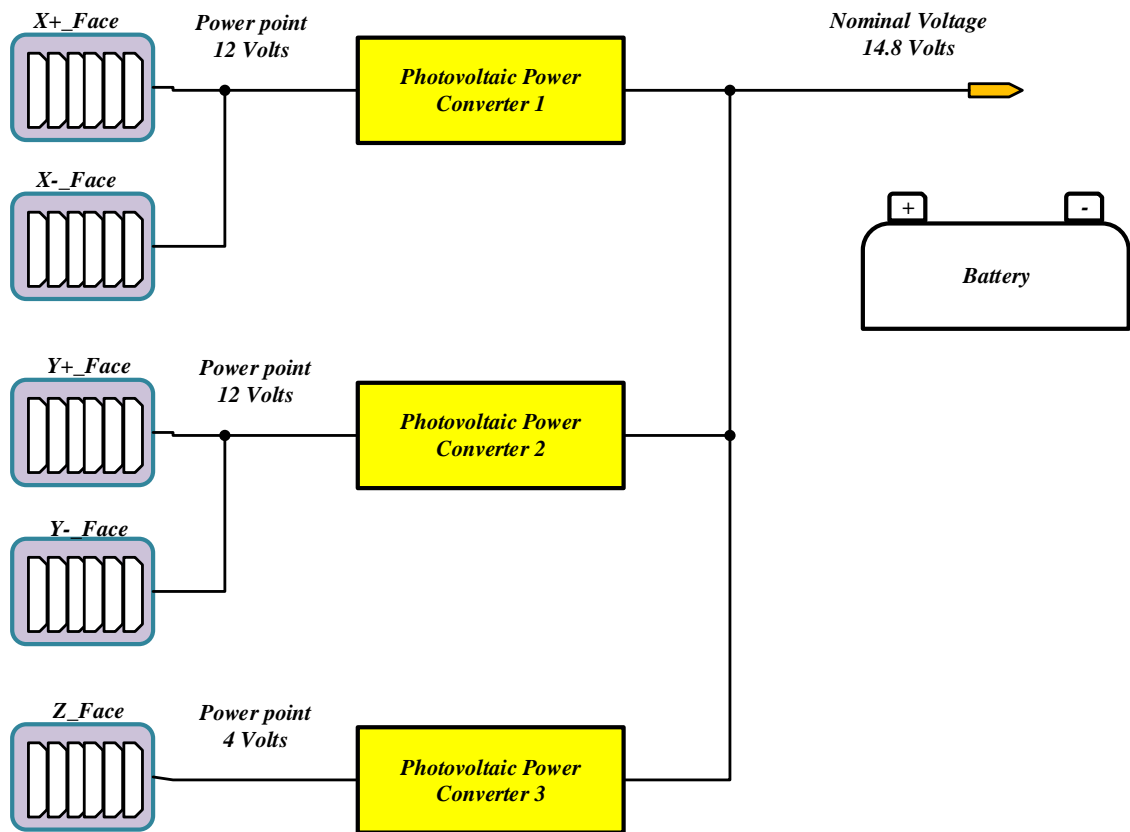


Figure 6.1: Photovoltaic arrays power system generator of a 3U nanosatellite

Furthermore, those solar cells can be grouped in sets of arrays in which each array can be constructed of numbers of parallel photovoltaic strings, series-parallel known as “SP” topology, or of numbers of series connected tiers, total cross tied known as “TCP” topology.

However, the practice of the photovoltaic generators on spacecraft has specific limitations provoked by the low efficiency per meters squared of the solar cells, the alternative process from days and nights which leads to a discontinuity of the solar source of light, the non-operation of the solar cells caused by electrical mismatches. But, it’s important to realize that in case distinctions are observed in the electrical characteristics of the solar cells forming a single photovoltaic module and on the photovoltaic modules forming a photovoltaic string; a firm reduction of the produced output power of the entire photovoltaic system generators can be seen. Under those circumstances, a gap will be made between the possible energy production and the current extracted energy. These days, efforts made by researchers and scientists contribute towards the improvement of conversion efficiency of those photovoltaic modules as well as those solar cells through new implementation and efficient algorithms for the power conversion unit and the maximum power point tracking algorithms known as MPPT algorithms. In other hands, researchers have pushed their way of thinking to actually bury the limitations that the MPPT algorithm and the power conversion plus efficient algorithm may have; those

researchers have led to the development of solar tracking strategies and an efficient algorithm for faults detection on a photovoltaic system generator.

Doubtlessly, a factual instrument can be utilized to compute the probability of the reliability state of a given solar cells array after a given length of its operating time. This is known as solar array reliability analysis tool. Whereby the calculated reliability noted “R” of the solar cell array is equal to the calculated probability of success known as “P_s” (Patel, 2005b):

$$P_s = R = e^{-\lambda t} \quad (\text{Equation 55})$$

Where:

λ = is the failure rate of the solar cell array

t = in the operating time or the number of temperature cycles as appropriate.

Thus, the probability failure known as “P_f” is determined as:

$$P_f = 1 - P_s \quad (\text{Equation 56})$$

Practically, a faulty solar cell can reach critical high temperature, which implies, the hotspot phenomenon and consequently electrical failure of the photovoltaic module can occur. Therefore, series-diodes and bypass diodes are used to avoid the hotspot and mismatch events.

In reality, the inserted diodes in the photovoltaic solar cells array will have a voltage drop across each of those elaborated diodes. Therefore, they will introduce losses and local maxima in the electrical characteristics of the photovoltaic module. Consequently, the produced electrical energy will decrease and will decrease the conversion efficiency of the solar cells.

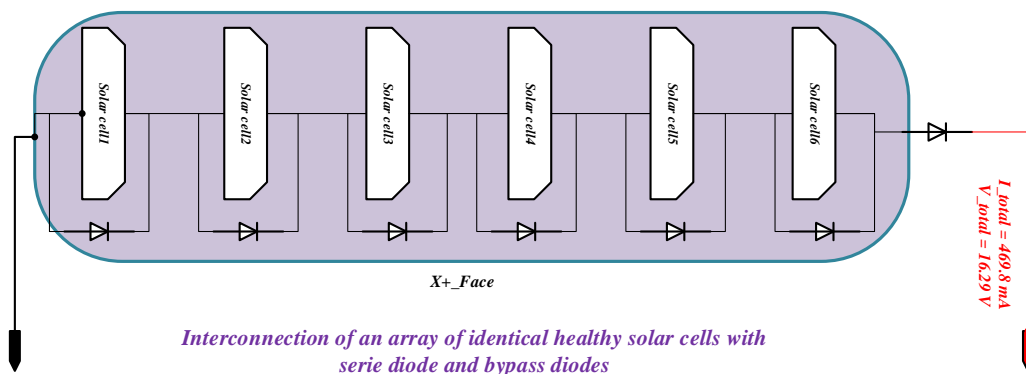


Figure 6.2: Interconnection of an array of solar cell with bypass and series diodes inserted

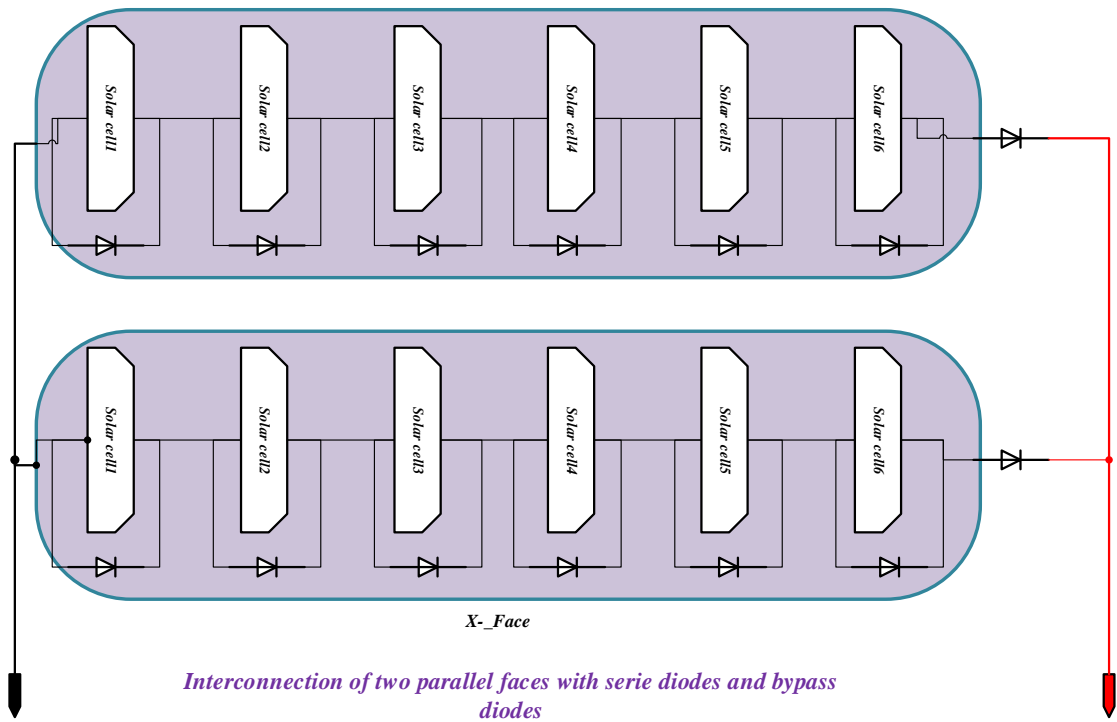


Figure 6.3: Interconnection of two parallel faces of the nanosatellites photovoltaic system

Let's highlight the fact that in a photovoltaic system of a nanosatellite, the solar cells are connected in various configurations. Habitually, the fixed solar cells array system of a nanosatellite as seen on the figure above is made by series and parallel connection of the solar cells array modules. The obtained series, parallel and series-parallel constitute the elemental configuration scheme in the photovoltaic system generator of a nanosatellite power supply.

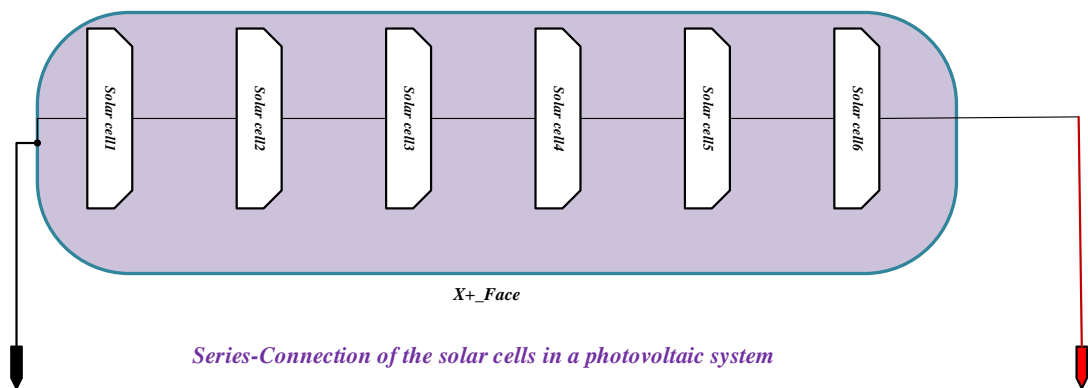


Figure 6.4: Series -Connection of solar cells known as the S-Connection mode

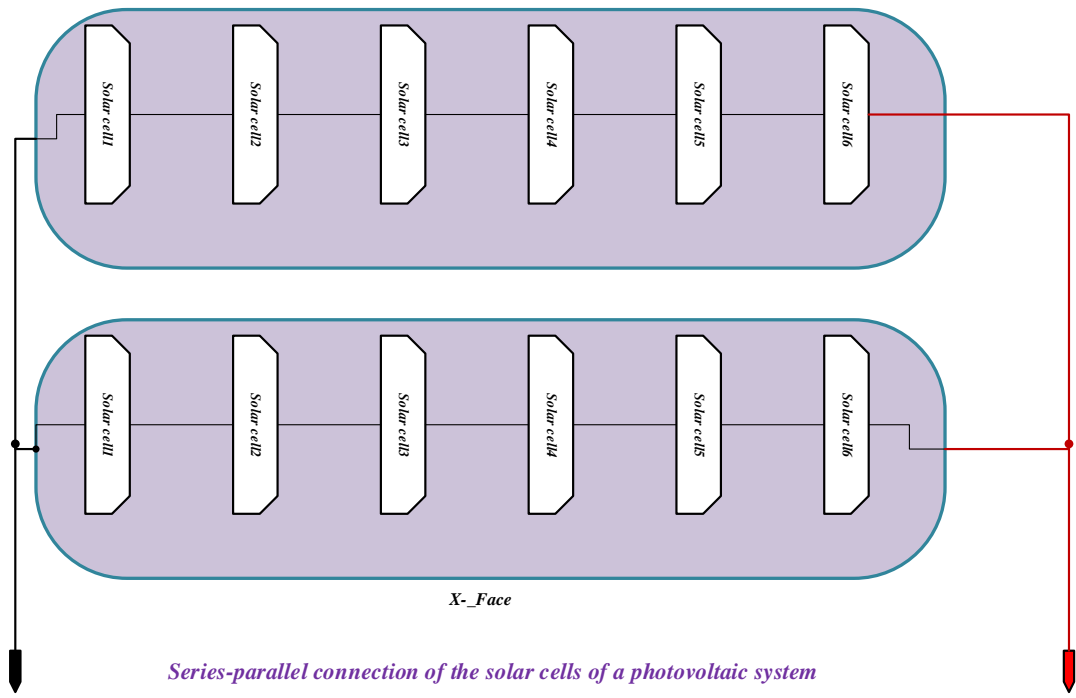


Figure 6.5: Series - Parallel Connection of solar cells known as the SP-Connection mode

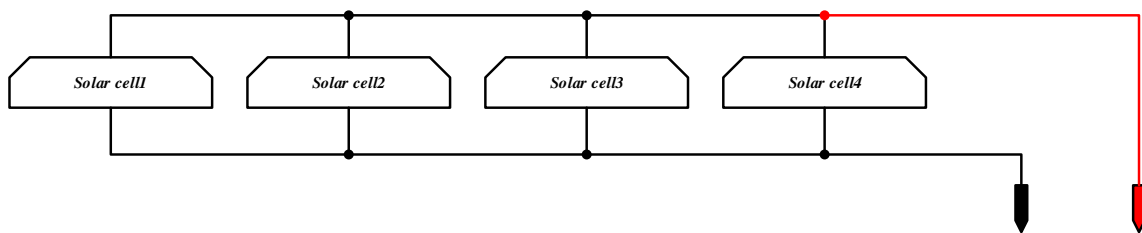


Figure 6.6: Parallel Connection of solar cells known as the P-Connection mode

Accordingly to the configuration scheme, the values on the current and the voltage produced by the solar cells available in the photovoltaic system will differ from one configuration scheme to another. Practically, those solar cells show a non-linear output characteristic called current-voltage (I-V) characteristics when exposed at a certain solar irradiance level and furthermore under a known degradation level. While originally those solar cells are mounted in a way that we can easily tabulate them as elements of a given matrix made of m times n identical solar cells linked in a series-parallel scheme so that a uniform solar irradiance can illuminate them when orbiting in space. The series-parallel configuration has been done considering the ideal model of those solar cells so that the setting can be done to realize an operation at their maximum power points which will contribute to the realization of a maximum output power production from the entire photovoltaic system that will fulfil the power demand of all the payloads connected to the power system unit of the designed nanosatellite.

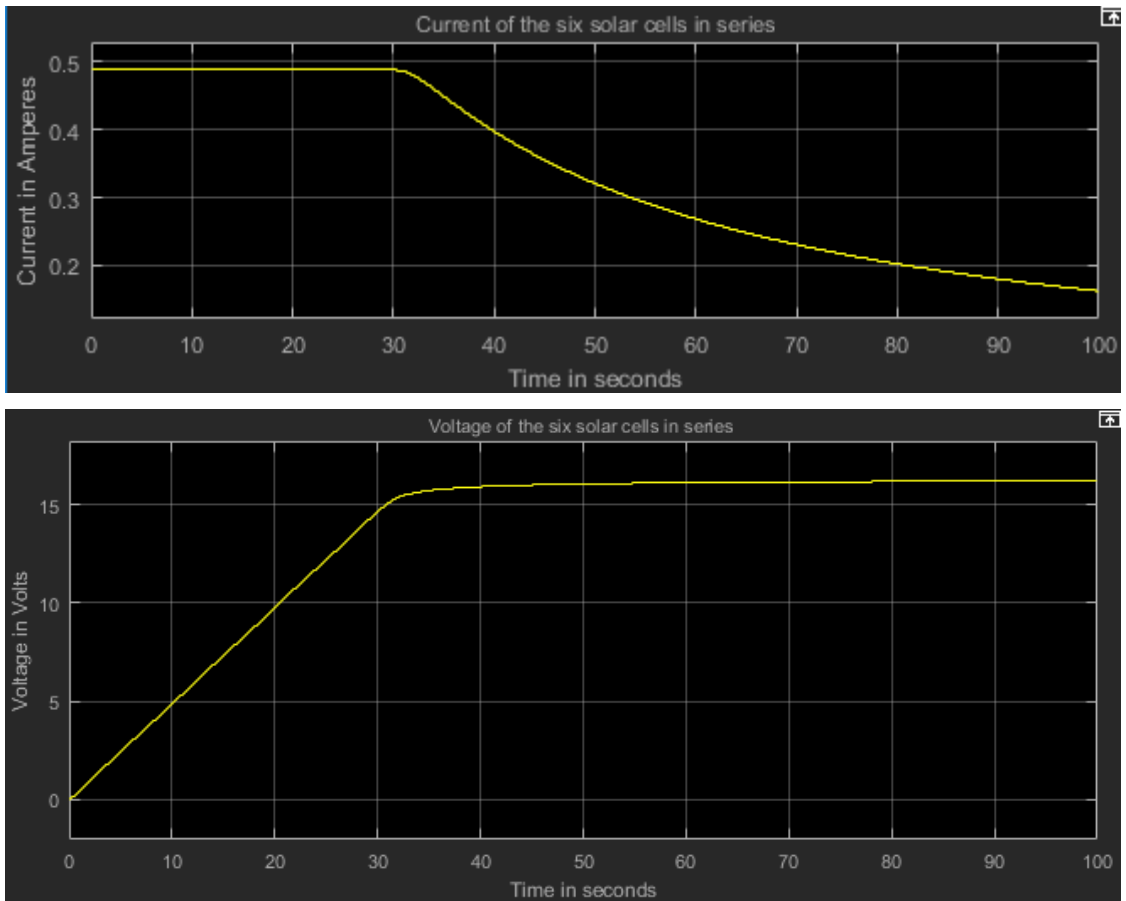


Figure 6.7: Current-Voltage characteristic of a face made of 6 healthy XTJ solar cells in Series – Connection

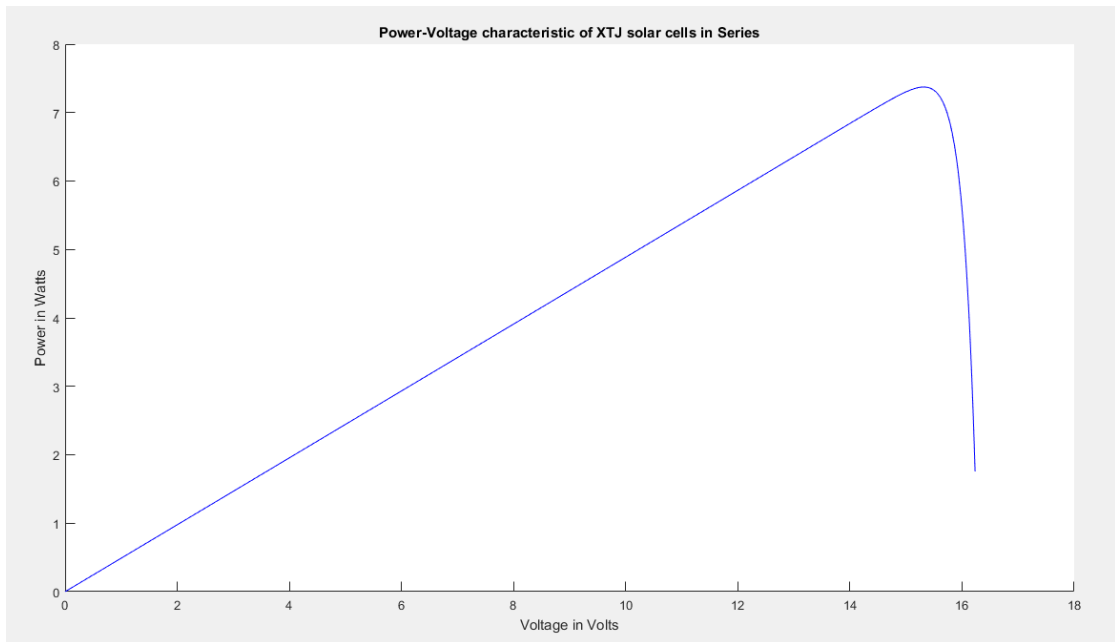
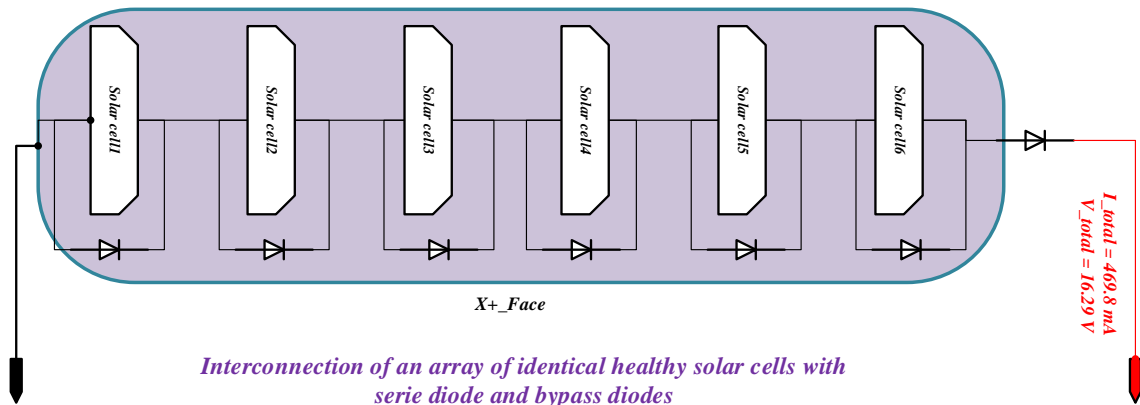


Figure 6.8: Power-Voltage characteristic of a face made of 6 healthy XTJ solar cells in Series – Connection



Interconnection of an array of identical healthy solar cells with serie diode and bypass diodes

XTJ_Prime multijunction solar cell with 30.7% efficiency

Voc= 2.715 Volts

Vmp= 2.39 Volts

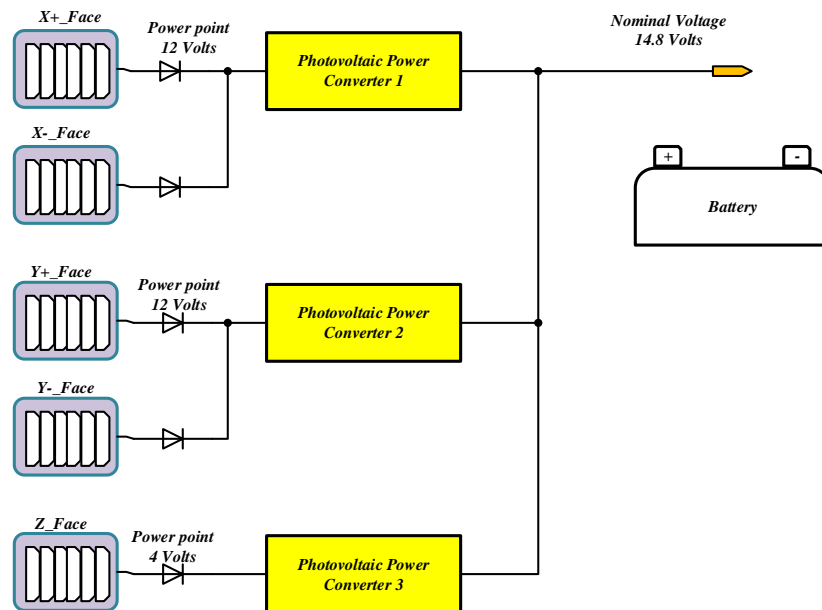
Imp= 469.8 milli Amperes

Isc= 488.7 milli Amperes

$P_{total} = I_{total} \cdot V_{total} = 7.653042$ Watts

Figure 6.9: Electrical parameters readings of the series-connection topology

Due to the failure probability of those solar cells when orbiting in space, series-diodes and bypass diodes are used to avoid the hotspot and mismatch events as shown in the picture figure below:

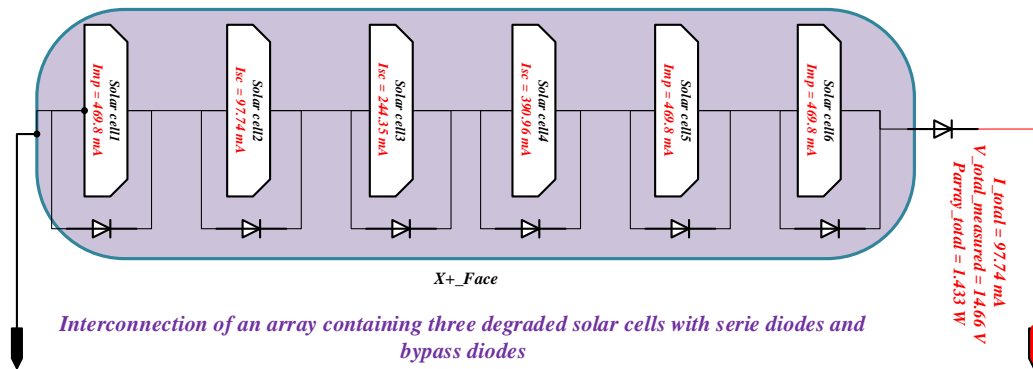


Solar Panel Setup with serie Diodes

Figure 6.10: Photovoltaic system of a 3U-Nano satellite with series diodes

Under the hotspot, mismatch events or degraded circumstances, the degraded solar cells mounted on the nanosatellite will diverge from their individual maximum power point which

will then contribute to a decrease of the produced output power of the entire photovoltaic system.



XTJ_Prime multijunction solar cell with 30.7% efficiency
 $V_{oc} = 2.715 \text{ Volts}$
 $V_{mp} = 2.39 \text{ Volts}$
 $I_{mp} = 469.8 \text{ milli Amperes}$
 $I_{sc} = 488.7 \text{ milli Amperes}$

Figure 6.11: Solar cells arrays with 3 degraded solar cells among them

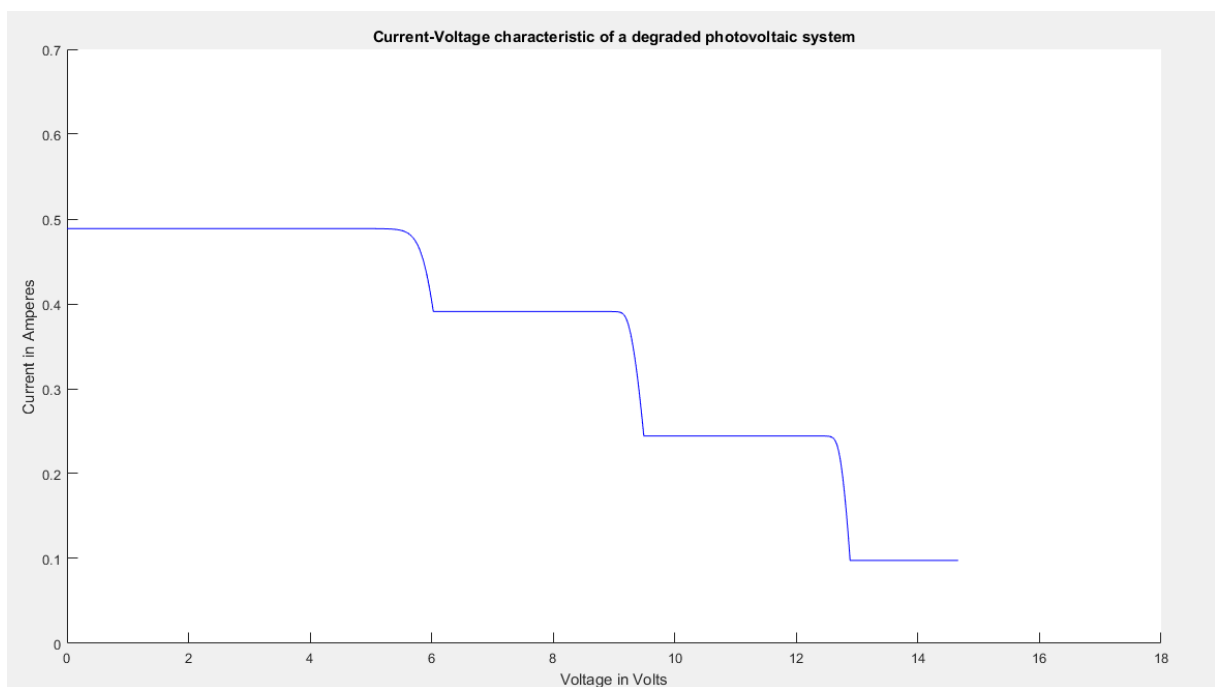


Figure 6.12: Current-Voltage characteristic of a photovoltaic system under degradation circumstances

Due to the fact that the degradation of the solar cell isn't uniform as shown in figure 6.11, therefore the variation of their short circuit current from 0 mA to 488.7 mA will influence the current voltage characteristic of the solar array. Initially, the short circuit current of the healthy solar cell is approximately 0 mA. During its degradation process, the stated short circuit value will gradually rise until it reaches 488.7 mA representing a fully degraded solar cell. Under degradation circumstances shown in figure 6.12, the low short circuit current of a solar will have a minor impact through the reduction of the overall current of the solar array but as soon

as the degradation of a consecutive solar cell is more effective than the previous one; the new degraded solar cell effect will take over the previous one. This mechanism leads towards the current voltage characteristic represented in figure 6.12 as a descending stair-case graph.

Consequently, the basic formula of the electric power of a solar cell is proportional to its current and its voltage. But figure 6.12 gave us the connection between those two parameters when the degradation process occurs on different solar cells. Thus, if the normal current is affected by the amount of current flowing through the short circuit path or diodes; then the influence of the short circuit current's value will have a physical impact on the power voltage characteristic of the overall solar array with degraded solar cell as seen in figure 6.13. There, the power of the overall healthy solar array has decreased due to degraded solar cells that are still connected in the solar array. The gradual degradation of those solar cells will imply a gradual shift on hitting the maximum power point of the solar array.

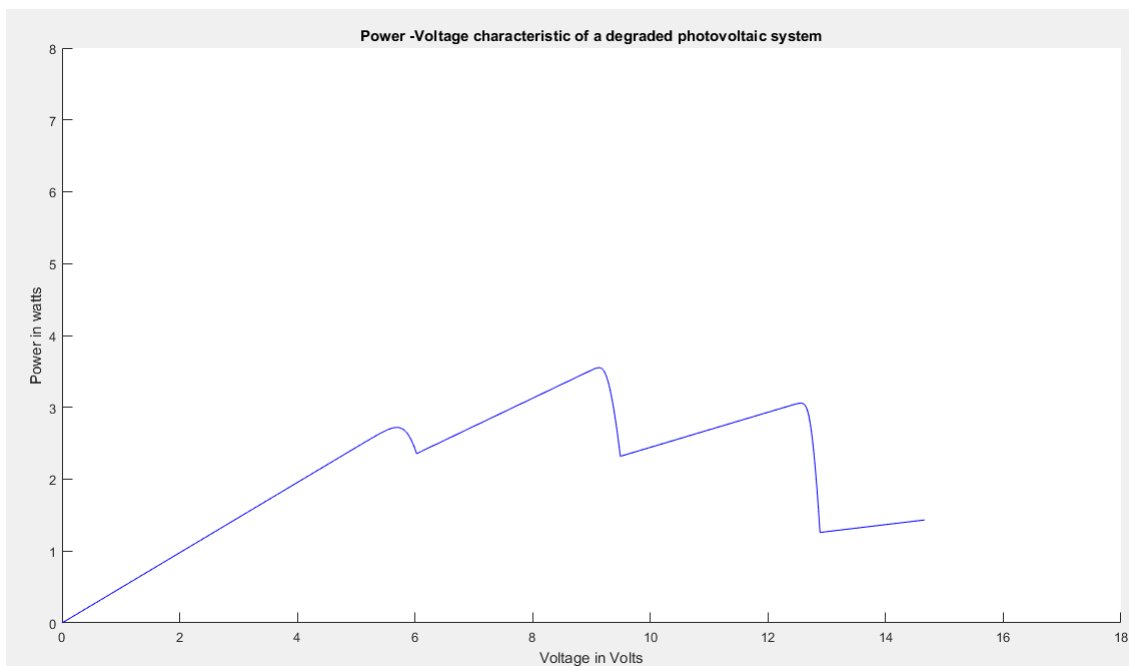


Figure 6.13: Power -Voltage characteristic of a photovoltaic system under degradation circumstances

Although, the mismatch, hotspot and degradation events have been defeated through insertions of series diodes and bypass diodes. An engineering point of view of that solution will be around the power losses and voltage drop generated by the inserted diodes based on the fact that an increase on power losses of the solar cells units will automatically decrease the efficiency of the photovoltaic system. Henceforth, an adequate selection in terms of the size, the connection scheme of the photovoltaic system will assist regarding the protection against sudden significant output power changes that lead to the photovoltaic system fluctuation.

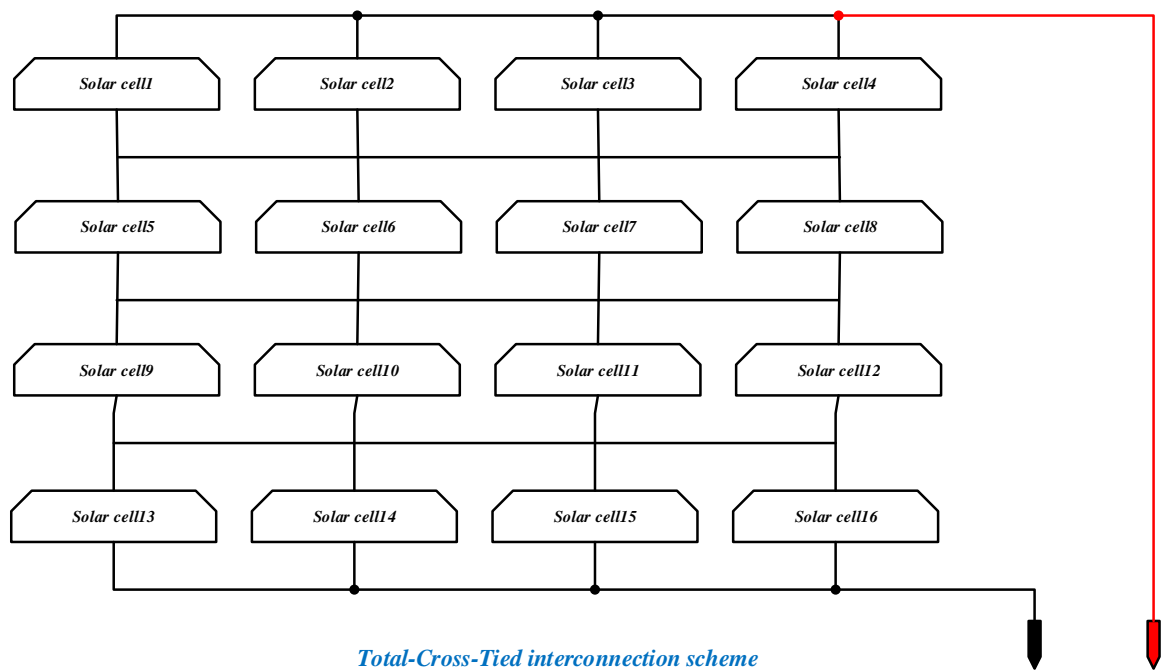
Now that we have seen the negative side of the bypass and series diodes used in a photovoltaic system, the effort and delivery of this research project is to develop a dynamic reconfigurable strategies which will dynamically change the connection scheme of solar cells contained in a photovoltaic of a Nano satellite power system with efficient ways. Consequently, it will improve the power output under electrical mismatch conditions caused by degradation or any other issues. Surely, each solar cells modules or sub-modules can to be attached to its own Maximum Power Point Tracking converter. Therefore an increase of the overall efficiency of the photovoltaic system will be achieved although a huge amount of DC to DC converter will be used or inserted in the power system of the nanosatellite. The electrical characteristics of other interconnection schemes different than the elemental connection schemes have been investigated and compared such as (*Kaushika and Gautam, 2003*):

- Total-cross-tied Connection topology known as TCT-Connection topology
- Bridge-linked Connection topology known as BL-Connection topology
- Hybrid Configuration Connection topology known as HC-connection topology

6.2.1 Total-Cross-Tied connection topology:

The total-cross-tied interconnection topology is basically an advanced or implemented series-parallel interconnection mode of solar cells where ties are connected across each row of junctions of the simple series-parallel interconnection mode of the solar cells array. On the positive side, the total-cross-tied topology facilitates the reduction of the comprehensive effects of mismatch and degradation of the solar cells.

A photovoltaic system made of a 4 by 4 solar cells matrix can be linked to each other using the total-cross-tied interconnection scheme as seen in figure 6.14:

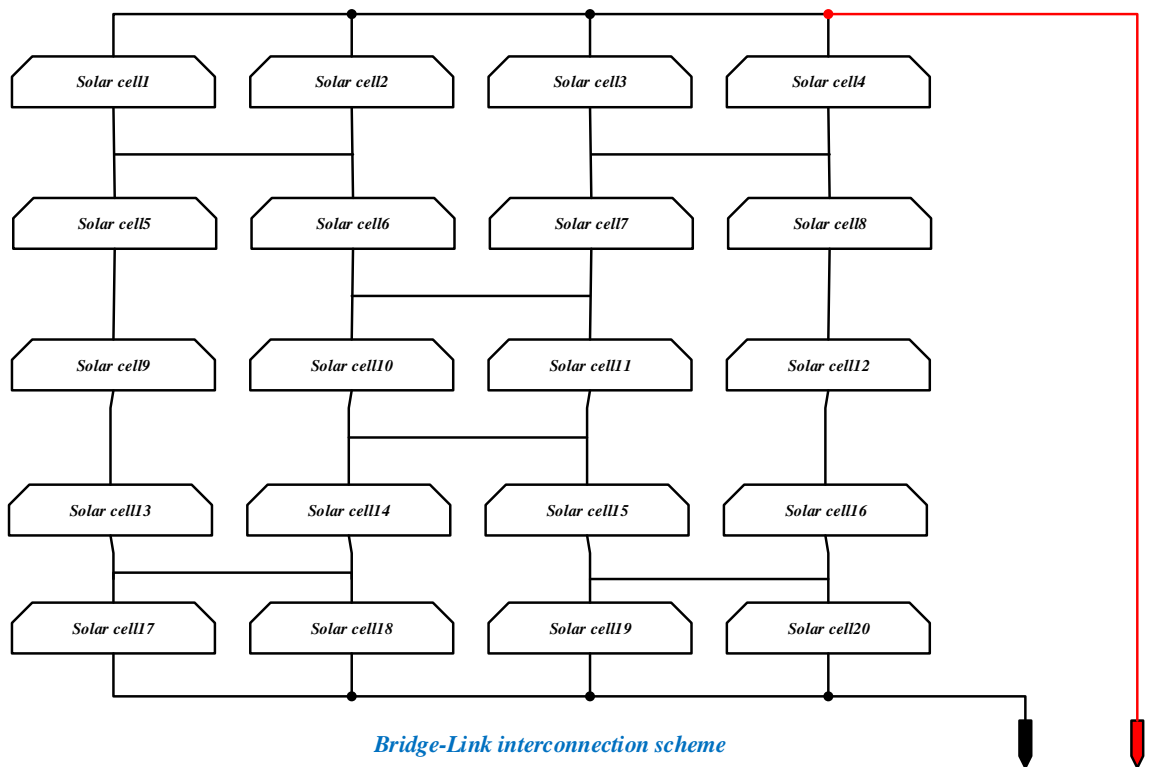


Total-Cross-Tied interconnection scheme

Figure 6.14: Total-Cross-Tied interconnection topology

6.2.2 Bridge-Linked connection topology:

Basically, the bridge-linked connection topology is obtained through reduction of some connections found in the total-cross-tied connection topology as seen in figure 6.15:



Bridge-Link interconnection scheme

Figure 6.15: Bridge-Linked interconnection topology

Having a proper understanding of the above figure will lead to the fact that the cells available in this particular topology are linked in a basic layout of a bridge rectifier. Using the bridge rectifier concept, we will notice that a bridge is made of four solar cells. Furthermore, ties are added between the bridges for interconnection purposes. Keeping in mind that in a bridge rectifier, two solar cells are firstly linked in series from each other and secondly connected in parallel, which will give a kind of series-parallel basic connection in a bridge rectifier layout.

6.2.3 Hybrid Configuration connection topology:

The Hybrid configuration also called Honey-comb connection topology is a result of modifications performed on the bridge-linked interconnection topology mentioned in the previous paragraph. This topology is a combination of the advantages found using the total-cross-tied interconnection scheme and the bridge-linked interconnection scheme. In addition, the hybrid configuration also provides the series-parallel feature beside the ones given by the total-cross-tied interconnection scheme and the bridge-linked interconnection scheme. The hybrid configuration interconnection topology can be drawn for a 4 times 4 solar cells photovoltaic system as shown in figure 6.16:

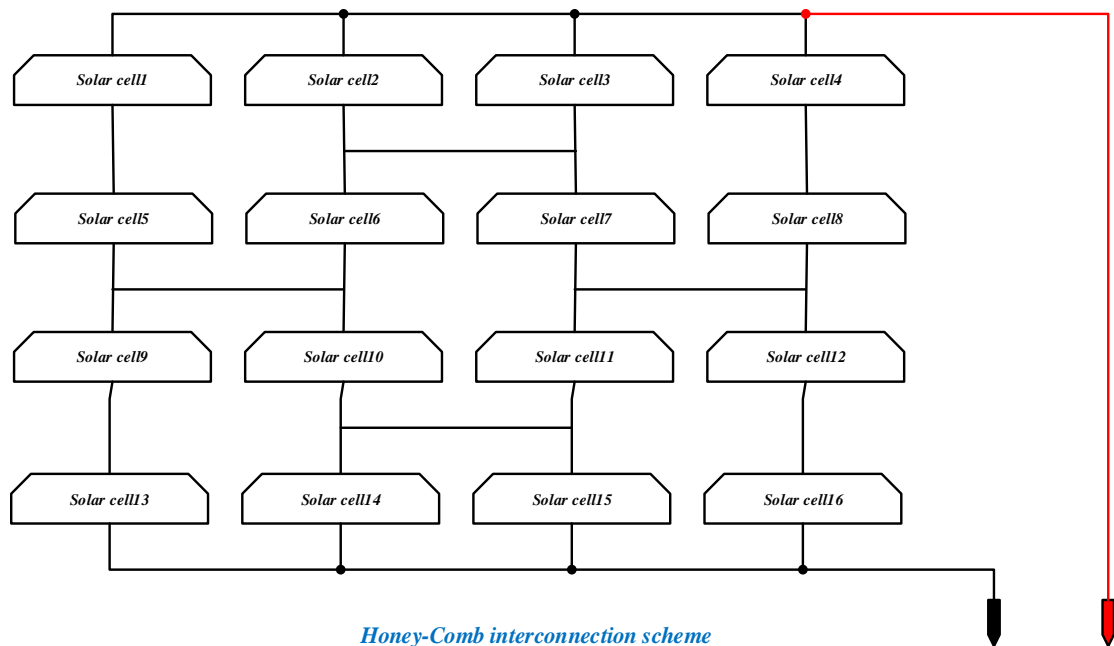


Figure 6.16: Honey-Comb interconnection style

Chapter 7: Degradation fault detection algorithm and system

Optimization of solar cells

7.1 Introduction:

In the previous chapters, we have highlighted the process of a photovoltaic power generation system of a nanosatellite and its elements. We mentioned that solar cells are one of the major elements of a photovoltaic system and we also described the fact that the conversion of the sun light into electricity using photovoltaic cells depends on numerous factors. Like any other system, we have to record or monitor the data provided by the power generator system so that we can clearly see or understand if the utilized system works correctly and is efficient. Moreover, bad efficiency of the photovoltaic system or photovoltaic cells can be obtained if there is a fault in the photovoltaic system, which will lead to permanent power losses on the system. Thus, monitoring the parameters of the photovoltaic cells will assist in terms of detecting if a fault occurred in the system. Under the faults circumstances, an adequate analysis must be done and a suitable photovoltaic array interconnection can be utilized to optimize the produced output power of the solar cells system.

7.2 Failures occurring in photovoltaic system:

Many analysing studies have been done to actually demonstrate the multiple types of failures, which occur in a photovoltaic system and photovoltaic cells. Engineering and scientifically speaking, the presence of faults in photovoltaic cells will extend the interest of the research in the field of solar cells monitoring, detection of faults and optimization due to the importance of producing an efficient and reliable photovoltaic system generator at the lowest cost possible for space applications. During the operation of a solar cell, the failures listed below can occur on the solar cell to produce power losses in the solar cell:

- The ethylene vinyl acetate discoloration over a solar cell's normal life span known as ethylene vinyl acetate yellowing and ethylene vinyl acetate browning;
- Delamination which arises when the separation of the bond within the plastics placed on the back and the glass placed on the front of the solar cell is made;
- Bubbles formed during the lamination process of the solar modules;
- Cracks in the solar cells which can result from the mechanical and thermal stresses at which the solar cells are exposed during transportation or installation process;
- Defects in the anti-reflecting coating seen as a faulty type of optical coating applied to the surface of the solar cells for reflection's reduction;

- Hotspots caused by the panel acting as load when there is a low current solar cell in the solar cell array of at least several high short-circuit solar cells;
- Delamination of the edge-seals incorporated around the perimeter of the photovoltaic technologies to prevent the penetration of the moisture from the sides;
- Newly cracked solar cells also seen as micro cracks that occur into the solar cells;
- Delamination over solar cells and interconnections;
- Fissure encapsulation over solar cells and interconnections;
- Standing out interconnections; and
- Degradation over time, which implies a significant drop in current.

According to the above list of failures that can be picked on a solar cell, various types of fault detection methods can result from it regarding the parameters, which will be used to identify the fault in that particular solar cell. Right now, during the presence of one of those highlighted faults in a photovoltaic system, the maximum power point tracking unit will be protected by triggering the current based protection devices of the photovoltaic system. The degradation of the solar cells over time will be the fault considered in this chapter for the design of a monitor and fault detection system which will allow a suitable interconnection scheme among the healthy solar cells so that we can optimize the produced output power of the photovoltaic system.

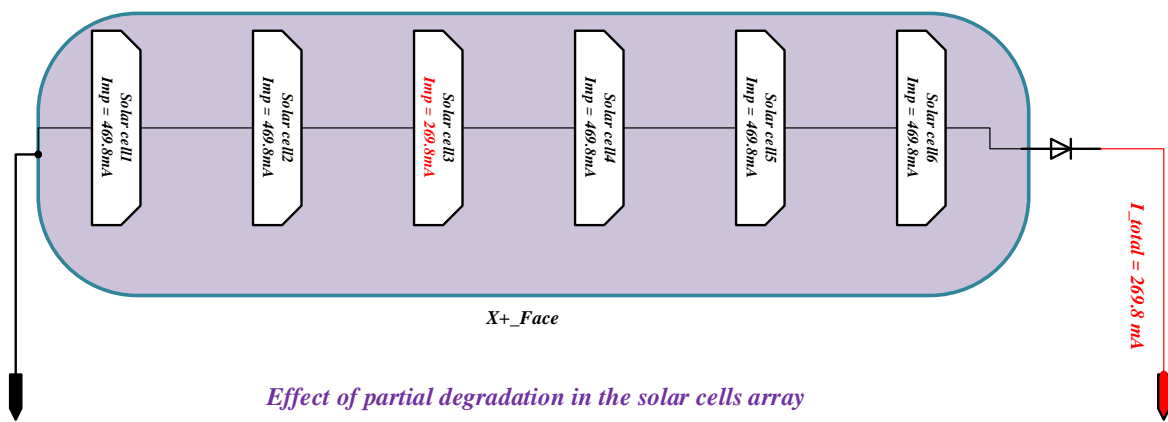
7.3 Degradation in photovoltaic system:

In a photovoltaic cell, the photovoltaic degradation can arise in various ways. Thus, a better understanding of those photovoltaic degradation ways is necessary before searching for a monitoring, detection method of photovoltaic degradation which can contribute to the reduction or the elimination of the photovoltaic degradation effect in a photovoltaic system. So far, some observed photovoltaic degradation ways seen in solar cells can be listed below (*Meyer and Dyk, 2004*):

- Front surface soiling;
- Optical degradation;
- Solar Cell degradation;
- Mismatched solar cells;
- Light-Induced degradation; and
- Temperature-Induced degradation

7.3.1 Front surface soiling:

The front surface of a solar cell can be ruined if there is an accumulation of dirt on the top surface of the solar cell. This process might take place during the assembling or transportation process of the nanosatellite before it has been launched. Consequently, the solar cell produced output power can be reduced up to ten percent losses of its normalized produced power under the front surface soiling condition. Due to the accumulated dirt on the top surface of the solar cell, the partially shade solar cell produces less current than the other cells contained in the same solar cells array. Henceforth, leading to a low overall current of the solar cells array as seen in the figure shown below:



Effect of partial degradation in the solar cells array

*XTJ_Prime multijunction solar cell with 30.7%
efficiency
Voc= 2.715 Volts
Vmp= 2.39 Volts
Imp= 469.8 milli Amperes
Isc= 488.7 milli Amperes*

Figure 7.1: Impact of soiling the top surface of a solar cell in a solar cells array

Due to the reduction in power of the solar cells array based on the impact of a soiled solar cell, this type of solar cell degradation can be detected by visual inspection of the solar cell and on ground field inspection (*Meyer and Dyk, 2004*).

7.3.2 Optical degradation:

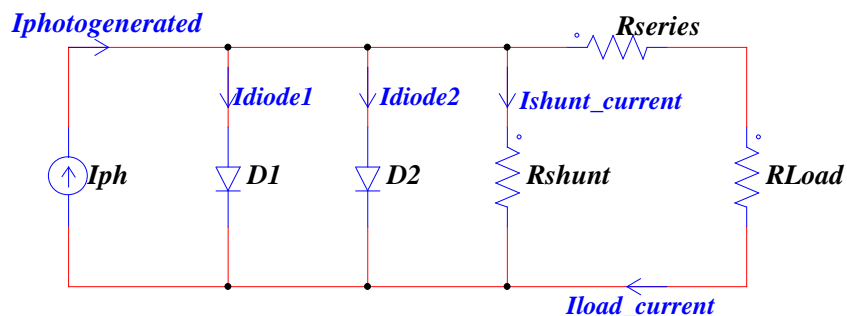
A consequence of the encapsulating material can be captured as an optical degradation. In space, this phenomenon is related to the light absorption impact on solar cells while orbiting in space. The effect of ultraviolet exposure, temperature, or humidity after a long-term exposure periods can lead to the yellowing of the encapsulating material named Ethylene vinyl acetate. There after the ethylene vinyl acetate will turn from yellow to brown. In addition, the browning ethylene vinyl acetate take in a huge portion of sunlight in the ultraviolet and visible region

therefore the required available photon responsible for the current generation is reduced which will lead to a decrease of the solar cell performance by fifty percent (Pern et al., 1991). The optical effect of ethylene vinyl acetate browning on solar cells efficiency can be picked up by illuminating the solar cell with a ultraviolet lamp (Pern et al., 1996).

7.3.3 Solar cell degradation:

Using the two diodes equivalent circuit of a solar cell illustrated by the figure 7.2, its solar cell degradation mode can be provoked based on three factors listed below:

- The increase of the solar cell's series resistance: it's noted that a solar cell's series resistance exists from the resistances in solar cells solder bonds, emitter and resistances in the junction box of its terminal. Applying ohm's law, an increase of that resistance value will increase the voltage drop across it and consequently a reduction of the voltage produced by the solar cell will be obtained. Thus, a monitoring process of the dark current through current-voltage measurement will assist towards the detection of an increase of the solar cell's series resistance;
- The decrease of the solar cell's shunt resistance: which stands for any parallel huge conductivity path of the solar cell. An increase of the shunt current will be obtained if there is a decrease on the shunt resistance value, which will lead also to a decrease of the load current flowing through the series resistance of the solar cell. The shunt current value can be monitored if a sensor's probe is connected to the shunt resistance of the solar cell to sense its value in case a significant change may occur; and
- The antireflection coating deterioration: a low reflectivity of the solar cell ameliorates both the short-circuit current and the open-circuit voltage parameters. Henceforth, an improvement on the solar cell's efficiency will be observed. Therefore, by sensing and monitoring both parameters, the detection of the solar cell through the antireflection coating deterioration way can be achieved.



Two-diodes equivalent circuit model of a solar cell

Figure 7.2: Equivalent circuit of a solar cell using the two diodes model

7.3.4 Mismatched solar cells:

Front surface soiling, encapsulated degradation, antireflective coating deterioration, manufacturing defects, micro solar cells cracking caused by thermal stress and hail damage, partial shading can be factors causing the mismatched solar cells in a photovoltaic system. The degradation of the solar cells array's performance will be the effect of mismatched solar cells in the solar cells array. This phenomenon is practically observed through the dissipated heat of the mismatched solar cells. Certain factors will be influenced by the hot spot formation generated through the mismatched conditions, these factors are given below:

- The efficiency of the solar cell;
- The open-circuit voltage of the solar cell;
- The short circuit current of the solar cell;
- The maximum power of the solar cell; and
- The fill factor of the solar cell.

A detection of this type of solar cell's degradation mode can be performed by using one of the methods listed below:

- Visual inspection;
- Current-voltage measurements;
- Hot-spot endurance testing; and
- Individual solar cell temperature monitoring during the forward biased operation of the solar cell.

7.3.5 Light-Induced degradation:

The exposure of a solar cell on to light arises the phenomenon of electrons-holes generation and recombination. During the recombination process, the energy released can be responsible for some broken weak bonds in the solar cell's depletion region. It's important to realize that meta-stable defects are formed by those broken bonds and an increase in defects disintegrate the material's quality which will be linked into the degradation of the solar cell performance. In the other hands, light-induced degradation of a solar cell can be identified through the following process:

- A continuous monitoring process of the short- circuit current and the open circuit voltage parameters of the solar cell.
- A periodic measurement of the current voltage characteristics of the solar cell.

7.3.6 Temperature-Induced degradation:

A decrease of the solar cell's band gap is usually found during the operation of a solar cell at higher temperatures, involving the absorption of longer wavelength photons. Similarly, an increase of the temperature leads to an increase of the minority carrier lifetime. The change on both temperature and minority carrier lifetime will increase the light generated current and therefore the short-circuit current will increase as well. An exponential decrease of the saturation current with an increase of the temperature can be noted (*van Dyk et al., 2000*). Thus, a measurement of the temperature dependence of the solar cells can be used to pick up the change in the temperature coefficient.

7.4 Degradation Analysis in photovoltaic system:

After a detailed explanation on the types of degradation modes happening in a solar cell, we can now be able to understand and identify a degraded solar cell in a photovoltaic system by using one of the given methods in the previous section of this chapter. In summary, it has been said previously that various procedures can be used to detect a degraded solar cell such as (*Meyer and Dyk, 2004*):

- The comprehensive visual inspection: whereby snapshots of the solar cell have to be taken so that a visual comparison needs to be performed to reveal faults like cracked solar cell, inadequate interconnections, browning of the solar cell and the hot spots formations. This method will be costly for space applications due to the fact that extra cameras need to be mounted above the solar cells to provide the required photographs;
- The light current-voltage measurement: in this case the current-voltage characteristics of the solar cell needs to be taken before outdoor deployment at the standard conditions. Thus, the collected characteristics will be important to identify any faulty solar cells due to the degradation effect seeing that the measurement will be done on a repeat sequence after a given fixed interval of time after each measurement. Through this method, the short circuit current value, the open voltage value, the maximum power of the solar cell are retrieved;
- The dark current –voltage measurement;
- The shunt resistance measurement;
- Hot spot investigation;
- Temperature dependence measurement; and
- Monitoring the short circuit current and the open circuit voltage parameters.

For the purpose of this research, a continuous monitoring process of the short circuit current has been used to identify the degraded solar cell. The measured short-circuit current will be compared to the given short-circuit current value under standard conditions.

7.5 Degraded solar cells detection in photovoltaic system:

Due to the fact that the decrease of the open circuit voltage causes a decrease on the short circuit current parameter, it can be used as a primary alert of a degraded solar cell in a solar cells array. Practically, a degraded solar will have a non-null current flowing across its bypass diode. Thus, sensing the current flowing through the bypass diode of a solar cell can assist to detect the solar cell's status either degraded or healthy. Furthermore, the open circuit voltage of each solar cell can be sensed to facilitate the degradation analysis of the measured solar cell. At the same time, the circuit or the embedded system performing the open circuit condition of the measured solar cell needs to be reliable and efficient to allow the correct data of the sensed voltage to be captured.

7.5.1 Detection of the degraded solar cell using the short-circuit current:

The short circuit current will be used to sense the degradation condition of the solar cells forming the photovoltaic system of the nanosatellite. For the purpose of the experimental design of the hardware which will be used to perform the fault detection algorithm and the reconfiguration switching scheme to maximize the produced output power regarding the presence of some degraded solar cells in the solar array; a high side current device will be mounted across each solar cell to sense the current flowing through the parallel path or the bypass diode of each solar cell as illustrated on the figure 7.3:

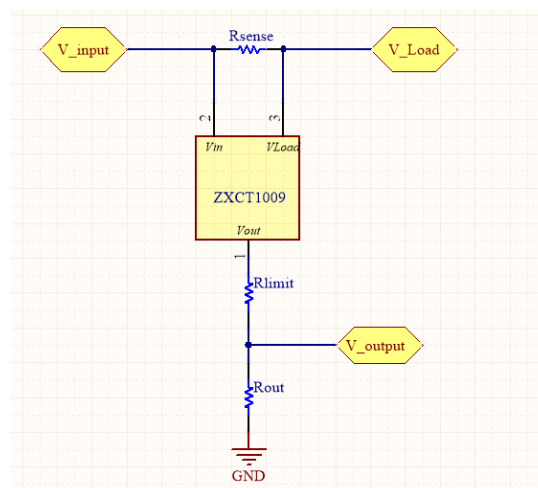


Figure 7.3: Unidirectional short-circuit current sensing system of a solar cell unit

For the design of the experimental hardware, the high side current sensor is represented by the ZXCT1009FTA. Due to the little size of the current sensor component, they can be easily mounted on board of the nanosatellite without any space and weight restrictions. In addition, the AZL solar cell 6Volts, 330 mA and 2 watts was used for the implementation of the reconfigurable algorithm. Therefore, practically we decided to translate the short circuit current of the purchased solar cell into a DC output voltage of 3.4 volts. Accordingly, the sense resistor will be choose so that the sense voltage will vary between 0.5 volts and 5 volts at full load condition.

$$V_{sense} = R_{sense} \times I_{short-circuit_full_Load} \quad (\text{Equation 57})$$

$$R_{sense} = \frac{V_{sense}}{I_{short-circuit_full_Load}} = \frac{3.4 \text{ Volts}}{3.34 \times 10^{-3}} = 1000 \text{ Ohms} \quad (\text{Equation 58})$$

$$R_{output} = \frac{V_{output}}{V_{sense} \times 0.01} = \frac{3.4}{3.4 \times 0.01} = 100 \text{ Ohms} \quad (\text{Equation 59})$$

The maximum value of the additional current limiting resistor depends on the value of the minimum input voltage, the maximum output voltage and the dropout voltage of the current sensor device. That current limiting resistor can be ignored in case the input voltage transients doesn't have significant impact on the output voltage.

Using equation 59, we can see that:

$$V_{output} = R_{output} \times V_{sense} \times 0.01 \quad (\text{Equation 60})$$

Replacing the expression of V_{sense} with the one gotten in equation 57, we will obtain:

$$V_{output} = R_{output} \times (R_{sense} \times I_{short-circuit_full_Load}) \times 0.01 \quad (\text{Equation 61})$$

Henceforth, each sensed and output given voltage from the high sensing circuit will be compared to a particular set point value to determine the degradation status of the allocated solar cell and the all the measurement data collected from each solar cells of the photovoltaic system will be log into a memory so that the read values can be used to compute the degradation detection algorithm as its primary mission and therefore will proceed with the algorithm in

charges of bypassing the degraded solar cells using low logic level controlled power electronic switches.

7.5.2 Degraded solar cell detection algorithm:

The reliability of a photovoltaic power supply unit is important these days especially for space application devices. Previously, we have highlighted the possible faults, which can occur on a photovoltaic cell, which is a component of the photovoltaic power supply unit. In fact, photovoltaic solar cell faults can be identified as faults caused during (*Bazzi et al., 2011*):

- The installation process;
- Harsh environmental effects of the sun on the photovoltaic cell's surface; and
- The degradation of the photovoltaic material

Currently, the number of man-made debris objects orbiting the earth, or orbital debris is alarmingly increasing; resulting in the increased probability of degradation, damage or destruction of operating spacecraft (*Englert et al., 2014*). Henceforth, it's important to start thinking on a way forward to reduce the amount of spacecraft debris in the space environment. Another key point is the significant of a faulty photovoltaic cell in a photovoltaic module, which is just an equivalent of an open circuit at the position of the faulty photovoltaic cell. The faulty photovoltaic cell surpasses to a reverse bias on the other photovoltaic cells that constitute the photovoltaic module or group. A consequence of that situation is the increase of hot spots in the photovoltaic cells, which can boost the number of faulty photovoltaic cells in the system. A solution of the raised matter can be the integration of bypass diodes with the photovoltaic cells (*Swaleh and Green, 1982*). But through the chapter, we will highlight an implemented method whereby the bypass diodes can be replaced by low power electronic switches to reduce the power losses of the bypass diodes in a photovoltaic module. Nevertheless, the harsh output power degradation observed in a photovoltaic system due to the presence of faulty solar cells has not been covered by the bypass diodes. Significantly, the output power loss due to faulty photovoltaic cells is way bigger than what one expects by a simple counting of healthy and faulty cells numbers. In reality, the output power degradation due to one faulty photovoltaic cell is 16.5 percent, based on the fact that the photovoltaic module is unable to keep on operating at its maximum power point when the balanced structure of a photovoltaic module is affected by degradation faults (*Lin et al., 2014*). The realization of manual degradation fault detection and fault elimination will be costly and on the other hand it will be almost impossible for photovoltaic systems used in orbital or deep space mission applications. Henceforth, the design of an embedded degradation fault detection in a photovoltaic system which can dynamically detect and bypass photovoltaic cell degradation faults for space application devices.

A degradation fault detection and fault elimination system is suitable for longer service life of a photovoltaic system. Its objective will be to locate any photovoltaic degraded cell in the photovoltaic module and secondly will eliminate the degraded cell by patterning a new photovoltaic module structure, which will reduce the output power loss generated by the faults of photovoltaic cell. Considering the photovoltaic power supply of a 3U Nanosatellite as shown in the figure below:

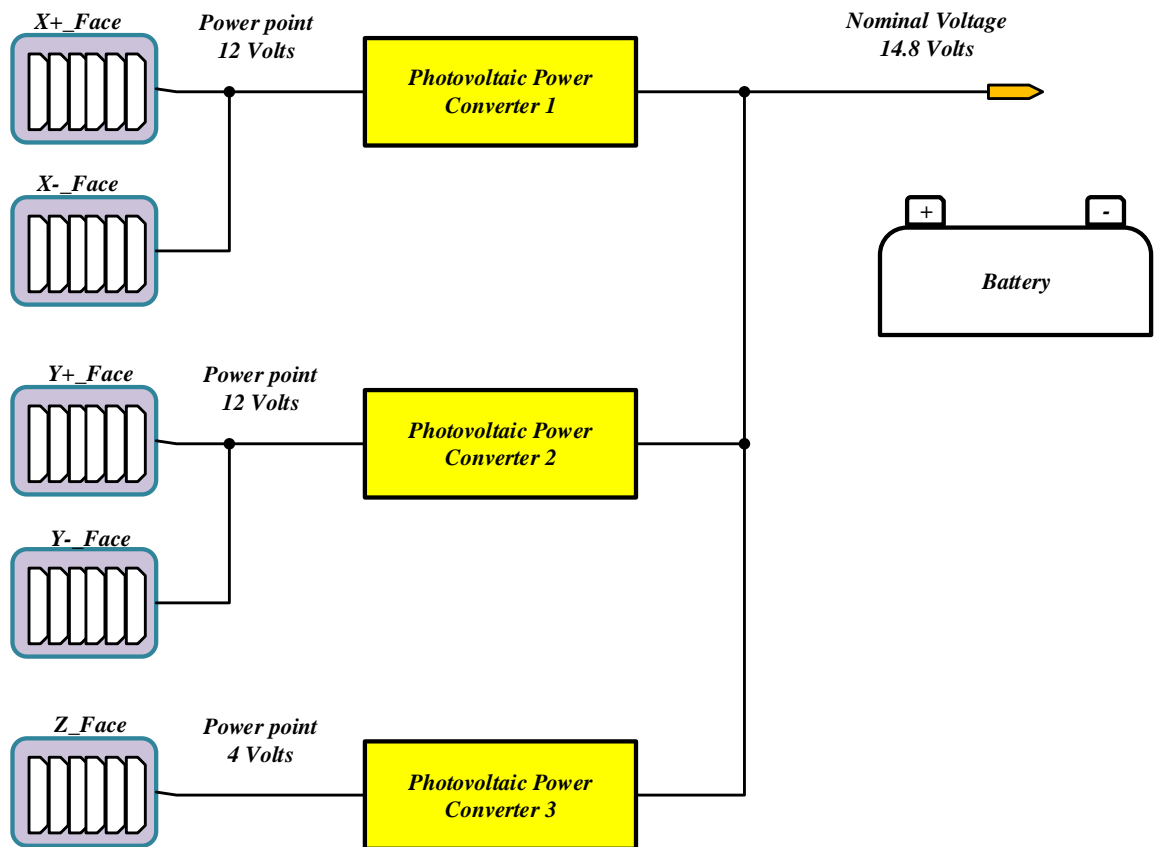


Figure 7.4: Zacube 2 power supply system

The photovoltaic module of that power supply system can be connected as a matrix of N by M size whereby the element of that matrix will be the representation of each photovoltaic cell during the normal operation mode of the photovoltaic power system. Moreover the degradation fault detection will require a formation of a multiple of M photovoltaic module in which the value of the multiple must be lower or equal to N; using the provided photovoltaic cells while the joined output power will be measured to determine the existence or not of a degraded photovoltaic cell in the photovoltaic module. Under the presence of degraded photovoltaic cells, a new formed N_{opt} times M_{opt} photovoltaic module will be constructed when the fault elimination system has successfully taken place. Thus, the system's output power will increase. In the case whereby degraded photovoltaic cells have been removed from the primary

photovoltaic module connection's style, we will obtain the new formed photovoltaic module known as the matrix (N_{opt}, M_{opt}) smaller the original matrix (N, M) of the initial photovoltaic module formed with only healthy photovoltaic cells. The matrix configuration mode of the photovoltaic module can be done using low power electronic switches as shown on the figure below where all the six solar cells of the face X^+ have been linked so that they can form a matrix $M(6,1)$:

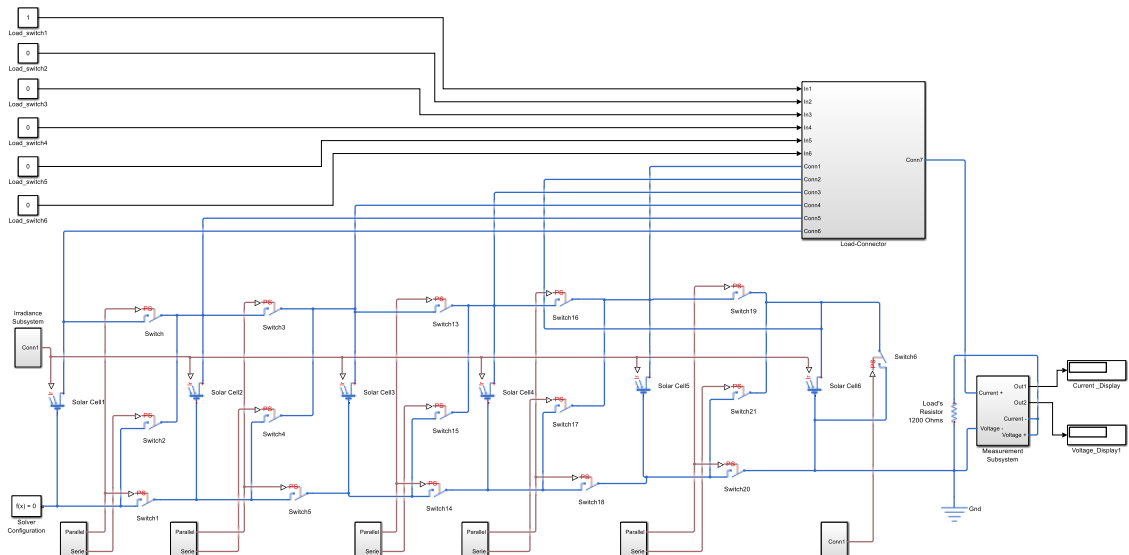


Figure 7.5: X^+ face interconnection used for degradation fault detection and fault elimination

Based on the above figure, an extra information can be drawn out of it regarding the switching scheme of all those low power electronic switches during the degradation fault detection and fault elimination just by turning them either ON state mode or OFF state mode. Therefore, the proposed degradation fault detection algorithm will be performed using of the interconnection shown in previous figure. The identification of a degraded photovoltaic cell with logarithmic time complexity will be the main task of the degradation fault detection algorithm. In other hands, the determination of the optimal interconnection style of the photovoltaic module will be the allocated task of the fault elimination algorithm. The single execution of the degradation fault detection algorithm will take place at a fixed interval of time known as Δt . It is important to realize that interval of time must be lower than the average interval time for a degradation fault to raise.

Initially, a comparison between the actual photovoltaic cell output and the theoretical output power of the photovoltaic cell will be performed by the degradation fault detection algorithm when there are no degraded photovoltaic cells. In the case of a variation between the

compared quantities, the degradation fault detection algorithm will end as a result of no degradation faults found when the detected variation is lower than a pre-specified threshold error. Contrarily, the degradation fault detection algorithm will keep on running to locate the presence of any degraded photovoltaic cells in the system, once a degraded cell is found then the fault elimination algorithm will take over through its execution by excluding degraded photovoltaic cells from the photovoltaic module. A confirmation of the absence of a new degraded photovoltaic cell will be the main task of the degradation fault detection algorithm. Thus, smaller will be the scientific computational of the degradation fault detection and the fault elimination algorithms. For the space application, the interval of time Δt at which the algorithm will be executed is configured regarding the pulse width of the nanosatellite over its allocated ground station, this will allow also a ground communication which the nanosatellite in terms of viewing or downloading the actual parameters states while passing its ground station in the space environment.

The degradation fault existence checking algorithm is actually the simplest way of fault search flowchart. This concept finds out whether a degraded photovoltaic cell is present in a group of: $\alpha \times M$ photovoltaic cells. The group maximum output power is tracked using the maximum power point tracking unit of the photovoltaic system. Let's keep in mind that: $\alpha \geq \alpha_{min}$; Here the threshold value is noted: α_{min} . Resulting to a huge output voltage of $\alpha \times M$ photovoltaic cells interconnection mode so that it can correctly be the charger's driver. In other words, in case we have a photovoltaic module smaller than $\alpha_{min} \times M$ photovoltaic cells interconnection mode, the degradation fault existence checking algorithm will be unable to perform. For the purpose of this research project, the degradation fault detection algorithm will be performed using two instructions:

- Firstly, the identification of the row allocated to the degraded faulty photovoltaic cells
- Secondly, the identification of the column allocated to the degraded faulty photovoltaic cells

Those enumerated instructions will be used to locate any degradation faults in a $N \times M$ photovoltaic cells configuration module. Under that circumstance, a primary run of the degradation fault existence checking algorithm on the entire photovoltaic module is done. In case no degraded faulty cells have been found the degradation fault detection algorithm will stop. Otherwise, the algorithm will move to its next stage of removing all degraded faulty cells and the fault elimination process will reconnect the remaining healthy photovoltaic cells so that we can reduce the power losses generated by the degraded photovoltaic cells in the system. The degradation fault detection algorithm of a photovoltaic module made of six photovoltaic cells

has been computed using Matlab to analyse the degradation state of each single cell using the monitored value of their short-circuit current and the open circuit voltage parameters. Considering that the six photovoltaic cells of a single face of the Zacube 2 nanosatellite can be configured as shown in the figure below during the last short-circuit current and open circuit voltage measurements:

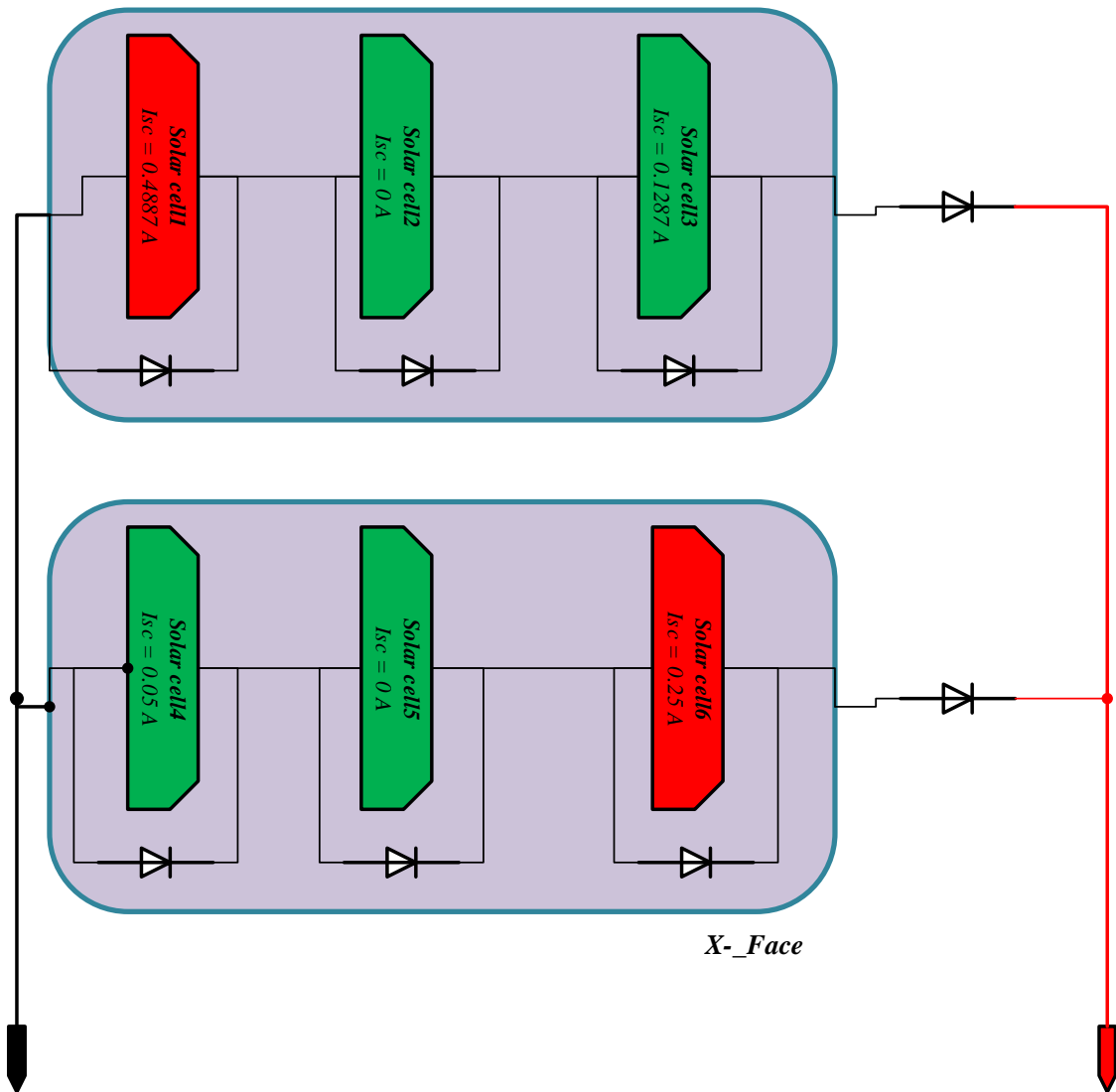


Figure 7.6: Short-circuit current monitoring results of the X+ face of the Zacube 2

We can clearly see that we’ve got two degraded photovoltaic cells shown in red where the short-circuit current is above fifty percent of the standard short-circuit current value of a XTJ-Prime solar cell. Using the data matrix concept mentioned earlier, the measured parameters of each photovoltaic cell will be kept in a $N \times M$ photovoltaic cells matrix as shown below:

$$Matrix(N, M) = \begin{bmatrix} 1^{row}, 1^{column} & \dots & 1^{row}, M^{column} \\ \vdots & \ddots & \vdots \\ N^{row}, 1^{column} & \dots & N^{row}, M^{column} \end{bmatrix} \quad (Equation 62)$$

Based on the interconnection style seen in figure 48, the collected data can be stored in a matrix using Matlab as shown below:

$$\text{Matrix}(2,3) = \begin{bmatrix} \text{solar cell1} & \text{solar cell2} & \text{solar cell3} \\ \text{solar cell4} & \text{solar cell5} & \text{solar cell6} \end{bmatrix} \quad (\text{Equation 63})$$

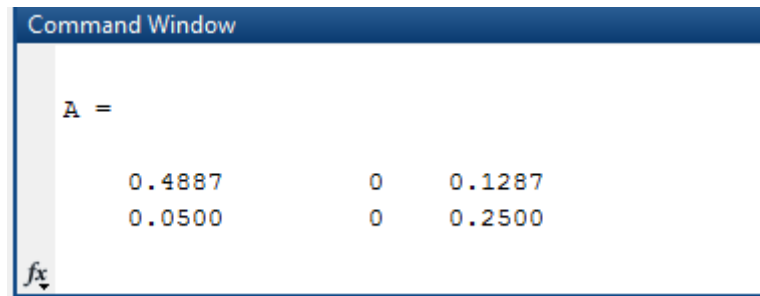


Figure 7.7: Snapshot of the command window after capturing the measured short-circuit current of each photovoltaic cell

After identification of the row number and column number of the degraded faulty photovoltaic cell, the degradation fault detection algorithm in matlab should tell the operator or the fault elimination unit the appropriate location coordinates of the degraded cells so that they can be excluded from the remaining healthy photovoltaic module. This is illustrated in the figure below:

$$\text{Number of string in parallel} = 2 \quad (\text{Equation 64})$$

$$\text{Number of cells in series} = 3 \quad (\text{Equation 65})$$

$$\text{Matrix}(2,3) = 0.4887 \quad 0.05 \quad 0 \quad 0 \quad 0.1287 \quad 0.25 \quad (\text{Equation 66})$$

$$M(2,3)\text{_Digital} = 0 \quad 1 \quad 1 \quad 1 \quad 1 \quad 0 \quad (\text{Equation 67})$$

After a rearrangement of the collected single or individual short-circuit current data measurement of the photovoltaic cells in a single array of photovoltaic cells using Matlab, the algorithm can easily analyse the collected information and identify the degraded photovoltaic cells. Accordingly, the figure below will be the search outcome of the degradation fault detection algorithm for the selected configuration of the matrix (2, 3) made from the interconnection given by the outcome shown below:

$$\text{Faulty solar cell's position} = 1 \quad 6 \quad (\text{Equation 68})$$

As we mentioned earlier, once the degraded photovoltaic cells have been identified; the fault elimination algorithm needs to take over to exclude the degraded photovoltaic cells from the healthy photovoltaic cells so that we can reduce the power losses caused by those degraded faulty photovoltaic cells. Thus, a newly formed configuration will be done using only the remaining healthy solar cells. The figure below will display the reduced number of healthy photovoltaic cells after elimination of the degraded ones:

$$\text{Healthy solar cells data} = 1 \quad 1 \quad 1 \quad 1 \quad \quad \quad (\text{Equation 69})$$

Using the remaining healthy photovoltaic cells, we can decide to reconnect them in a suitable way so that the required power demand from the connected load can be supplied with higher efficiency. The figure below illustrates the possible combinations possibility that can be made from a presented scenario of having 4 healthy photovoltaic cells on the single face of Zacube 2 in space:

$$\text{Reconfigurable_Serie_Parallel} = \begin{bmatrix} 1 & 1 \\ 1 & 1 \end{bmatrix} \quad \quad \quad (\text{Equation 70})$$

$$\text{Reconfigurable_Serie} = \begin{bmatrix} 1 \\ 1 \\ 1 \\ 1 \end{bmatrix} \quad \quad \quad (\text{Equation 71})$$

$$\text{Reconfigurable_Parallel} = [1 \quad 1 \quad 1 \quad 1] \quad \quad \quad (\text{Equation 72})$$

The indices of the healthy photovoltaic cells have to be then sent to the Simulink model of a six photovoltaic cells used to validate the results and the outcomes of this research project. In addition, the bypass diodes used in the standard configuration are replaced by low logic level power mosfets, which will allow the interconnection of those photovoltaic cells from one unit to another. An illustration of the interconnection of six XTJ-Prime solar cells in series using mosfets is shown using the figures below:

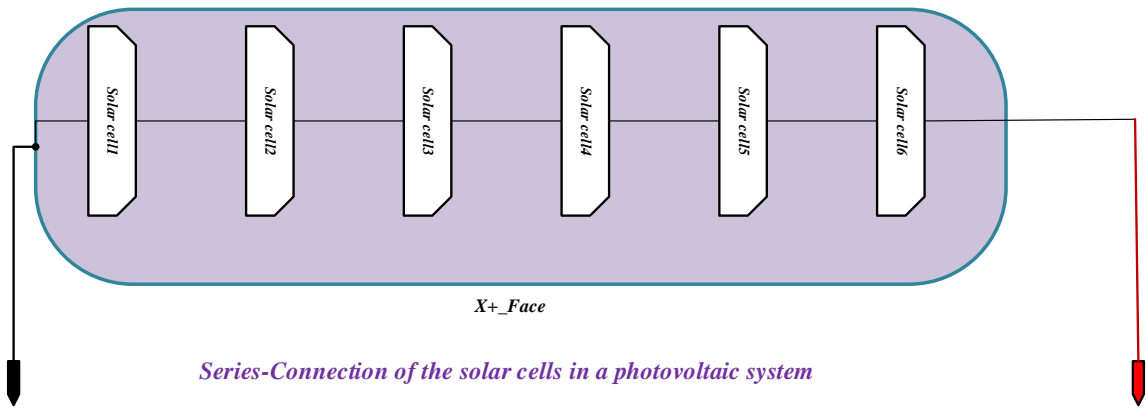


Figure 7.8: Six solar cells (XTJ-Prime) connected in series using simple wires

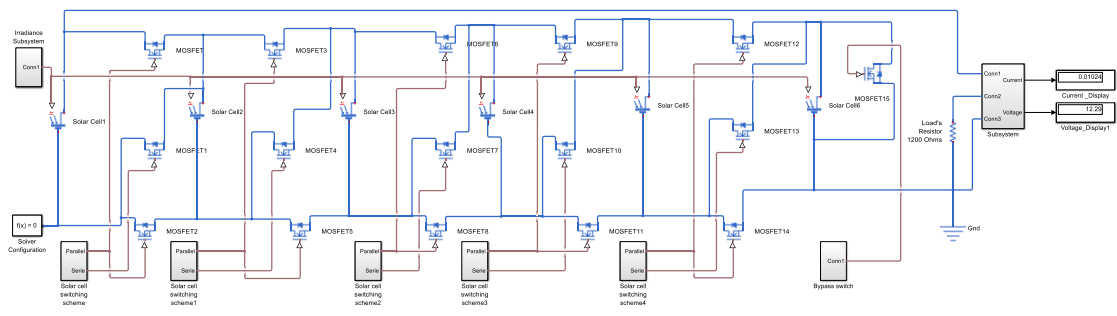


Figure 7.9: Six solar cells (XTJ-Prime) connected in series using simple Mosfets

The optimal interconnection style of the photovoltaic module will be all worked out through the fault elimination algorithm operation process. Consequently, the produced output power losses generated by the faulty degraded photovoltaic cells of the photovoltaic module will be reduced. Through the result of the degradation fault detection algorithm, the amount of the healthy photovoltaic cells will be known. Accordingly, a decision will be required for the optimal interconnection style of the photovoltaic module so that the electrical demand can be fulfilled by the photovoltaic system in charge. Considering that the number of non-degraded and active photovoltaic cells is represented by: S , then the function of those non-degraded photovoltaic cells will be given by: (S) . Given a general configuration of a photovoltaic module of $N \times M$ photovoltaic cells whereby the number of its faulty degraded photovoltaic cells is given by the variable name: *faulty*. Under that circumstance, the maximum of non-degraded active photovoltaic cells of the given photovoltaic module will be expressed by:

$$S_{\text{maximum}} = (N \times M) - (\text{faulty}) \quad (\text{Equation 73})$$

Firstly a set of proposed S values in ascending classification will be determined so that the equation below can be true:

$$[S + F(S)] \geq [S_{maximum} + F(S_{maximum})] \quad (\text{Equation 74})$$

Thus, the number of possible interconnections style of the photovoltaic module using that amount of S non-degraded active photovoltaic cells will be: $F(S)$. Running those possible interconnections styles, there must be an optimal configuration that produces the maximum output power $P_{max}(S)$ of the rest of the photovoltaic module once the faulty degraded photovoltaic cells have been excluded.

Chapter 8: The constructed reconfigurable photovoltaic module

8.1 Introduction:

The content of this chapter addresses the manufacturing process of the reconfigurable photovoltaic module which will allow the exclusion of faulty degraded photovoltaic cells in a photovoltaic array as illustrated in figure 8.1:

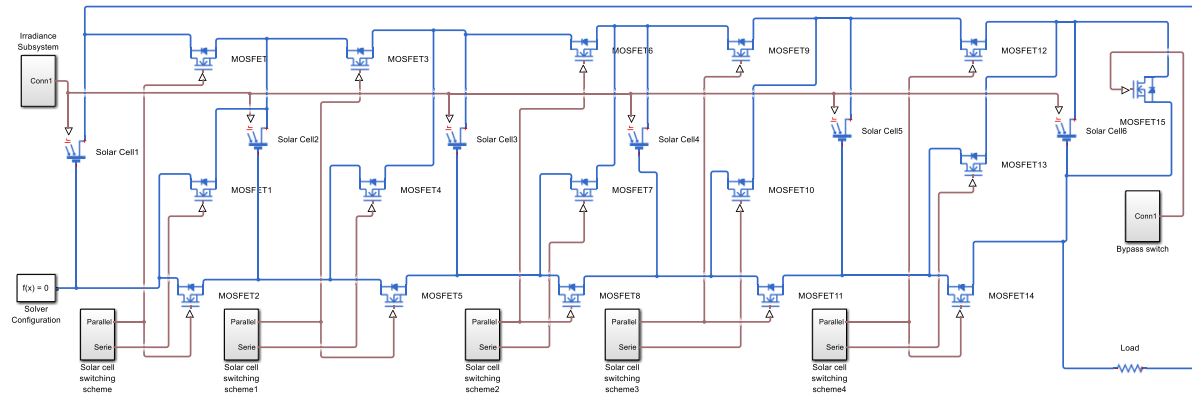


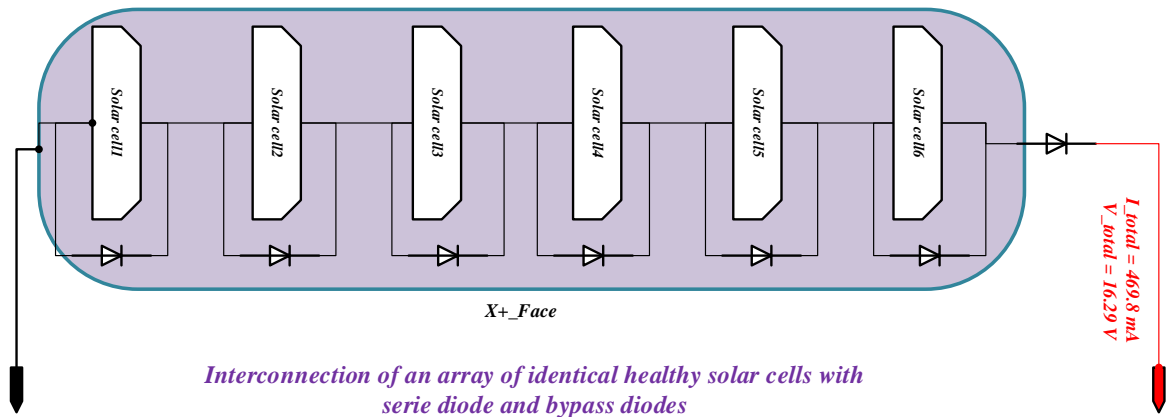
Figure 8.1: Reconfigurable photovoltaic module architecture of the X+ Face using Simulink

8.2 Modelling and simulation of the reconfigurable module:

Considering a single face of the Zacube 2 photovoltaic system generator, we can clearly notice that we got a series interconnection of six XTJ-Prime photovoltaic cells. Based on the reconfigurable architectural style, the Zacube 2 photovoltaic cells can be modelled using Simulink as shown on the above figure. Using the above given Simulink model, the electrical parameters of the photovoltaic module can be monitored such as:

- The current-voltage characteristic known as I-V characteristic
- The power-voltage characteristic known as P-V characteristic

The implemented version of that Simulink model which allows the monitoring of those stated characteristics is given in figure 8.2:



Interconnection of an array of identical healthy solar cells with serie diode and bypass diodes

XTJ_Prime multijunction solar cell with 30.7% efficiency

$V_{oc} = 2.715$ Volts

$V_{mp} = 2.39$ Volts

$I_{mp} = 469.8$ milli Amperes

$I_{sc} = 488.7$ milli Amperes

$P_{total} = I_{total} \cdot V_{total} = 7.653042$ Watts

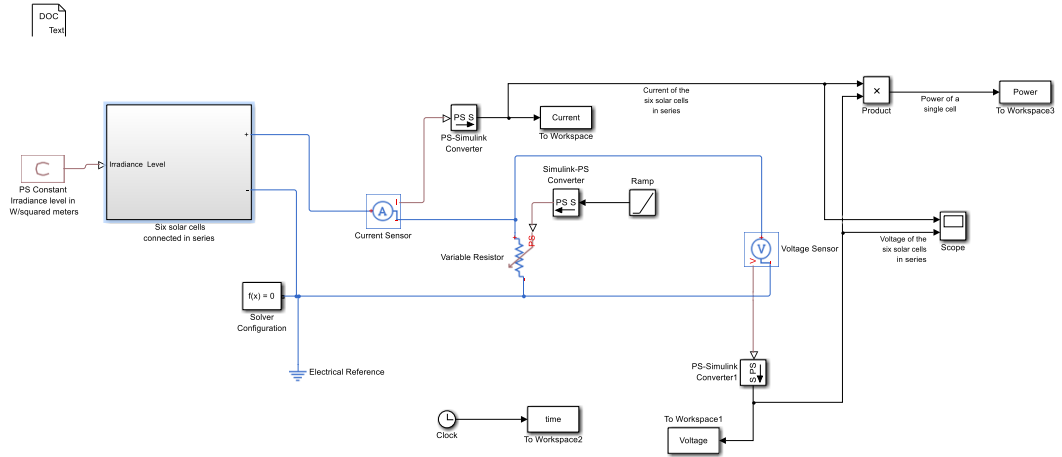
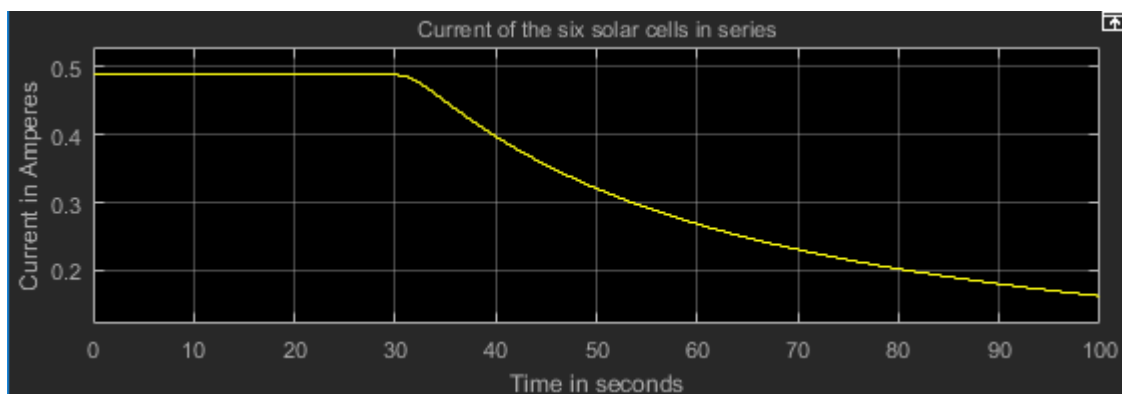


Figure 8.2: Current-Voltage Characteristic Simulink model of a healthy X+ Face of the Zacube 2



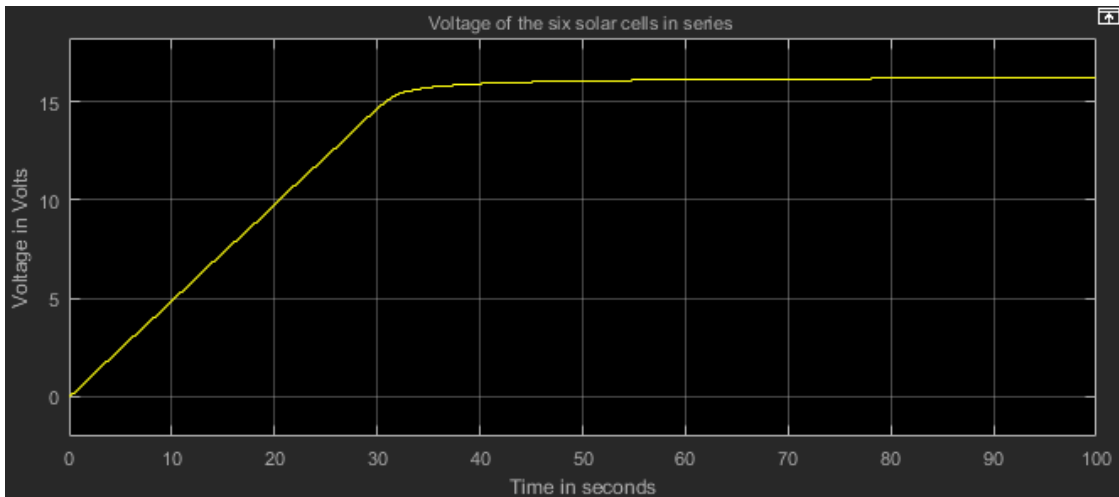


Figure 8.3: Individual Current-Voltage Characteristic curve of a healthy X+ Face of the Zacube 2

Practically, it can be noticed in figure 8.3 that both voltage and short circuit current of the combination of 6 healthy XTJ_Prime solar cells don't reach their nominal values at the moment they have been exposed to the sun. They will take a while for both parameters to reach their expected values while working under standard conditions.

We can note from those curves displayed in figure 8.4 that the actual total current of the healthy face is less than 0.5 Amperes approximately 0.48 Amperes. While the total produced voltage is a little bit above 16 Volts.

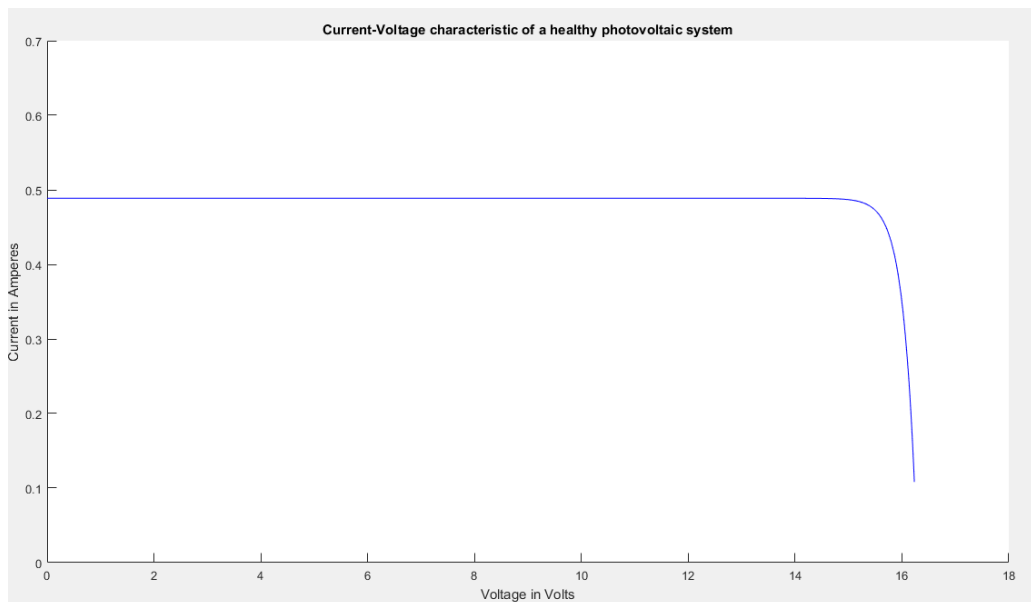


Figure 8.4: Current-Voltage (I-V) Characteristic curve of a healthy X+ Face of the Zacube 2

Through the above figure, the produced maximum current and voltage can be derived which will help in terms of the determination of the maximum power which is one of the main role of the maximum power point tracking unit in the power supply of the nanosatellite.

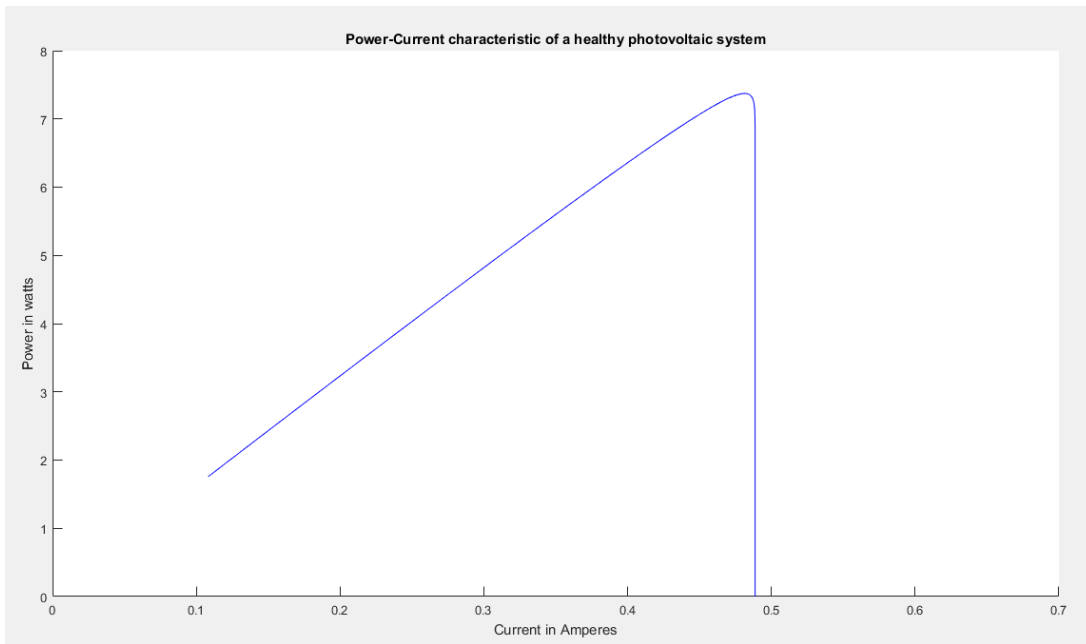


Figure 8.5: Power-Current ($P-I$) Characteristic curve of a healthy X+ Face of the Zacube 2

A flexible reconfiguration with degraded faulty cells elimination which allows the connection of the load no matter the reference voltage point is given using the figure 8.6:

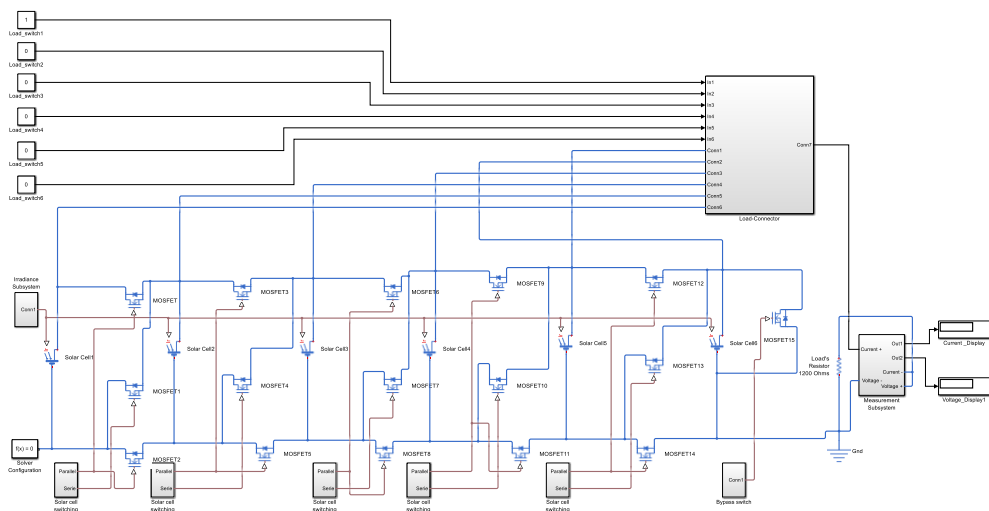


Figure 8.6: Implemented reconfigurable architecture of the X+ face photovoltaic module

8.3 Design of the printed circuit board of the reconfigurable module:

The printed circuit board of the above implemented reconfigurable architecture using surface mounted Mosfets is shown below:

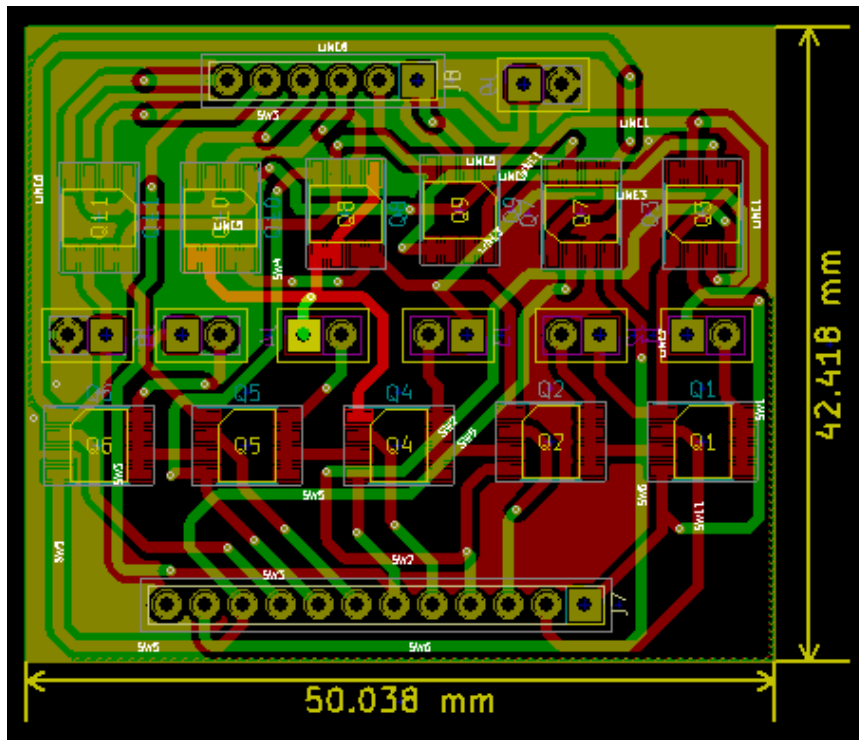


Figure 8.7: Top and Bottom layer PCB tracks of the implemented reconfigurable photovoltaic module architecture

Due to the space limitation in a nanosatellite, the design of the printed circuit board has been done over 51 mm by 43 mm. This will facilitate its insertion on the nanosatellite structure. However, the printed circuit board has been designed using both top layer and bottom layer to reduce the amount of jumpers required during the realization of some connections.

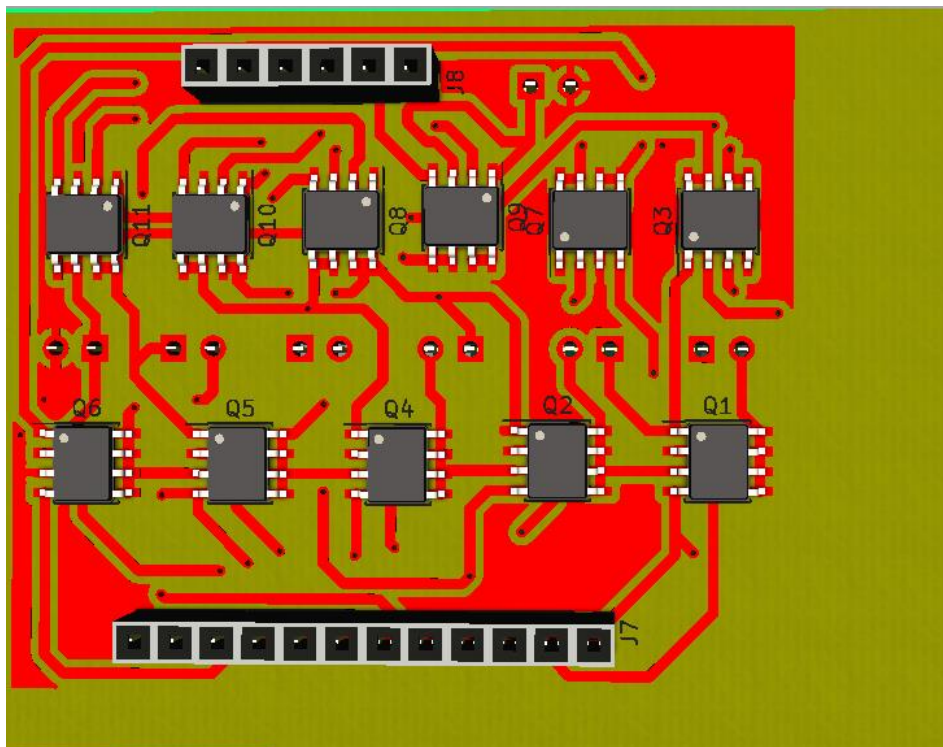


Figure 8.8: Populated Top-layer of the reconfigurable photovoltaic module's PCB

The top-layer has been realized using the dual N-channel power mosfet FDMA1028NZ surface mounted type. The dual package type contributes toward the reduction of the components list used for the construction of the circuitry. Those low power mosfets do not require any external mosfet drivers.

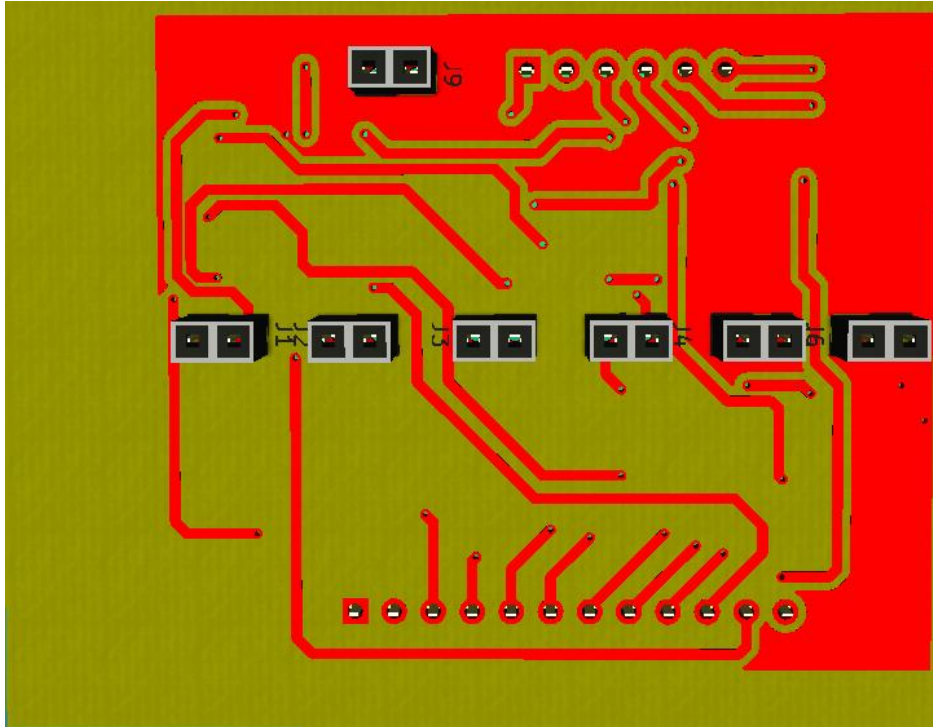


Figure 8.9: Populated Bottom-layer of the reconfigurable photovoltaic module's PCB

8.4 Experimental setups:

According to the block diagram presented in figure 8.10, individual solar cell mounted on the nanosatellite will be monitored using current sensing module. Firstly, the current sensing module will have the ability to measure the short circuit current of each solar cell. Secondly, the measured parameters will be stored in a memory. That operation will allow the comparison between the measured value and the short circuit reference value. The outcome of the comparison will trigger the logic level mosfet either on or off. The on and off control of those low power mosfets leads to the reconfiguration of the entire solar cells array.

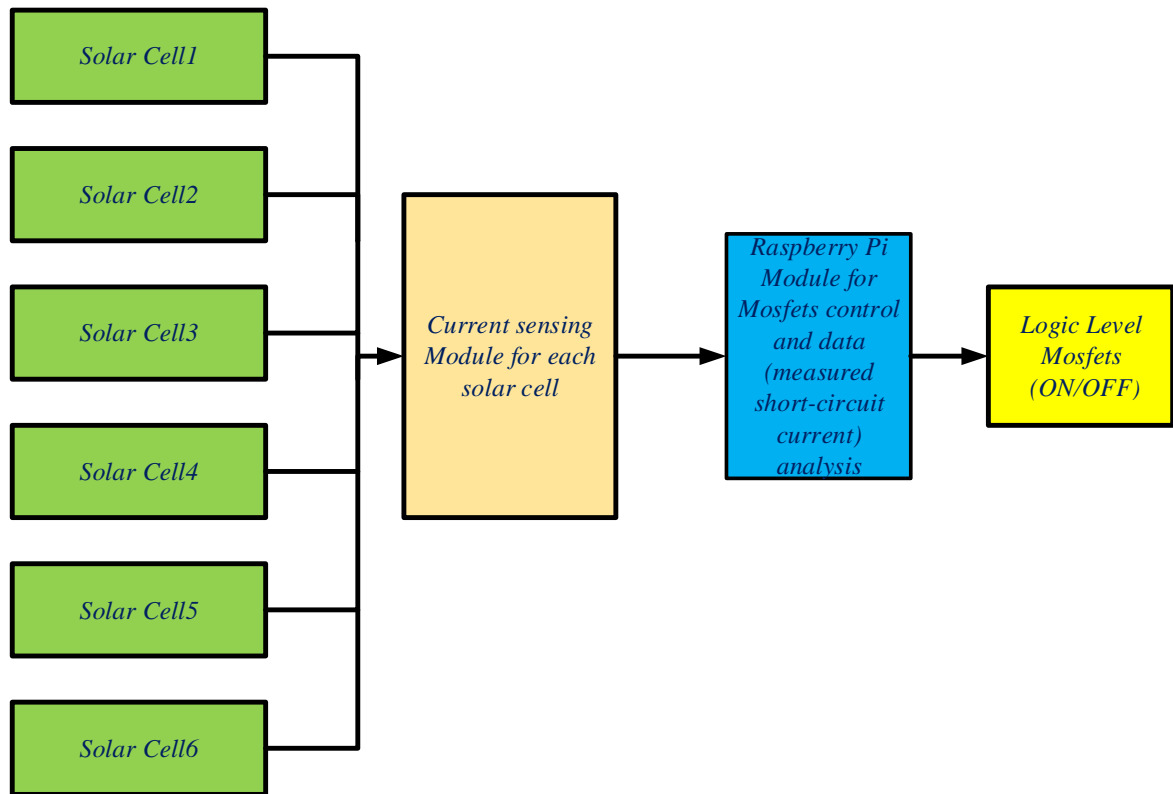


Figure 8.10: Block diagram of the experimental setup layout of the designed reconfigurable photovoltaic module



Figure 8.11: Experimental Set up for measurement of the produced output

8.5 Conclusion:

The initial purpose of the design of a nanosatellite like any other spacecraft is to operate dependably throughout their operational life. But this can only be achieved through stringent quality control and testing of parts and subsystems during the construction of the satellite and before its launch into the space orbit. In chapter one of this thesis, the enumerated steps have been highlighted as a terrestrial approach regarding the successful design of a spacecraft on earth. Meanwhile into its orbit in space, the components used for the construction of the particular spacecraft exposed to environmental constraints such as the degradation of some subsystems in the van Allen radiations belts. The description of the harsh environmental conditions at which the spacecraft is exposed in space has been given in the first chapter and the effects or consequences of have been mentioned in order to clearly see the impact of the harsh environmental conditions on the nanosatellites. Furthermore, current available predicting methods have been discussed through chapter one to show how they are useful in terms of the development of a practical and physical monitoring system of the nanosatellite's module using the logged data gotten from the spacecraft while orbiting in space.

Seeing that a better understanding of where exactly the designed and built nanosatellite will operate in terms of the involved environmental conditions; was brought out through the first chapter of this thesis. The consecutive chapter briefly introduce the technology inserted in a nanosatellite for its operation in the space orbit. The area of focus in chapter two is known as the electrical power system of a nanosatellite. A general overview of the current on-going Zacube 2 electrical power system has been drawn with its different payload subsystems and its satellite bus. In this chapter, based on the given orbital parameters; the visibility angle of the nanosatellite can be calculated as well as the adequate time at which the nanosatellite will be facing its ground station here in south Africa so that the status of the nanosatellite's electrical power system can be retrieved through telemetry communication and instructions can be sent from the ground station to the Nanosatellite in that time of visibility.

In chapter three, a breakdown of the photovoltaic system has been covered. A definition of solar cells devices and its classification based on its generation have been discussed through the third chapter. The performances of a photovoltaic cell was measured and plotted in that chapter as well as the derivation of the formulas used to calculate the electrical parameters of a photovoltaic system and its power conversion efficiency.

Chapter four has presented the photovoltaic cell's modelling, together with the representation of its electrical quantities. The single diode and the double diode representation of a photovoltaic cell were drawn using PSIM software. An implementation was done into the

simplified equivalent model of a single junction photovoltaic cell whereby the material resistivity and the ohmic losses due to levels of contact are taken into consideration during the modelling of the photovoltaic cell. For the fact that a multiple junction solar cell is the product of successive single junction solar cell, using the drawn model of a single junction solar cell; the modelling of a n-layer of semiconductors into a multijunction solar cell has been given in that chapter using PSIM software.

The degradation in different solar cell technologies was discussed in chapter five whereby a study on the factors involved of the degradation of a solar cell was enumerated, the degradation process and the way to predict, monitor and prevent the degradation of that solar cell technology was elaborated.

In chapter six, various types of configuration of photovoltaic cells were illustrated. Due to various factors such as aging of the solar cells, degradation of the solar cells; the initial configurations of the solar arrays or modules will receive a modification in order to increase the photovoltaic system's output power close or equal to its optimized output power. Henceforth, the system reconfiguration ability allows the photovoltaic system to be more efficient, it also excludes the faulty photovoltaic cells from the remaining healthy system.

The difference between those interconnections topologies mentioned in chapter six appears in the reduction or insertion of connections links between the solar cells. This action is performed using switches. The switching algorithm scheme with the computing of its flowchart has been discussed in chapter six. In addition to that it has been mentioned that the more inserted interconnection link in the topology, the more complex the computation of the switching algorithm will be.

Through this project, a general technique has been used to monitor the health status of solar cells based on their degradation process. The periodic measurement of an individual short circuit current of each solar cell will assist in terms of monitoring its degradation rate within its lifetime. The measured short-circuit current will then be compared to a reference given value of the short circuit current which will then be used to reconfigure or to exclude the degraded photovoltaic cell from the healthy photovoltaic system. Furthermore, it has been realised that the voltage drop across a logic level mosfet is lower than the voltage drop across a bypass diode. Thus, the insertion of logic level power electronic switches instead of bypass diodes will increase the reliability of the photovoltaic module.

Based on the work done with regards to this research project, my contribution in the research environment can be listed as shown below:

- The development of a Simulink model which can perform the estimated electrical characteristics of a face of the photovoltaic system mounted on a nanosatellite using the XTJ triple junction solar cells.
- The development of the short circuit current monitoring module for each photovoltaic cell.
- The development of a reconfigurable solar cells array mounted on the single face of a nanosatellite with exclusion of the degraded solar cell from the photovoltaic array.

Chapter 9: Recommendations and Future work

9.1 Recommendations:

The future research work falling under the outcomes of this thesis can be presented as follows:

- A study on the relationship between the degradation rate and the short-circuit current of a multijunction photovoltaic cell;
- Analysis of the power electronic switches used for reconfigurable photovoltaic modules for space applications; and
- The development of a wide range DC power converter used with a reconfigurable photovoltaic modules for space application

9.2 Future research work:

1. Development of a reconfigurable photovoltaic module for the entire six faces of a nanosatellite power system.
2. Analysis of the impact of the power used to control the switching algorithm on the available power found or required by the nanosatellite's operational system

References:

- 3 Generations of Solar Cells: Solar Facts and Advice [WWW Document], n.d. URL <http://www.solar-facts-and-advice.com/solar-cells.html> (accessed 7.6.17).
- Adamo, B., Anderson, R., Butler, T., Buddington, B., Capone, J., Davis, J., Hejny, N.E., Jackson, J.W., Janjic, T., Johnson, K., others, n.d. EE External Advisory Council CURRENT MEMBERS.
- Alurralde, M., 2004. Experimental and theoretical radiation damage studies on crystalline silicon solar cells. *Sol. Energy Mater. Sol. Cells*. <https://doi.org/10.1016/j.solmat.2003.11.029>
- Azzouzi, M., 2016. A study of the degradation of organic solar cells. Universitat Politècnica de Catalunya.
- Bailey, S., Raffaele, R., 2003. Space solar cells and arrays. *Handb. Photovolt. Sci. Eng.* 413–448.
- Bazzi, A.M., Kim, K.A., Johnson, B.B., Krein, P.T., Dominguez-García, A., 2011. Fault impacts on solar power unit reliability, in: *Applied Power Electronics Conference and Exposition (APEC), 2011 Twenty-Sixth Annual IEEE*. IEEE, pp. 1223–1231.
- Bekhti, M., 2013. Radiation analysis of InGaP/GaAs/Ge and GaAs/Ge solar cell: A comparative study. *Internatioal J. Renew. Energy Res.* 3.
- Bester, J., Groenewald, B., Wilkinson, R., 2012. Electrical power system for a 3U CubeSat nanosatellite incorporating peak power tracking with dual redundant control. *Przegląd Elektrotechniczny Sel. Full Texts* 88, 300–304.
- Comment les satellites transforment-ils l'énergie du soleil en électricité - Articles | Airbus Defence and Space [WWW Document], n.d. URL <http://www.space-airbusds.com/fr/actualites/comment-les-satellites-transforment-ils-l-energie-du-soleil-en-electricite.html> (accessed 7.19.16).
- Deneuville, A., Bruyère, J.C., Mini, A., Hamdi, H., Kahil, H., 1980. Cellules solaires: quelques aspects des structures «Schottky» à base de silicium amorphe hydrogéné. *Rev. Phys. Appliquée* 15, 233–240.
- Dryden, H.L., Von Doenhoff, A.E., 1961. Solar energy in the exploration of space. *Proc. Natl. Acad. Sci.* 47, 1253–1261.
- ECLIPSE ET VISIBILITE D'UN SATELLITE [WWW Document], n.d. URL http://mecaspa.cannes-aero-patrimoine.net/COURS_SA/VISIBILI/VISIBILI.htm#calcul_éclipse (accessed 4.7.17).
- Englert, C.R., Bays, J.T., Marr, K.D., Brown, C.M., Nicholas, A.C., Finne, T.T., 2014. Optical orbital debris spotter. *Acta Astronaut.* 104, 99–105.
- esa, n.d. Call for a sustainable future in space [WWW Document]. Eur. Space Agency. URL http://www.esa.int/Our_Activities/Operations/Space_Debris/Call_for_a_sustainable_future_in_space (accessed 9.22.17).
- Faraday, B.J., Statler, R.L., Tauke, R.V., 1968. Thermal annealing of proton-irradiated silicon solar cells. *Proc. IEEE* 56, 31–37. <https://doi.org/10.1109/PROC.1968.6136>
- Fehr, M., Schnegg, A., Rech, B., Lips, K., Astakhov, O., Finger, F., Pfanner, G., Freysoldt, C., Neugebauer, J., Bittl, R., Teutloff, C., 2011. Combined multifrequency EPR and DFT study of dangling bonds in a -Si:H. *Phys. Rev. B* 84. <https://doi.org/10.1103/PhysRevB.84.245203>
- F'SATI [WWW Document], n.d. URL <http://www.fsati.org/index.php/fr/?limit=4&start=4> (accessed 4.10.17).
- Galrinho, M., 2016. Least squares methods for system identification of structured models. KTH Royal Institute of Technology.
- Hacke, P., Uesugi, M., Matsuda, S., 1994. A study of the relationship between junction depth and GaAs solar cell performance under a 1 MeV electron fluence. *Sol. Energy Mater. Sol. Cells* 35, 113–119.
- How do Photovoltaics Work? | Science Mission Directorate [WWW Document], n.d. URL <https://science.nasa.gov/science-news/science-at-nasa/2002/solarcells> (accessed 7.6.17).
- Ibrahim, A.A.E., Ramadan, M.R.I., Aboul-Enein, S., ElSebaei, A.A.-A., El-Broullesy, S.M., 2011. Short Circuit Current Isc as a Real Non-Destructive Diagnostic Tool of a Photovoltaic Modules Performance. *Int. J. Renew. Energy Res. IJRER* 1, 162–168.
- Image: ZACUBE-2 - eoPortal Directory - Satellite Missions [WWW Document], n.d. URL https://www.google.co.za/imgres?imgurl=https%3A%2F%2Fdirectory.eoportal.org%2Fdocuments%2F163813%2F2241228%2FZACUBE2_Auto0.jpeg&imgrefurl=https%3A%2F%2Fdirectory.eoportal.org%2Fweb%2Feoportal%2Fsatellite-missions%2Fv-w-x-y-z%2Fzacube-2&docid=SzBr3SOa2nvYDM&tbnid=AcWan3A77a8HzM%3A&vet=1&w=875&h=541&bih

- =566&biw=988&q=ZAcube-2%20schematics&ved=0ahUKEwiY8uHA4JHSAhVLC8AKHQn8Cx8QMwghKAIwAg&iact=mrc&uact=8 (accessed 4.24.17).
- Imalka Jayawardena, K.D.G., J. Rozanski, L., A. Mills, C., J. Beliatas, M., Aamina Nismy, N., P. Silva, S.R., 2013. 'Inorganics-in-Organics': recent developments and outlook for 4G polymer solar cells. *Nanoscale* 5, 8411–8427. <https://doi.org/10.1039/C3NR02733C>
- Jordan, D.C., Kurtz, S.R., 2013. Photovoltaic degradation rates—an analytical review. *Prog. Photovolt. Res. Appl.* 21, 12–29.
- Kaushika, N.D., Gautam, N.K., 2003. Energy yield simulations of interconnected solar PV arrays. *IEEE Trans. Energy Convers.* 18, 127–134. <https://doi.org/10.1109/TEC.2002.805204>
- Kenny, R.P., Nikolaeva-Dimitrova, M., Dunlop, E.D., 2006. Performance Measurements of CIS Modules: Outdoor and Pulsed Simulator Comparison for Power and Energy Rating, in: 2006 IEEE 4th World Conference on Photovoltaic Energy Conference. Presented at the 2006 IEEE 4th World Conference on Photovoltaic Energy Conference, pp. 2058–2061. <https://doi.org/10.1109/WCPEC.2006.279907>
- Khaligh, A., Onar, O.C., 2010. Energy harvesting: solar, wind, and ocean energy conversion systems, Energy, power electronics, and machines series. CRC Press, Boca Raton, Fla.
- Kiefer, K., Dirnberger, D., Müller, B., Heydenreich, W., Kröger-Vodde, A., 2010. A degradation analysis of PV power plants, in: Proceedings of the 25th European Photovoltaic Solar Energy Conference. pp. 5032–5037.
- Kim, H., Parkhideh, B., Bongers, T.D., Gao, H., 2013. Reconfigurable Solar Converter: A Single-Stage Power Conversion PV-Battery System. *IEEE Trans. Power Electron.* 28, 3788–3797. <https://doi.org/10.1109/TPEL.2012.2229393>
- Kumar, P., 2017. Organic solar cells: device physics, processing, degradation, and prevention. CRC Press, Taylor & Francis Group, Boca Raton, FL.
- Lansel, S., 2005. Technology and future of III-V multi-junction solar cells. Retrieved April 21, 1–16. *Layers of the Sun, 2015.* . Sun Today.
- LE, C.F., n.d. C OP- Y_.
- Lee, D.-W., Cho, W.-J., Song, J.-K., Kwon, O.-Y., Lee, W.-H., Park, C.-H., Park, K.-E., Lee, H., Kim, Y.-N., 2015. Failure analysis of Cu(In,Ga)Se₂ photovoltaic modules: degradation mechanism of Cu(In,Ga)Se₂ solar cells under harsh environmental conditions. *Prog. Photovolt. Res. Appl.* 23, 829–837. <https://doi.org/10.1002/pip.2497>
- Lin, X., Wang, Y., Pedram, M., Kim, J., Chang, N., 2014. Designing Fault-Tolerant Photovoltaic Systems. *IEEE Des. Test* 31, 76–84. <https://doi.org/10.1109/MDAT.2013.2288252>
- Ljung, L., 1998. System Identification, in: Signal Analysis and Prediction, Applied and Numerical Harmonic Analysis. Birkhäuser, Boston, MA, pp. 163–173. https://doi.org/10.1007/978-1-4612-1768-8_11
- Loff, S., 2015. CubeSats Overview [WWW Document]. NASA. URL http://www.nasa.gov/mission_pages/cubesats/overview (accessed 2.3.17).
- Mac Kenzie, C.M., 1967. Solar power systems for satellites in near-earth orbits.
- Markvart, T., Castañer, L., 2003. Principles of solar cell operation. *Pract. Handb. Photovolt. Fundam. Appl.* 2.
- Messenger, S.R., Jackson, E.M., Warner, J.H., Walters, R.J., 2010. Scream: A new code for solar cell degradation prediction using the displacement damage dose approach, in: 2010 35th IEEE Photovoltaic Specialists Conference. Presented at the 2010 35th IEEE Photovoltaic Specialists Conference, pp. 001106–001111. <https://doi.org/10.1109/PVSC.2010.5614713>
- Messenger, S.R., Jackson, E.M., Warner, J.H., Walters, R.J., Cayton, T.E., Chen, Y., Friedel, R.W., Kippen, R.M., Reed, B., 2011. Correlation of Telemetered Solar Array Data With Particle Detector Data On GPS Spacecraft. *IEEE Trans. Nucl. Sci.* 58, 3118–3125. <https://doi.org/10.1109/TNS.2011.2172957>
- Messenger, S.R., Summers, G.P., Burke, E.A., Walters, R.J., Xapsos, M.A., 2001. Modeling solar cell degradation in space: A comparison of the NRL displacement damage dose and the JPL equivalent fluence approaches†. *Prog. Photovolt. Res. Appl.* 9, 103–121. <https://doi.org/10.1002/pip.357>
- Messmer, E.R., 2013. Solar Cell Efficiency vs. Module Power Output: Simulation of a Solar Cell in a CPV Module. <https://doi.org/10.5772/52707>

- Meyer, E.L., Dyk, E.E. van, 2004. Assessing the reliability and degradation of photovoltaic module performance parameters. *IEEE Trans. Reliab.* 53, 83–92. <https://doi.org/10.1109/TR.2004.824831>
- Meyers, P.V., Asher, S., Al-Jassim, M.M., 1996. A Search for Degradation Mechanisms of CdTe/CdS Solar Cells. *MRS Online Proc. Libr. Arch.* 426. <https://doi.org/10.1557/PROC-426-317>
- NREL, Swiss Scientists Power Past Solar Efficiency Records | NREL | NREL [WWW Document], n.d. URL <https://www.nrel.gov/news/press/2017/swiss-scientists-power-past-solar-efficiency-records.html> (accessed 10.3.17).
- O'Brien, T.P., 2009. SEAES-GEO: A spacecraft environmental anomalies expert system for geosynchronous orbit. *Space Weather* 7, S09003. <https://doi.org/10.1029/2009SW000473>
- Odenwald, S.F., Green, J.L., 2007. Forecasting the impact of an 1859-caliber superstorm on geosynchronous Earth-orbiting satellites: Transponder resources. *Space Weather* 5, S06002. <https://doi.org/10.1029/2006SW000262>
- Our Solar System - Overview | Planets [WWW Document], n.d. . NASA Sol. Syst. Explor. URL <http://solarsystem.nasa.gov/planets/solarsystem> (accessed 7.6.17).
- Patel, M.R., 2005a. *Spacecraft power systems*. CRC Press, Boca Raton, Fla.
- Patel, M.R., 2005b. *Spacecraft power systems*. CRC Press, Boca Raton.
- Pern, F.J., Czanderna, A.W., Emery, K., Dhere, R.G., 1991. Weathering degradation of EVA encapsulant and the effect of its yellowing on solar cell efficiency, in: *Proc. 22nd IEEE Photovoltaic Specialists Conference*. pp. 557–561 vol.1. <https://doi.org/10.1109/PVSC.1991.169275>
- Pern, F.J., Eisgruber, I.L., Micheels, R.H., 1996. Spectroscopic, scanning laser OBIC and I-V/QE characterizations of browned EVA solar cells, in: *Conference Record of the Twenty Fifth IEEE Photovoltaic Specialists Conference - 1996*. Presented at the Conference Record of the Twenty Fifth IEEE Photovoltaic Specialists Conference - 1996, pp. 1255–1258. <https://doi.org/10.1109/PVSC.1996.564360>
- Photovoltaic effect - Energy Education [WWW Document], n.d. URL http://energyeducation.ca/encyclopedia/Photovoltaic_effect (accessed 7.6.17).
- Plantevin, O., Fortuna, F., Bachelet, C., n.d. Matière Bat. 104-108 Orsay TP dégradation des cellules solaires sous irradiation.
- Quintana, M.A., King, D.L., McMahon, T.J., Osterwald, C.R., 2002. Commonly observed degradation in field-aged photovoltaic modules, in: *Photovoltaic Specialists Conference, 2002. Conference Record of the Twenty-Ninth IEEE. IEEE*, pp. 1436–1439.
- Read “The Sun to the Earth -- and Beyond: A Decadal Research Strategy in Solar and Space Physics” at NAP.edu, n.d.
- reconfigurable-PV - CAD4X Laboratory [WWW Document], n.d. URL <http://www.cad4x.kaist.ac.kr/research/reconfigurable-pv> (accessed 8.23.16).
- Renewable energy [WWW Document], n.d. . ScienceDaily. URL https://www.sciencedaily.com/terms/renewable_energy.htm (accessed 7.6.17).
- Sauvage, F., 2014. A review on current status of stability and knowledge on liquid electrolyte-based dye-sensitized solar cells. *Adv. Chem.* 2014.
- Shekoofa, O., Wang, J., 2015. Multi-diode modeling of multi-junction solar cells, in: *2015 23rd Iranian Conference on Electrical Engineering*. Presented at the 2015 23rd Iranian Conference on Electrical Engineering, pp. 1164–1168. <https://doi.org/10.1109/IranianCEE.2015.7146389>
- Solar Cells: A Guide to Theory and Measurement – Ossila [WWW Document], n.d. URL <https://www.ossila.com/pages/solar-cells-theory> (accessed 2.10.18).
- Solar Performance and Efficiency [WWW Document], n.d. . Energy.gov. URL <https://energy.gov/eere/energybasics/articles/solar-performance-and-efficiency> (accessed 7.7.17).
- Sopori, B., Basnyat, P., Devayajanam, S., Shet, S., Mehta, V., Binns, J., Appel, J., 2012. Understanding light-induced degradation of c-Si solar cells, in: *2012 38th IEEE Photovoltaic Specialists Conference*. Presented at the 2012 38th IEEE Photovoltaic Specialists Conference, pp. 001115–001120. <https://doi.org/10.1109/PVSC.2012.6317798>
- Srour, J.R., McGarrity, J.M., 1988. Radiation effects on microelectronics in space. *Proc. IEEE* 76, 1443–1469. <https://doi.org/10.1109/5.90114>
- Stöckmann, F., 1973. Photoconductivity — A centennial. *Phys. Status Solidi A* 15, 381–390. <https://doi.org/10.1002/pssa.2210150202>

- Study raises questions on what causes silicon solar cell degradation [WWW Document], n.d. URL <https://phys.org/news/2011-06-silicon-solar-cell-degradation.html> (accessed 2.23.17).
- Sumita, T., Imaizumi, M., Matsuda, S., Ohshima, T., Ohi, A., Itoh, H., 2003. Proton radiation analysis of multi-junction space solar cells. *Nucl. Instrum. Methods Phys. Res. Sect. B Beam Interact. Mater. At.* 206, 448–451.
- Suparta, W., Zulkeple, S.K., 2015. An Assessment of the Space Radiation Environment in a Near Equatorial Low Earth Orbit Based on Razaksat-1 Satellite. *ArXiv Prepr. ArXiv151103837*.
- Swaleh, M.S., Green, M.A., 1982. Effect of shunt resistance and bypass diodes on the shadow tolerance of solar cell modules. *Sol. Cells* 5, 183–198. [https://doi.org/10.1016/0379-6787\(82\)90026-6](https://doi.org/10.1016/0379-6787(82)90026-6)
- Systems Tool Kit - Technology | Space Foundation [WWW Document], n.d. URL <https://www.spacefoundation.org/programs/space-certification/certified-products/space-technology/systems-tool-kit-technology> (accessed 4.21.17).
- Taherbaneh, M., Ghafoofard, H., Rezaie, A.H., Rahimi, K., 2011. Evaluation end-of-life power generation of a satellite solar array. *Energy Convers. Manag.* 52, 2518–2525. <https://doi.org/10.1016/j.enconman.2010.12.024>
- Tamrakar, V., S.C. G., Sawle, Y., 2015. Single-Diode Pv Cell Modeling And Study Of Characteristics Of Single And Two-Diode Equivalent Circuit. *Electr. Electron. Eng. Int. J.* 4, 13–24. <https://doi.org/10.14810/elelij.2015.4302>
- tax, * All products require an annual contract Prices do not include sales, n.d. Number of satellites in space by country 2016 | Statistic [WWW Document]. Statista. URL <https://www.statista.com/statistics/264472/number-of-satellites-in-orbit-by-operating-country/> (accessed 2.2.17).
- Toorian, A., Diaz, K., Lee, S., 2008. The CubeSat Approach to Space Access, in: 2008 IEEE Aerospace Conference. Presented at the 2008 IEEE Aerospace Conference, pp. 1–14. <https://doi.org/10.1109/AERO.2008.4526293>
- Types of Solar Cells - Generation of Solar Cells, 2015. . WiFi Notes.
- van Dyk, E. e., Meyer, E. l., Leitch, A. w. r., Scott, B. j., 2000. Temperature dependence of performance of crystalline silicon photovoltaic modules. *South Afr. J. Sci.* 96, 198–200.
- Vasudevan, R., Poli, I., Deligiannis, D., Zeman, M., Smets, A.H.M., 2017. Light-Induced Effects on the a-Si:H/c-Si Heterointerface. *IEEE J. Photovolt.* 7, 656–664. <https://doi.org/10.1109/JPHOTOV.2016.2633800>
- Visoly-Fisher, I., Dobson, K. d., Nair, J., Bezalel, E., Hodes, G., Cahen, D., 2003. Factors Affecting the Stability of CdTe/CdS Solar Cells Deduced from Stress Tests at Elevated Temperature. *Adv. Funct. Mater.* 13, 289–299. <https://doi.org/10.1002/adfm.200304259>
- Walker, D.H., Statler, R.L., 1988. A satellite experiment to study the effects of space radiation on solar cell power generation. *Sol. Cells* 23, 245–268.
- Walters, R., Summers, G.P., Warner, J.H., Messenger, S., Lorentzen, J.R., Morton, T., Lei, F., 2007. SPENVIS Implementation of end-of-life solar cell calculations using the displacement damage dose methodology, in: 19th Space Photovoltaic Research and Technology Conference. p. 25.
- Walters, R.J., Messenger, S.R., Cotal, H.L., Summers, G.P., Burke, E.A., 1996. Electron and proton irradiation-induced degradation of epitaxial InP solar cells. *Solid-State Electron.* 39, 797–805.
- Walters, R.J., Messenger, S.R., Summers, G.P., Burke, E.A., Keavney, C.J., 1991. Space radiation effects in InP solar cells. *IEEE Trans. Nucl. Sci.* 38, 1153–1158. <https://doi.org/10.1109/23.124088>
- Weinberg, I., Brinker, D.J., 1988. Progress in InP solar cell research.
- Wertz, J.R., Larson, W.J. (Eds.), 1999. Space mission analysis and design, 3rd ed. ed, Space technology library. Microcosm ; Kluwer, El Segundo, Calif. : Dordrecht ; Boston.
- Yamaguchi, M., 2001. Radiation-resistant solar cells for space use. *Sol. Energy Mater. Sol. Cells* 68, 31–53.
- Yang, W., Yao, Y., Wu, C.-Q., 2013. Mechanisms of device degradation in organic solar cells: Influence of charge injection at the metal/organic contacts. *Org. Electron.* 14, 1992–2000. <https://doi.org/10.1016/j.orgel.2013.04.036>
- ZACUBE 2 (ZA 004) - Gunter's Space Page - Gunter's Space Page [WWW Document], n.d. URL http://space.skyrocket.de/doc_sdat/zacube-2.htm (accessed 4.10.17).
- ZACube-1 (TshepisoSAT) | AMSAT-NA, n.d.

ZACUBE-2 - eoPortal Directory - Satellite Missions [WWW Document], n.d. URL
<https://directory.eoportal.org/web/eoportal/satellite-missions/v-w-x-y-z/zacube-2> (accessed 4.10.17).

ZAcube-2 schematics - Google Search [WWW Document], n.d. URL

https://www.google.co.za/search?q=ZAcube-2+schematics&biw=988&bih=566&tbm=isch&imgil=W8E1jrQX0bYEbM%253A%253BIWwt_YiGYznmLM%253Bhttps%25253A%25252F%25252Famsat-uk.org%25252Ftag%25252Fzacube-2%25252F&source=iu&pf=m&fir=W8E1jrQX0bYEbM%253A%252CIWwt_YiGYznmLM%252C_&usg=__VIs0j4a1mWfiaSWOrqPsGctWC54%3D&ved=0ahUKEwiugdK84JHSAhXpDsAKHc93AsQQyjciMw&ei=pRqkWO6aEemdGAbP74mgDA#imgrc=W8E1jrQX0bYEbM:
(accessed 2.15.17).

Zell, H., 2015. Solar Irradiance [WWW Document]. NASA. URL

http://www.nasa.gov/mission_pages/sdo/science/solar-irradiance.html (accessed 7.12.17).